VU Research Portal

Towards 3D-Printed Bioactive Calcium Phosphate Scaffolds for Bone Tissue Engineering

Kelder, Cindy Linda

2021

document version
Publisher's PDF, also known as Version of record

Link to publication in VU Research Portal

citation for published version (APA)
Kelder, C. L. (2021). *Towards 3D-Printed Bioactive Calcium Phosphate Scaffolds for Bone Tissue Engineering*. s.n.

General rights
Copyright and moral rights for the publications made accessible in the public portal are retained by the authors and/or other copyright owners and it is a condition of accessing publications that users recognise and abide by the legal requirements associated with these rights.

- Users may download and print one copy of any publication from the public portal for the purpose of private study or research.
- You may not further distribute the material or use it for any profit-making activity or commercial gain
- You may freely distribute the URL identifying the publication in the public portal ?

Take down policy
If you believe that this document breaches copyright please contact us providing details, and we will remove access to the work immediately and investigate your claim.

E-mail address:
vuresearchportal.ub@vu.nl

Download date: 13. Sep. 2021

Towards 3D-Printed Bioactive Calcium Phosphate Scaffolds for Bone Tissue Engineering

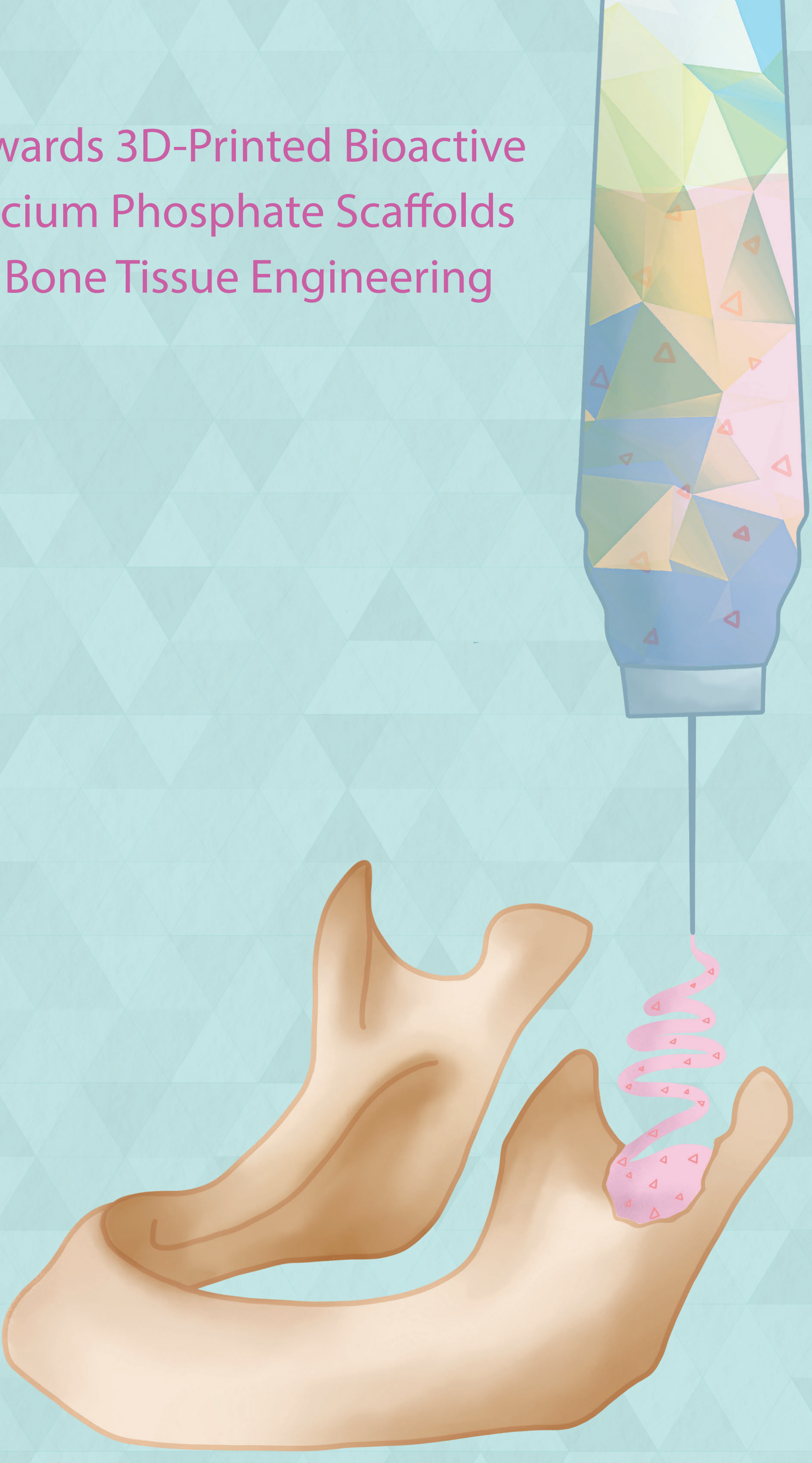

Cindy L. Kelder

Towards 3D-Printed Bioactive Calcium Phosphate Scaffolds for Bone Tissue Engineering

Cindy L. Kelder

Towards 3D-Printed Bioactive Calcium Phosphate Scaffolds for Bone Tissue Engineering
ISBN/EAN: 978-94-6419-226-1

Copyright © 2021 Cindy Kelder
Layout and Cover design by Yasmin Katlich, persoonlijkproefschrift.nl
Printed by Gildeprint Enschede, gildeprint.nl

Printed by All rights reserved. No part of this thesis may be reproduced, stored or transmitted in any way or by any means without the prior permission of the author, or when applicable, of the publishers of the scientific papers.

The studies described in this thesis were conducted at the department of Oral Cell Biology and the department of Oral Implantology and Prosthetic Dentistry at the Academic Centre of Dentistry Amsterdam (ACTA)

ACTA ACADEMISCH CENTRUM
TANDHEELKUNDE AMSTERDAM

VRIJE UNIVERSITEIT

Towards 3D-Printed Bioactive Calcium Phosphate Scaffolds for Bone Tissue Engineering

ACADEMISCH PROEFSCHRIFT

ter verkrijging van de graad Doctor
aan de Vrije Universiteit Amsterdam,
op gezag van de rector magnificus
prof.dr. V. Subramaniam,
in het openbaar te verdedigen
ten overstaan van de promotiecommissie
van de Faculteit der Tandheelkunde
op vrijdag 9 juli 2021 om 11.45 uur
in de aula van de universiteit,
De Boelelaan 1105

door

Cindy Linda Kelder

geboren te Wageningen

promotoren: prof.dr. D. Wismeijer
dr. A.D. Bakker
copromotoren: prof.dr. C.J. Kleverlaan
dr.ir. T.J. de Vries

“If we knew what it is, we were doing, it would not be called research. Would it?”

-Albert Einstein

Contents

Chapter 1 General introduction 8

Chapter 2 Burst, Short, and Sustained Vitamin D_3 Applications Differentially Affect Osteogenic Differentiation of Human Adipose Stem Cells 19

Chapter 3 Cells Derived from Human Long Bone Appear More Differentiated and More Actively Stimulate Osteoclastogenesis Compared to Alveolar Bone-Derived Cells 47

Chapter 4 The 3D Printing of Calcium Phosphate with K-Carrageenan under Conditions Permitting the Incorporation of Biological Components—A Method 79

Chapter 5 Physical and biological aspects of 3D calcium phosphate scaffolds containing vitamin D_3 95

Chapter 6 General discussion 115

Chapter 7 Summary 127

Chapter 8 Nederlandse samenvatting 133

Chapter 9 Appendices 139

List of publications 140

Contributing authors 142

PhD portfolio 149

Acknowledgements 150

About the author 154

1

General Introduction

Clinical problem

Noncritical size bone defects may heal without planned surgical reconstruction and secondary surgery. Critical-size bone defects do not spontaneously heal and are a major clinical and socio-economic problem. The most common regenerative procedure for critical-sized bone defects is placing bone grafts to aid the healing [1,2]. The exact minimum dimensions for a critical size defect are not clear, but in long bones, it is defined as a defect with a length that exceeds the diameter of the affected bone by 2 to 2.5 times [3] or 'the smallest osseous defect that will not spontaneously heal during the lifespan of the patient or animal' [2]. Such critical-size defects can be caused by trauma, infections requiring debridement of the bone, resection of bone tumors, and skeletal diseases, and are sometimes accompanied by pain. Due to multiple operations and longer hospitalization, the management of such large bone defects have a negative impact on the patients' quality of life and offers a significant disease burden. Therefore, other options focused on rapid healing of these defects are needed.

Bone

Bone is a hard, calcified connective tissue with many essential functions, such as support, protection of the internal organs and marrow cavities, and calcium and phosphate storage [4]. It is continuously remodeled and, when broken (non-critical size defect), can repair itself due to its good intrinsic healing capacity. This healing starts with hematoma formation, which is accompanied by an inflammatory response. During this response, mesenchymal stem cells are recruited, and blood vessel formation is stimulated, through the local production of cytokines and growth factors (e.g., interleukins, tumor necrosis factor-alfa (TNF-α), bone morphogenetic proteins (BMPs), and vascular endothelial growth factor (VEGF)). A callus is formed to stabilize the fracture, which generally first undergoes chondrogenesis and subsequently calcifies before being remodeled into lamellar bone [5,6].

Bone remodeling

Continuous remodeling of healthy bone (bone metabolism) is carried out by osteoclasts and osteoblasts and occurs in three stages: resorption, reversal, and formation. In the resorption stage, preosteoclasts are attracted and mature into osteoclasts on the bone surface, where they resorb part of the bone [7]. Osteoclasts are multinucleated cells derived from the hematopoietic lineage and resorb bone in two steps: First, the inorganic components of the bone are dissolved through the formation of a sealing zone and lowering of the pH, followed by the digestion and degradation of the organic components such as collagen by proteolytic enzymes [8]. In the reversal stage, the resorption processes are coupled to the formation processes. During this coupling, osteoclasts and osteoblasts influence each other by sending coupling signals [9]. Bone lining cells prepare the surface of the resorbed pit for bone formation and give signals for the migration and differentiation of osteoblasts [10]. In the last stage, the formation stage, osteoblast produce new bone. Osteoblasts are mononuclear cells derived from mesenchymal stem cells and lay down the new bone in the resorbed pits. They synthesize the organic matrix, the osteoid, which is then mineralized [11]. Osteoblasts frequently are incorporated into the matrix, where they differentiate into osteocytes – by far the most abundant cell type in bone –, they become lining cells, or they undergo apoptosis. The remodeling process ends with bone lining cells covering the surface [4,7].

Autologous bone grafts

Despite the functional intrinsic healing capacity of bone, the reconstruction of critical-size bone defects, as a consequence of injury or cancer, remains challenging. The ‘golden standard’ to treat these large defects is an autologous bone graft [12]. Such grafts are considered the ‘golden standard’ since it provides an osteoconductive as well as osteoinductive environment due to the presence of both living cells and growth factors [13]. Autologous bone grafts are harvested from the patient, often from the iliac crest, the cranium, or from the symphysis of the chin or ascending ramus in the case of orofacial defects. Such grafts are used in several fields such as dentistry, oral and maxillofacial surgery, and orthopedic surgery, to stimulate the formation of new bone. However, this treatment has its limitations, i.e. limited volume of available tissue graft, extended anesthesia time, additional surgical resources, and donor site morbidity. Also, poor results have been reported [14]. Alternative approaches for bone reconstruction, such as bone tissue engineering, could overcome these limitations

Bone tissue engineering

To stimulate bone formation, bone tissue engineering approaches combine the use of scaffolds, cells, and physical and/or chemical stimuli [5]. Chemical stimuli include bone morphogenetic protein-2 (BMP-2) [15,16], vascular endothelial growth factor (VEGF) [17] and 1,25$(OH)_2$ vitamin D_3 (vitD_3) [18–20]. Scaffolds for bone tissue engineering can be comprised of many materials and preferably degrade at the same speed as the new bone is formed, as scaffolds are not intended to be permanent implants [21]. Ceramics are a class of biomaterials that are often used in bone tissue engineering since the crystals in calcium phosphate (CaP)-containing scaffolds resemble the hydroxyapatite (HA) in natural bone and such materials are osteoconductive [5]. In addition, most forms of CaP dissolve chemically or are resorbed by osteoclasts, making these scaffolds bioresorbable [22]. Subsequently, the CaP can re-precipitate, thereby transforming the scaffold surface, which stimulates the formation of bone [23,24]. Fabrication of CaP-containing scaffolds can be performed in several ways, e.g. gel casting [25,26] foaming [27,28] , freeze casting [29,30] and coatings [31,32]. The achieved fit of scaffolds produced with these fabrication methods is not always precise, leaving lacunae in the area between the scaffolds and the border of the defect. This may impair the bone healing as the cells at the defect border are not in contact with the scaffold, thereby acquiring fewer cues to form bone, which may prolong the healing period. 3D-printing can offer a solution. With 3D-printing, scaffolds designed and fabricated with precise dimensions and a defect-specific fit can be produced, enabling and possibly stimulating bone regeneration.

3D-printing

Techniques that create objects in a layer-by-layer fashion can all be described by the term '3D-printing'. Charles W. Hull described the first 3D-printing technique in 1984 when he invented stereolithography (SLA) [33]. In this technique, solved monomers are photo-polymerized to fabricate a layer. Several 3D-printing techniques are used in tissue engineering, such as SLA, selective laser sintering (SLS), and extrusion-based printing. The properties of the material used and its application dictates which 'printing' technique can best be used. In SLS, a laser is used to sinter particles in a powder bed. This technique is often used in bone tissue engineering since structures with high porosity can be formed. Materials often printed using the SLS technology are HA, polycaprolactone (PCL), and poly (l-lactic acid) (PLLA). This technique is limited by its smallest attainable feature, which depends on the diameter of the laser and the size of the particles in the powder bed. Another downside is the impossibility to incorporate bioactive components, as the laser denatures these bioactive components. More and more research is done on extrusion-based printing, where materials are extruded from a nozzle. This technique allows for the fabrication of 3D scaffolds enhanced with biological components and/or cells because it can be carried out at room temperature, thereby facilitating the opportunity to incorporate biological components and/or cells [34,35]. This technique is also compatible with the fabrication of CaP containing scaffolds. It is often based on the combination of CaP particles with a polymer, for instance, the combination of HA particles combined with polylactic-co-glycolic acid (PLGA) [36]. 3D-printing of CaP containing scaffolds for drug and growth factor delivery is a challenge. By using polymers like PLGA and PCL, often organic solvents, such as chloroform or dichloromethane are needed. However, these can denature the incorporated biological components. A solution can be found in the use of natural binders such as collagen and carrageenan. Collagen is an abundant part of the extracellular matrix, which makes it an interesting component for scaffolds. Carrageenan is derived from red seaweed, which makes it abundantly available and cheap. Furthermore, it resembles the glycosaminoglycans in the extracellular matrix [37].

Most 3D-printed constructs with incorporated biological components designed for bone tissue engineering use BMP-2 [38,39] because, BMP-2 is an FDA approved (for anterior lumbar interbody fusion, acute open tibial fractures, and sinus and alveolar ridge augmentation [40]) osteogenic agent, which promotes bone formation. Unfortunately, when applied in high concentrations it can also have negative side effects such as ectopic bone formation and inflammatory complications [41]. $VitD_3$ is another biological component often used in bone tissue engineering as it can promote the osteogenic differentiation of stem cells by upregulation of alkaline phosphatase (ALP) thus enhancing mineralization [19,20,42]. $VitD_3$ can also influence osteoclastogenesis by inducing RANKL [43]. In this way, scaffolds that release $vitD_3$ may promote osteogenesis while also stimulating remodeling of the formed bone.

Previous research in our group showed that a slow-release system of precipitated CaP with incorporated BMP-2 promotes bone formation and induces ectopic ossification in rats [44,45]. To achieve a better fit in the bone defects in patients we see as a next stage the development of a method to 3D-print a similar system, where biological components are released to enhance the bone formation.

Aim and Outline of this thesis

The main aim of this thesis was to develop a 3D-printing method for calcium phosphate combined with biological components that 1) are capable of being released from the scaffold, and 2) retain their biological activity. This thesis is subdivided into four chapters.

To optimize 3D-printed scaffolds it is essential to know in which time frame biological components should be released from these scaffolds. In **chapter 2**, we investigated which release kinetic of $vitD_3$ is more optimal for osteogenic differentiation of adipose stem cells in vitro. Based on previous research in our group, we hypothesized that a short incubation of 30 minutes would be more optimal for the osteogenic differentiation of adipose stem cells.

Bone tissue engineering constructs are placed in a bony environment. As there are different skeletal sites, the question arises if different bony-surroundings are differentially affected by such constructs. In **chapter 3**, we compared cells derived from human alveolar bone with cells derived from human long bone when studying their osteogenic and osteoclastogenic potential. We hypothesized that due to the higher turn-over of alveolar bone cells, these cells would have an increased osteogenic and osteoclastogenic potential.

In **chapter 4**, we developed a method in which we can 3D-print precipitated calcium phosphate combined with natural binder κ-carrageenan. We investigate whether the incorporation of a biological component is possible and whether it is released from the printed constructs.

In **chapter 5**, we assessed the clinical relevance of 3D-printed constructs consisting of calcium phosphate paste and κ-carrageenan, enhanced with biological component vitD$_{3.}$ The printability, cytotoxicity, and apparent stiffness of the material were assessed. The effects of constructs with and without vitD$_3$ on a human osteosarcoma cell line was also assessed.

Finally, the overall findings of this thesis are discussed in **chapter 6** and summarized in **chapter 7.**

References

1. Kiernan, C.; Knuth, C.; Farrell, E. Endochondral ossification: Recapitulating bone development for bone defect repair. In *Developmental Biology and Musculoskeletal Tissue Engineering: Principles and Applications*; Elsevier, 2018; pp. 125–148 ISBN 9780128114674.
2. Ben-David, D.; Fishman, B.; Rubin, G.; Novak, A.; Laevsky, I.; Kadouri, A.; Nishri Katz, Y.; Burger, O.; Zaretsky, A.; Bor, N.; et al. Autologous cell-coated particles for the treatment of segmental bone defects - A new cell therapy approach. *J. Orthop. Surg. Res.* **2019**, *14*, 1–11.
3. Gugala, Z.; Lindsey, R.W.; Gogolewski, S. New Approaches in the Treatment of Critical-Size Segmental Defects in Long Bones. *Macromol. Symp.* **2007**, *253*, 147–161.
4. Clarke, B. Normal bone anatomy and physiology. *Clin. J. Am. Soc. Nephrol.* 2008, *3 Suppl 3*, S131.
5. Amini, A.R.; Laurencin, C.T.; Nukavarapu, S.P. Bone tissue engineering: recent advances and challenges. *Crit. Rev. Biomed. Eng.* **2012**, *40*, 363–408.
6. Fazzalari, N.L. Bone Fracture and bone fracture repair. In Proceedings of the Osteoporosis International; Springer, 2011; Vol. 22, pp. 2003–2006.
7. HADJIDAKIS, D.J.; ANDROULAKIS, I.I. Bone Remodeling. *Ann. N. Y. Acad. Sci.* **2006**, *1092*, 385–396.
8. Boyce, B.F.; Rosenberg, E.; de Papp, A.E.; Duong, L.T. The osteoclast, bone remodelling and treatment of metabolic bone disease. *Eur. J. Clin. Invest.* 2012, *42*, 1332–1341.
9. Sims, N.A.; Martin, T.J. Osteoclasts Provide Coupling Signals to Osteoblast Lineage Cells Through Multiple Mechanisms. *Annu. Rev. Physiol.* **2020**, *82*, 507–529.
10. Everts, V.; Delaissié, J.M.; Korper, W.; Jansen, D.C.; Tigchelaar-Gutter, W.; Saftig, P.; Beertsen, W. The bone lining cell: Its role in cleaning Howship's lacunae and initiating bone formation. *J. Bone Miner. Res.* **2002**, *17*, 77–90.
11. Sanz-Herrera, J.A.; Reina-Romo, E. Bone Remodeling BT - Encyclopedia of Nanotechnology. In; Bhushan, B., Ed.; Springer Netherlands, 2012; pp. 345–354 ISBN 978-90-481-9751-4.
12. Azi, M.L.; Aprato, A.; Santi, I.; Kfuri Jr., M.; Masse, A.; Joeris, A. Autologous bone graft in the treatment of post-traumatic bone defects: a systematic review and meta-analysis. *BMC Musculoskelet. Disord.* **2016**, *17*, 465.
13. Myeroff, C.; Archdeacon, M. Autogenous Bone Graft: Donor Sites and Techniques. *J. Bone Jt. Surgery-American Vol.* **2011**, *93*, 2227–2236.
14. Keating, J.F.; Simpson, A.H.R.W.; Robinson, C.M. The management of fractures with bone loss. *J. Bone Jt. Surg. - Ser. B* 2005, *87*, 142–150.
15. Kim, B.S.; Choi, M.K.; Yoon, J.H.; Lee, J. Evaluation of bone regeneration with biphasic calcium phosphate substitute implanted with bone morphogenetic protein 2 and mesenchymal stem cells in a rabbit calvarial defect model. *Oral Surg. Oral Med. Oral Pathol. Oral Radiol.* **2015**, *120*, 2–9.

16. Li, C.; Vepari, C.; Jin, H.J.; Kim, H.J.; Kaplan, D.L. Electrospun silk-BMP-2 scaffolds for bone tissue engineering. *Biomaterials* **2006**, *27*, 3115–3124.
17. Des Rieux, A.; Ucakar, B.; Mupendwa, B.P.K.; Colau, D.; Feron, O.; Carmeliet, P.; Préat, V. 3D systems delivering VEGF to promote angiogenesis for tissue engineering. *J. Control. Release* **2011**, *150*, 272–278.
18. Vu, A.A.; Bose, S. Vitamin D3 Release from Traditionally and Additively Manufactured Tricalcium Phosphate Bone Tissue Engineering Scaffolds. *Ann. Biomed. Eng.* **2020**, *48*, 1025–1033.
19. Song, I.; Kim, B.S.; Kim, C.S.; Im, G. Il Effects of BMP-2 and vitamin D3 on the osteogenic differentiation of adipose stem cells. *Biochem. Biophys. Res. Commun.* **2011**, *408*, 126–131.
20. Liu, P.; Oyajobi, B.O.; Russell, R.G.G.; Scutt, A. Regulation of Osteogenic Differentiation of Human Bone Marrow Stromal Cells: Interaction Between Transforming Growth Factor-β and 1,25(OH)2 Vitamin D3In Vitro. *Calcif. Tissue Int.* **1999**, *65*, 173–180.
21. O'Brien, F.J. Biomaterials & scaffolds for tissue engineering. *Mater. Today* 2011, *14*, 88–95.
22. Ducheyne, P.; Radin, S.; King, L. The effect of calcium phosphate ceramic composition and structure on in vitro behavior. I. Dissolution. *J. Biomed. Mater. Res.* **1993**, *27*, 25–34.
23. Radin, S.R.; Ducheyne, P. The effect of calcium phosphate ceramic composition and structure on in vitro behavior. II. Precipitation. *J. Biomed. Mater. Res.* **1993**, *27*, 35–45.
24. Barrère, F.; van Blitterswijk, C.A.; de Groot, K. Bone regeneration: molecular and cellular interactions with calcium phosphate ceramics. *Int. J. Nanomedicine* **2006**, *1*, 317–332.
25. Potoczek, M.; Zima, A.; Paszkiewicz, Z.; Ślósarczyk, A. Manufacturing of highly porous calcium phosphate bioceramics via gel-casting using agarose. *Ceram. Int.* **2009**, *35*, 2249–2254.
26. Sánchez-Salcedo, S.; Werner, J.; Vallet-Regí, M. Hierarchical pore structure of calcium phosphate scaffolds by a combination of gel-casting and multiple tape-casting methods. *Acta Biomater.* **2008**, *4*, 913–922.
27. Montufar, E.B.; Vojtova, L.; Celko, L.; Ginebra, M.P. Calcium phosphate foams: Potential scaffolds for bone tissue modeling in three dimensions. In *Methods in Molecular Biology*; Humana Press Inc., 2017; Vol. 1612, pp. 79–94.
28. Ginebra, M.P.; Montufar, E.B. Injectable biomedical foams for bone regeneration. In *Biomedical Foams for Tissue Engineering Applications*; Elsevier Ltd., 2014; pp. 281–312 ISBN 9780857096968.
29. Deville, S.; Saiz, E.; Tomsia, A.P. Freeze casting of hydroxyapatite scaffolds for bone tissue engineering. *Biomaterials* **2006**, *27*, 5480–5489.
30. Shazni, Z.A.; Mariatti, M.; Nurazreena, A.; Razak, K.A. Properties of Calcium Phosphate Scaffolds Produced by Freeze-Casting. *Procedia Chem.* **2016**, *19*, 174–180.
31. Liu, Y.; Schouten, C.; Boerman, O.; Wu, G.; Jansen, J.A.; Hunziker, E.B. The kinetics and mechanism of bone morphogenetic protein 2 release from calcium phosphate-based implant-coatings. *J. Biomed. Mater. Res. Part A* **2018**, *106*, 2363–2371.
32. Habibovic, P.; Barrère, F.; Blitterswijk, C.A.; Groot, K.; Layrolle, P. Biomimetic Hydroxyapatite Coating on Metal Implants. *J. Am. Ceram. Soc.* **2004**, *85*, 517–522.
33. Hull, C.W. Apparatus for production of three-dimensional objects by stereolithography 1986.

34. Bae, E.-B.; Park, K.-H.; Shim, J.-H.; Chung, H.-Y.; Choi, J.-W.; Lee, J.-J.; Kim, C.-H.; Jeon, H.-J.; Kang, S.-S.; Huh, J.-B. Efficacy of rhBMP-2 Loaded PCL/β-TCP/bdECM Scaffold Fabricated by 3D Printing Technology on Bone Regeneration. *Biomed Res. Int.* **2018**, *2018*, 2876135.
35. Zhu, W.; Cui, H.; Boualam, B.; Masood, F.; Flynn, E.; Rao, R.D.; Zhang, Z.Y.; Zhang, L.G. 3D bioprinting mesenchymal stem cell-laden construct with core-shell nanospheres for cartilage tissue engineering. *Nanotechnology* **2018**, *29*.
36. Huang, Y.H.; Jakus, A.E.; Jordan, S.W.; Dumanian, Z.; Parker, K.; Zhao, L.; Patel, P.K.; Shah, R.N. Three-Dimensionally Printed Hyperelastic Bone Scaffolds Accelerate Bone Regeneration in Critical-Size Calvarial Bone Defects. *Plast. Reconstr. Surg.* **2019**, *143*, 1397–1407.
37. Vignesh, S.; Gopalakrishnan, A.; M.R, P.; Nair, S. V; Jayakumar, R.; Mony, U. Fabrication of micropatterned alginate-gelatin and k-carrageenan hydrogels of defined shapes using simple wax mould method as a platform for stem cell/induced Pluripotent Stem Cells (iPSC) culture. *Int. J. Biol. Macromol.* **2018**, *112*, 737–744.
38. Huang, K.H.; Lin, Y.H.; Shie, M.Y.; Lin, C.P. Effects of bone morphogenic protein-2 loaded on the 3D-printed MesoCS scaffolds. *J. Formos. Med. Assoc.* **2018**, *117*, 879–887.
39. Koons, G.L.; Mikos, A.G. Progress in three-dimensional printing with growth factors. *J. Control. Release* **2019**, *295*, 50–59.
40. Ramly, E.P.; Alfonso, A.R.; Kantar, R.S.; Wang, M.M.; Siso, J.R.D.; Ibrahim, A.; Coelho, P.G.; Flores, R.L. Safety and Efficacy of Recombinant Human Bone Morphogenetic Protein-2 (rhBMP-2) in Craniofacial Surgery. *Plast. Reconstr. Surg. - Glob. Open* **2019**, *7*, e2347.
41. James, A.W.; Lachaud, G.; Shen, J.; Asatrian, G.; Nguyen, V.; Zhang, X.; Ting, K.; Soo, C. A Review of the Clinical Side Effects of Bone Morphogenetic Protein-2.
42. Lou, Y.-R.; Toh, T.C.; Tee, Y.H.; Yu, H. 25-Hydroxyvitamin D3 induces osteogenic differentiation of human mesenchymal stem cells. *Sci. Rep.* **2017**, *7*, 42816.
43. Haussler, M.R.; Whitfield, G.K.; Kaneko, I.; Haussler, C.A.; Hsieh, D.; Hsieh, J.-C.; Jurutka, P.W. Molecular Mechanisms of Vitamin D Action. *Calcif. Tissue Int.* **2013**, *92*, 77–98.
44. Liu, Y.; De Groot, K.; Hunziker, E.B. BMP-2 liberated from biomimetic implant coatings induces and sustains direct ossification in an ectopic rat model. *Bone* **2005**, *36*, 745–757.
45. Zheng, Y.; Wu, G.; Liu, T.; Liu, Y.; Wismeijer, D.; Liu, Y. A Novel BMP2-Coprecipitated, Layer-by-Layer Assembled Biomimetic Calcium Phosphate Particle: A Biodegradable and Highly Efficient Osteoinducer. *Clin. Implant Dent. Relat. Res.* **2014**, *16*, 643–654.

2

Burst, Short, and Sustained Vitamin D_3 Applications Differentially Affect Osteogenic Differentiation of Human Adipose Stem Cells

International journal of molecular sciences (2020)

Abstract

Incorporation of 1,25$(OH)_2$ vitamin D_3 (vitD_3) into tissue-engineered scaffolds could aid the healing of critical-sized bone defects. We hypothesize that shorter applications of vitD_3 lead to more osteogenic differentiation of mesenchymal stem cells (MSCs) than a sustained application. To test this, release from a scaffold was mimicked by exposing MSCs to exactly controlled vitD_3 regimens. Human adipose stem cells (hASCs) were seeded onto calcium phosphate particles, cultured for 20 days, and treated with 124 ng vitD_3, either provided during 30 min before seeding ([200 nM]), during the first two days ([100 nM]), or during 20 days ([10 nM]). Alternatively, hASCs were treated for two days with 6.2 ng vitD_3 ([10 nM]). hASCs attached to the calcium phosphate particles and were viable (~75%). Cell number was not affected by the various vitD_3 applications. VitD_3 (124 ng) applied over 20 days increased cellular alkaline phosphatase activity at Days 7 and 20, reduced expression of the early osteogenic marker *RUNX2* at Day 20, and strongly upregulated expression of the vitD_3 inactivating enzyme *CYP24*. VitD_3 (124 ng) also reduced *RUNX2* and increased *CYP24* applied at [100 nM] for two days, but not at [200 nM] for 30 min. These results show that the 20-day application of vitD_3 has more effect on hASCs than the same total amount applied in a shorter time span.

Introduction

Bone defects can occur as a consequence of birth defects, injury, cancer, or inflammation. Despite the good intrinsic healing capacity of bone, the reconstruction of critical size defects remains challenging. Currently, the "golden standard" for critical size bone defects is the use of autologous bone grafts [1]. These grafts are taken from the patient, often from the iliac crest, or in the case of orofacial defects from the symphysis of the chin or ascending ramus. Autologous bone is generally still considered the "gold standard" since it provides both an osteogenic and osteoconductive environment, due to the presence of live cells and the cocktail of growth factors present in the matrix [2]. However, this method suffers from two major drawbacks: donor site morbidity and lack of available tissue [3]. These drawbacks could be overcome by alternative approaches for bone reconstruction, such as methods employing principles of bone tissue engineering.

To regenerate bone, bone tissue engineering combines the use of biomaterials, e.g., polymer-based or calcium phosphate-based materials, cells, and physical, mechanical, and/or chemical stimuli [4], such as bone morphogenetic protein-2 (BMP-2) and vascular endothelial growth factor (VEGF) [5,6]. Another biological component used as a chemical stimulus in bone regeneration is $1,25(OH)_2$ vitamin D_3 (vitD_3), which promotes osteogenic differentiation of bone marrow-derived mesenchymal stem cells (BMSCs) and hASCs by upregulation of alkaline phosphatase (ALP) and enhancing mineralization [7–9].

For the delivery of biological components, for example, BMP-2 and vitD_3, multiple delivery methods can be considered. Here, we focus on the three main delivery methods. First, an injection of bioactive factors into a carrier or injured site, or adsorption to a surface. This leads to a burst release where the biological component is depleted after a couple of days, as has been described for BMP-2 [10]. Supra-physiological concentrations are often used in this case, which may lead to negative effects such as a growth-inhibition when vitD_3 is used [11,12] or ectopic bone formation for BMP-2 [13]. Furthermore, in the case of expensive biological components such as BMP-2, this method can become costly. As a second method of release, avoiding supra-physiological concentrations, biomaterials can be used as release vehicles allowing a more sustained release [14–16]. A drawback of longer stimulation with biological components is that it can lead to the formation of inhibitors. For example, BMP-2 induces the expression of its antagonist noggin [17,18] and vitD_3 induces the expression of Cytochrome P450 family 24 subfamily A member 1 (CYP24a1), an enzyme that inactivates vitD_3 [19,20]. In addition, in natural bone development or healing, cytokines, growth factors, or extracellular matrix components are usually transiently expressed [21,22]. Sustained expression of these factors hinders the progression of healing or development [23]. The third method is a short stimulation of stem cells with a bioactive factor (30 min or less) of cells, after which the biological component is washed away [24]. Mokhtari-Jafari et al. showed that such a short stimulation with vitD$_3$ can lead to the differentiation of adipose stem cells into the osteogenic lineage [25]. Short incubation (15 or 30 min) with growth factors or other bioactive compounds suffices to induce long-lasting (weeks) effects on hASCs in cell culture [23,24]. In some cases, these effects even become more pronounced over time. To give an example, short incubation of BMP-2 triggers expression of the late marker osteocalcin in hASCs after 21 days of culture, but not at earlier time points [23]. Short stimulation can be used in a one-step surgery where the cells are harvested, stimulated shortly, and combined with a biomaterial serving as a scaffold, which can then be implanted, in one procedure. In this way, no exogenous ligands are placed into the body, avoiding possible side effects.

To shed light on the ongoing discussion whether short, burst or sustained release is the best method for the application of biological factors for bone tissue engineering, we designed an experiment where the in vivo situation was mimicked in a cell culture environment of hASCs seeded on BCP particles, allowing precise manipulation of doses and timing of application of a biologically active factor. We used vitD$_3$, since we successfully used this factor to stimulate osteogenic differentiation of hASCs in conventional 2D cultures. Our aim was to investigate which application of vitD$_3$, i.e., mimicking short exposure of cells ([200 nM] for 30 min), burst release from scaffolds ([100 nM] for two days), or sustained release from scaffolds ([10 nM] for 20 days), leads to optimal osteogenic differentiation of hASCs (Figure 1). We hypothesized that shorter applications of vitD$_3$ are more beneficial for osteogenic differentiation than a sustained application because longer applications may lead to the formation of inhibitors.

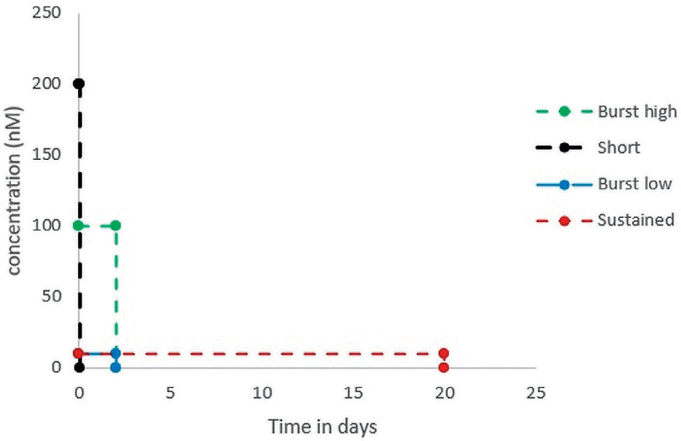

Figure 1. Schematic representation of the different vitamin D_3 applications**.** A total of 124 ng of vitD_3 was added for either 30 min before seeding at a concentration of 200 nM (Short), for two days at a concentration of 100 nM (Burst high) to mimic a burst release, or for 20 days with a concentration of 10 nM (Sustained) to mimic a sustained release. Alternatively, cells were exposed to 10 nM vitD_3 for two days (Burst low).

Materials and Methods

The release of vitD_3 from scaffolds was mimicked by exposing the hASCs seeded on a 3D biomaterial to controlled vitD_3 applications, and the viability, proliferation, and differentiation were measured.

Calcium Phosphate Particles

Clinically relevant, biphasic calcium phosphate (BCP, Straumann® BoneCeramic 60/40, Institut Straumann AG, Basel, Switzerland) particles with a particle size of 500–1000 µm and a porosity of 90% were used to mimic calcium phosphate-containing scaffolds in vitro.

Isolation of hASCs

For the isolation of hASCs, subcutaneous adipose tissue from the abdominal wall was harvested from donors who underwent plastic surgery at the Tergooi Hospital Hilversum, the Netherlands. The study was conducted in accordance with the Declaration of Helsinki and the protocol was approved by the Ethical Review Board of the VU Medical Center, Amsterdam, the Netherlands (number 2016/105). Informed consent was obtained from all donors. Four of the donors were female and between 33 and 56 years of age. Information on the fifth donor is unavailable.

To isolate hASCS, adipose tissue was cut into pieces and digested enzymatically with 0.1% collagenase A (Roche Diagnostics GmbH, Mannheim, Germany) which was added to phosphate-buffered saline (PBS; Thermo Fisher Scientific, Waltham, MA, USA) containing 1% bovine serum albumin (Roche Diagnostics GmbH) under stirring conditions for 45 min at 37 °C. This was followed by a Ficoll® density-centrifugation step (Lymphoprep; 1000× *g*, 20 min, – = 1.077 g/mL Ficoll®, osmolarity 280 ± 15 mOsm; Axis-Shield, Oslo, Norway) and the cell-containing interface was harvested and resuspended in Dulbecco's modified Eagle's medium (Life Technologies Europe BV, Bleiswijk, the Netherlands). hASCS were counted and stored in liquid nitrogen [24]. All experiments were conducted using the same five donors, but sometimes data from only four donors were available.

Platelet Lysate

Bloodbank Sanquin (Sanquin, Amsterdam, the Netherlands) provided pooled platelet products from multiple donors, which contained approximately 1×10^9 platelets per mL PAS-E/plasma (ratio 65:35) [47]. Platelets were lysed by a temperature shock at –80 °C to obtain platelet lysate (PL). Before use, PL was thawed and centrifuged at 600× *g* for 10 min to remove the remaining platelet fragments. Finally, the supernatant was added to the medium at 5% (*v/v*) for the culturing of cells and 2% (*v/v*) for the experiments [48]. PL was used as a human cell culture supplement rather than bovine serum.

Culture and Treatment of hASCs

hASCs (1×10^5) from five independent donors were seeded, separately, on top of 20 ± 1 mg BCP particles in 2 mL Eppendorf tubes. Before seeding, the BCP particles were soaked in 500 µL of Minimum Essential Medium ALPHA (α-MEM; Thermo Fisher Scientific) complemented with 1% Antibiotic Antimycotic Solution 100´ (Sigma, St Louis, MO, USA), 10 IU/mL heparin (Leo Pharma, Amsterdam, the Netherlands), 2% PL, and 50 µM ascorbic acid-2-phosphate (vitamin C; Sigma) for 30 min. For the short stimulation, the hASCs were treated with 124 ng of vitD$_3$ for 30 min ([200 nM]), before seeding. Then, cells (all treatments) were allowed to attach to the BCP particles for 1 h at 37 °C and transferred to 12 well plates with transwell inserts (pore size 3.0 µm; Greiner Bio-one, Alphen aan de Rijn, the Netherlands) with 0.5 mL of medium in the insert and 1 mL of medium in the well. For Burst and Sustained-release this medium was supplemented with the total amount of 124 ng of vitD$_3$ (Sigma, stock: 30 µM in 100% ethanol, stored at -80 °C, in the absence of light) per well. Control cultures contained the same concentration of alcohol as in the sustained condition (3.35 µL 100% alcohol per 10 mL of medium). The vitD$_3$ treatment was provided either over the first two days (Burst-release high: [100 nM]) or over the total culture period of 20 days (sustained-release: [10 nM]). In the condition "Burst-release low" (Burst low), the hASCs were treated for two days after seeding with 6.2 ng vitD_3 ([10 nM]) per day. A schematic representation of the applications is depicted in Figure 1. The medium of all conditions was refreshed daily.

Attachment and Viability

Attachment and viability were assessed using fluorescent microscopy. After two days, inserts were emptied, by cutting the membrane of the insert, in a clean 12-well plate. The medium was removed and the BCP particles with cells were washed once with PBS and incubated for 10 min with 5´ live/dead staining (Abcam, Cambridge, UK) in PBS. The dye was removed and 100 µL of PBS was added to the samples. The staining was analyzed with a fluorescence microscope (Leica Microsystems, Wetzlar, Germany) with a Nikon camera (Nikon, Tokyo, Japan). Brightness and contrast were adapted to enhance the visibility of the cells with Adobe Photoshop® 19.1.1 (Adobe Systems, San Jose, CA, USA). The number of live (green) and dead (red) cells were manually counted, but due to the difficulty of discerning individual cells, only qualitative assessments were made.

Metabolic Activity

The metabolic activity of hASCs was measured with AlamarBlue™ Cell viability reagent (Invitrogen, Carlsbad, CA, USA). Metabolic activity was measured on Days 2, 7, and 20. Inserts with BCP particles were placed in a new set of wells and incubated for 4 h at 37 °C with medium containing 10% AlamarBlue reagent (500 µL in the well and 500 µL in the insert). After incubation, the medium in the insert was mixed with the medium in the well. From each sample, 100 µL (in duplicate) were transferred to a black 96-well plate and fluorescence was measured at 530–560 nm with Synergy HT® spectrophotometer (BioTek Instruments, Winooski, VT, USA). Medium without cells and with 10% AlamarBlue reagent was autoclaved to fully reduce the AlamarBlue reagent and used as a positive control. Samples are presented as a percentage of the positive control.

Alkaline Phosphatase (ALP)

hASCs were cultured on BCP particles for 7 and 20 days with the different vitD_3 applications or without vitD_3. Cells were washed with PBS and lysed with 300 µL Milli-Q water and frozen at –20 °C for storage. After three freeze-thaw cycles, samples were collected by scraping. ALP was measured according to the method described by Lowry [49] using 4-nitrophenyl phosphate disodium salt at pH 10.3 as a substrate for ALP. Absorbance was measured at 405 nm with the Synergy HT® spectrophotometer. To correct for cell number, protein levels were measured using a bicinchoninic acid (BCA) Protein Assay Kit according to the manufacturers' instructions (Pierce, Rockford, IL, USA) and absorbance was read at 540 nm with Synergy HT® spectrophotometer. ALP was expressed as nmol/µg protein.

Quantitative Polymerase CHAIN reaction (qPCR)

After 7 and 20 days of culture, the inserts with the BCP particles were transferred to a clean 12-well plate. Total RNA was isolated with TRIzol® reagent (Invitrogen) following the manufacturer's protocol. The concentration and 260/280 ratio of RNA were measured using a Synergy HT® spectrophotometer and 750 ng RNA was reverse-transcribed to cDNA using RevertAid™ First Strand cDNA Synthesis Kit 1612 (Fermentas, St. Leon-Rot, Germany) according to the manufacturer's protocol. For the qPCR reaction, cDNA was diluted 5´ and 1 µL was used, together with 3 µL PCR-H_2O, 0.5 µL (20 µM) forward primer, 0.5 µL (20 µM) reverse primer, and 5 µL LightCycler® 480 SYBR Green I Mastermix (Roche Diagnostics). All measurements with a Ct value higher than 36 were considered unreliable and discarded. The values of all genes were normalized to hypoxanthine phosphoribosyltransferase (HPRT) following the comparative cycle threshold (C_t) method and presented as the mean relative fold expression ($2^{-\Delta Ct}$). All primer sequences are listed in Table 1.

Table 1. *Primer sequences.*

Gene (Human)	Forward Sequence	Reverse Sequence
KI67	*5′ CGAGACGCCTGGTTACTATCAA 3′*	*5′ GGATACGGATGTCACATTCAATACC 3′*
RUNX2	*5′ CCAGAAGGCACAGACAGAAGCT 3'*	*5' AGGAATGCGCCCTAAATCACT 3′*
COL1	*5′ GCATGGGCAGAGGTATAATG 3′*	*5′ GGTCCTTTGGGTCCTACAA 3′*
BAX	*5′ TGTCGCCCTTTTCTACTTTGC 3′*	*5′ CTGATCAGTTCCGGCACCTT 3′*
BCL-2	*5′ AGAGCCTTGGATCCAGGAGAA 3′*	*5′ GCTGCATTGTTCCCATAGAGTTC 3′*
VDR	*5′ GACACAGCCTGGAGCTGAT 3′*	*5′ CAGGTCGGCTAGCTTCTGGA 3′*
CYP24a1	*5′ CAAACCGTGGAAGGCCTATC 3′*	*5′ AGTCTTCCCCTTCCAGGATCA 3′*
HPRT	*5′ GCTGACCTGCTGGATTACAT 3′*	*5′ CTTGCGACCTTGACCATCT 3′*
OPN	*5′ TTCCAAGTAAGTCCAACGAAAG 3′*	*5′ GTGACCAGTTCATCAGATTCAT 3′*
PPAR- γ	*5′ CGACCAGCTGAATCCAGAGT 3′*	*5′ GATGCGGATGGCCACCTCTT 3′*

Statistical Analysis

Data were obtained from cultures of five independent donors (*n* = 5), performed in duplicate, and are presented as mean ± standard deviation (SD). Since the *n* was small, and the data are not normally distributed, the data were transformed with a log transformation. A paired t-test was conducted to test for statistical differences in gene expression levels between control and vitD_3 applications per time point and treatment, for results depicted as single point graphs. Statistical comparisons of the treatment groups (short, burst high, burst low, and sustained) in Alamar blue, protein content, ALP activity, and average gene expression levels were performed using repeated-measures ANOVA with Tukey's post hoc test. *P* values of <0.05 were considered significantly different. Analyses were performed using GraphPad Prism 5.0 (GraphPad Software, San Diego, CA, USA).

Results

hASCs Attached to BCP Particles and Survived, in the Presence and Absence of Vitamin D_3

Before identifying the optimal vitD_3 application, it needs to be established whether the hASCs are attached to the BCP particles. In Figure 2, representative micrographs for samples without vitD_3 (Figure 2A, B) and with vitD_3 (Figure 2C, D) are shown. The micrographs with vitD_3 are from samples with the short application (200 nM: 30 min) of vit$D_{3.}$ These micrographs are representative for all vitD_3-treated samples. By manual counting of green and red cells, it was determined that a comparable number of hASCs had attached to the BCP particles at Day 2, regardless of vitD_3 treatment. In all vitD_3 treated groups, as well as in the control group, the percentage of viable (green) cells was approximately 75%. No exact quantification is given per group, as this would misrepresent the reliability with which these numbers can be established, since it is extremely difficult to reliably visualize and discern individual cells in 3D seeded particles (Figure 2A–D).

Apoptosis induced by vitD_3 was measured by gene expression of pro-apoptotic protein B-cell lymphoma protein 2 associated X (*BAX*) and its inhibitor B-cell lymphoma 2 (*BCL-2*) (Figure 2E, F). The balance between *BCL-2* and *BAX* protein expression strongly affects apoptosis in bone cells, whereby an excess of *BCL-2* protects against apoptosis. In the current paper, *BAX* gene expression is therefore considered a pro-apoptotic marker, whereas enhanced BCL-2 gene expression is seen as a marker correlated with inhibition of apoptosis. At Day 7, Sustained application significantly increased the relative expression of *BAX* compared to the control and at Day 20. Burst high application of vitD_3 significantly increased the expression of *BAX* at Day 20 compared to the control (Figure 2E). All other applications did not affect the gene expression of this pro-apoptotic factor. Average *BAX* expression did not significantly differ between vitD_3-treated groups (Figure 2F). None of the vitD_3 treatments had an effect on the expression of *BCL-2* (Figure 2G). In general, the expression of *BCL-2* appeared to be upregulated at later time points compared to earlier time points within the same vitD_3 treatment group, but this was not statistically tested (Figure 2G).

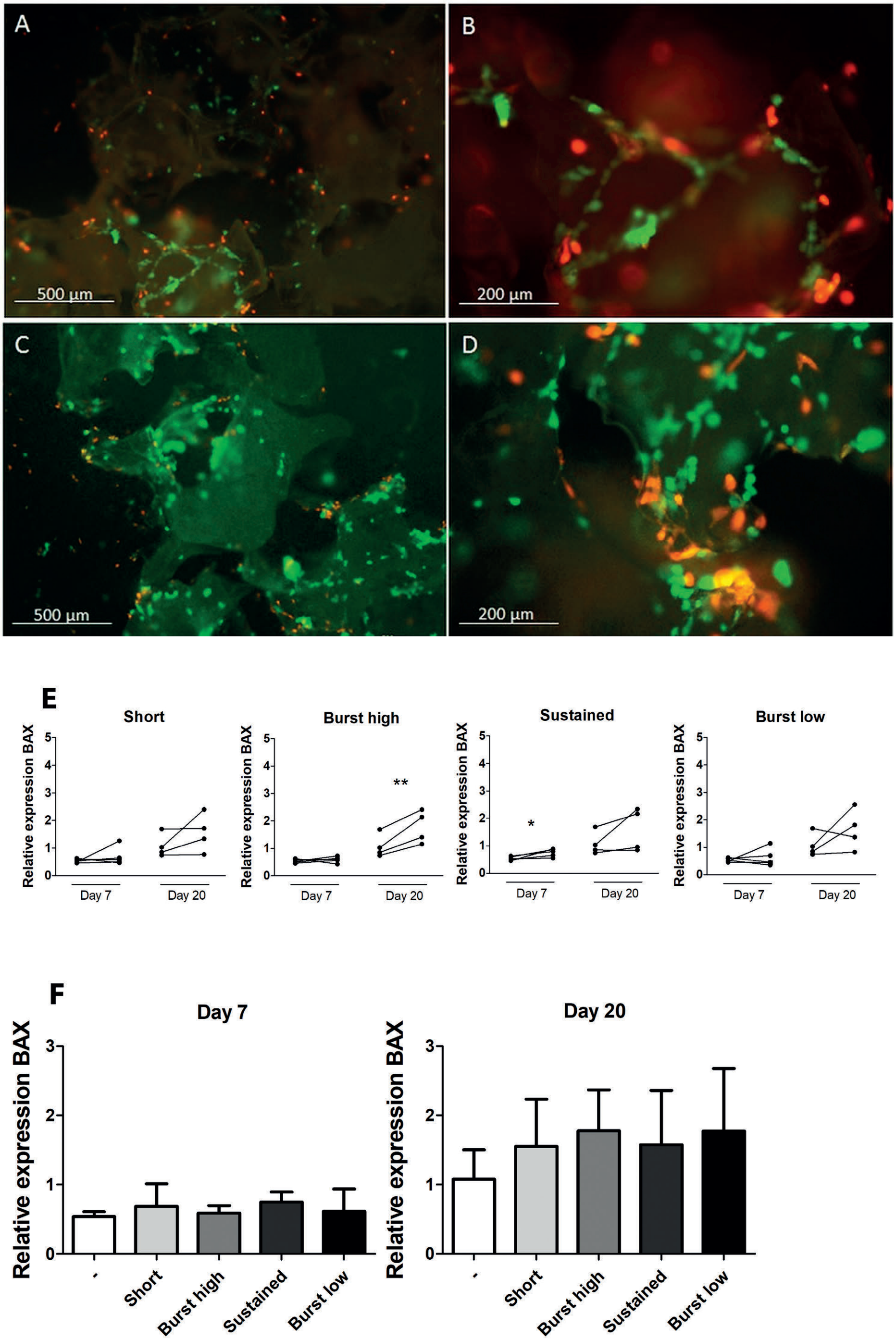
A
500 µm
B
200 µm
C
500 µm
D
200 µm
E
Short
Burst high
**
Sustained
*
Burst low
Relative expression BAX
0
1
2
3
4
5
Day 7
Day 20
F
Day 7
Day 20
Relative expression BAX
0
1
2
3
-
Short
Burst high
Sustained
Burst low

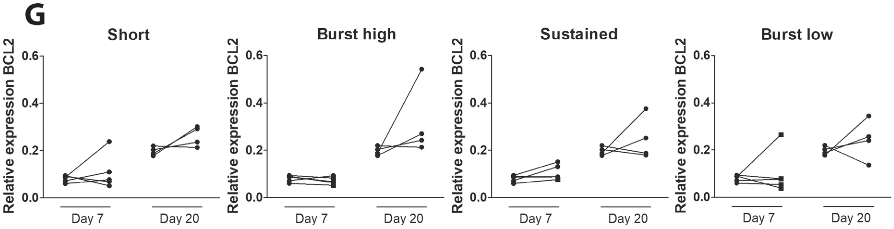

Figure 2. Effect of vitamin D_3 on the viability of hASCs on BCP particles. Fluorescence microscopy of live/dead staining shows the attachment and viability of hASCs on Day 2 after seeding. Living cells are stained green, while the red-stained cells are dead/dying. (**A**, **B**) Sample without vitD_3 treatment, where (B) is a higher magnification of the same sample as (A). (**C**, **D**) A representative sample with vitD_3 treatment (highest concentration, i.e., [200 nM]) is depicted. Both (C, D) were made in the same sample. (**E**) Gene expression of pro-apoptotic marker *BAX* measured at Days 7 and 20. Gene expression in controls (left) and vitD_3-treated cultures (right) of the same donor are connected by a line. (**F**) Relative expression of *BAX* at Days 7 and 20. Data represent mean + SD of four or five independent donors. (**G**) Gene expression of anti-apoptotic marker *BCL-2* measured at Days 7 and 20. Gene expression in controls (left) and vitD_3-treated cultures (right) of the same donor are connected by a line. * Significant effect ($p < 0.05$) of vitD_3 compared to the control at one-time point. ** $p < 0.01$. All gene expression levels were normalized to *HPRT*.

Vitamin D_3 Did not Affect Proliferation of hASCS on BCP Particles

Having established that hASCs indeed attached to BCP particles and were viable in the early stage (Figure 2), we next assessed the effect of vitD_3 on hASC proliferation. Alamar blue assay, gene expression of *Ki67*, and total protein levels were used as measures of cell number. Over time, between Days 2 and 20 the percentage of conversed Alamar blue, used as an indirect measure of cell number, increased on average 4.7-fold in all groups (Figure 3A). Compared to the control, VitD_3 did not significantly affect the percentage of conversed Alamar blue for any mode of application, at any time point tested. The effect of the different vitD_3-treatment kinetics on cell proliferation was also assessed by quantification of gene expression of the cell proliferation marker *Ki67*, which was not affected by vitD_3 treatment (Figure 3B). For confirmation of cell number, total protein per condition was analyzed. In line with earlier results, total protein was comparable between the groups treated with and without vitD_3 at Days 7 and 20 (Figure 3C). Between Days 7 and 20, total protein seemed to increase similarly for all groups, but this was not statistically tested.

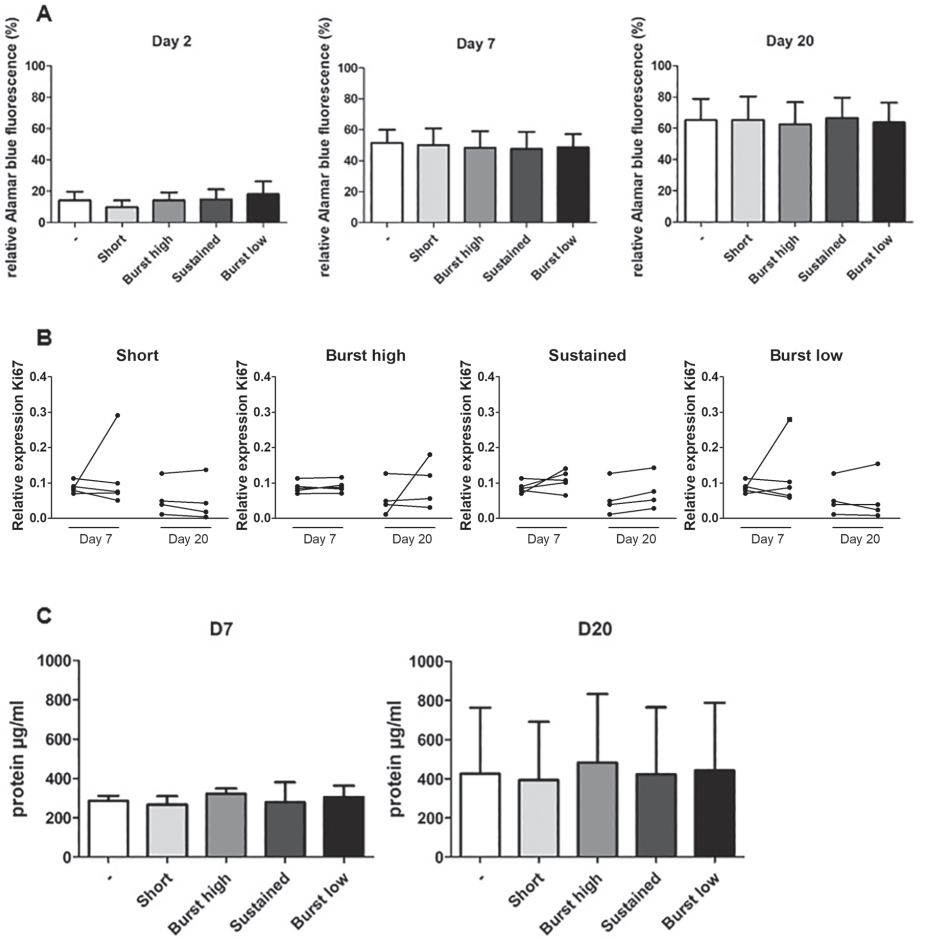

Figure 3. Effect of vitamin D_3 on proliferation and protein content of hASCs. hASCs were subjected to the various vitD_3 treatment modalities and Alamar blue was measured at Days 2, 7, and 20; the gene expression of *Ki67* was measured at Days 7 and 20, and total protein content was measured at Days 7 and 20. (**A**) VitD_3 treatment did not affect Alamar blue measurement between any of the groups, at any time point measured. (**B**) Gene expression of proliferation marker *Ki67* did not significantly differ between vitD_3-treated and control groups. Gene expression in controls (left) and vitD_3-treated cultures (right) of the same donor are connected by a line. (**C**) Total protein content was similar between all vitD_3-treated groups on Day 7, as well as on Day 20. Data represent four or five independent donors (mean + SD). Gene expression data were normalized to *HPRT*.

Regime Mimicking Sustained Release of Vitamin D_3 Affects ALP and RUNX2

The activity of ALP is an indication of early differentiation of the hASCs. ALP activity was measured on Days 7 and 20 and was divided by total protein (µg) levels to correct for approximate cell number. Sustained application of vitD_3 significantly increased cellular ALP (Figure 4A). At Day 7, Sustained application increased the activity of ALP on average by 2.7-fold, compared to all the other conditions. On Day 20, this increase was 6.0-fold. Gene expression of runt-related transcription factor 2 (*RUNX2*), osteopontin (*OPN*), and collagen type 1a (*COL1a*) were measured as positive osteogenic differentiation markers. Adipogenic marker peroxisome proliferator-activated receptor gamma (*PPAR-γ*) was quantified as a negative marker for osteogenic differentiation. *RUNX2* is an early differentiation marker which in general appeared to be upregulated at Day 20 compared to Day 7 within the same vitD_3 treatment group, but this was not statistically tested. The Burst high application at Days 7 and 20 and the Sustained vitD_3 application at Day 20 significantly downregulated the expression of *RUNX2* compared to their (paired) untreated controls (Figure 4B). When the rather variable *RUNX2* expression levels were expressed as average, no significant difference in gene expression between the different vitD_3-treated groups, and the control was found (Figure 4C). VitD_3 did not significantly affect *OPN*, *COL1a*, or *PPAR-γ* expression at any concentration, at any time point (Figure S1).

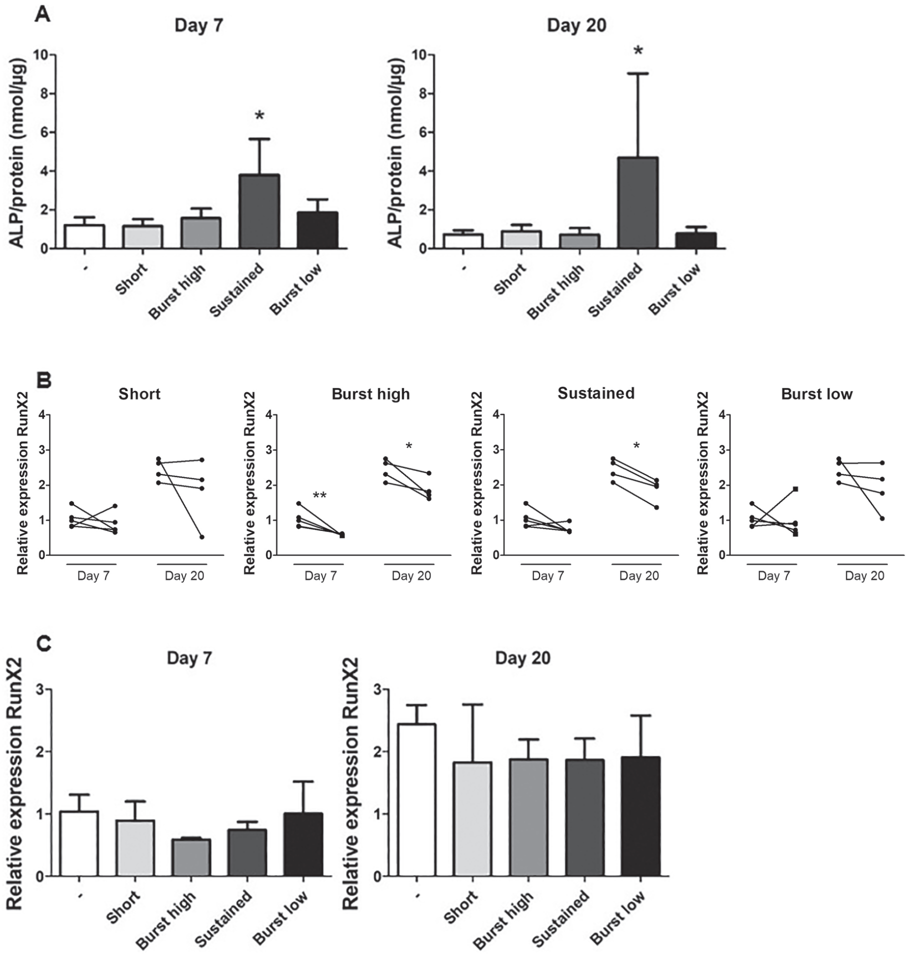

Figure 4. Effect of vitamin D_3 on ALP activity and *RUNX2* expression. (**A**) Cellular ALP, as a measure for early osteogenic differentiation, was measured on Days 7 and 20. Sustained-release significantly increased ALP activity compared to all other groups at both time points. (**B**) *RUNX2* expression, in general, seemed to be higher at Day 20 compared to Day 7, although no statistical comparison was made. VitD_3 seemed to reduce *RUNX2* expression in general. This effect of vitD_3 was significant for burst high at Days 7 and 2 and sustained application at Day 20. Gene expression in controls (left) and vitD_3-treated cultures (right) of the same donor are connected by a line. (**C**) Average relative expression of *RUNX2* at Days 7 and 20. Data represent four or five independent donors (mean + SD). All gene expression levels were normalized to *HPRT*. * Significant difference ($p < 0.05$) between control and vitD_3 treatment at the same time point ** $p < 0.01$.

Sustained Application of Vitamin D_3 Highly Upregulates CYP24a1 Expression

To analyze whether vitD_3 stimulates a feedback loop causing insensitivity of the cells for vitD_3 and inactivation of the vitD_3 itself [26], the expression of vitamin D receptor (*VDR*) and *CYP24a1* was measured. *VDR* was expressed at low levels on Day 7, regardless of the addition of vitD_3. At Day 20, vitD_3 seemed to have an overall stimulating, rather than inhibiting, effect on the expression of *VDR*. The stimulating effect of vitD_3 on

VDR expression by hASCs was significant for Sustained and Burst low applications (Figure 5A). Average expression levels of *VDR* did not significantly differ between groups (Figure 5B). *CYP24a1* converts the active form of vitD_3 in Calcitroic acid, an inactive vitamin D metabolite [26]. All vitD_3 applications, except for the condition “Short”, enhanced the expression of *CYP24a1* compared to the control condition at Day 7. At Day 20, Sustained and Burst low significantly increased *CYP24a1* compared to the control (Figure 5C). At Days 7 and 20 Sustained vitD_3 application strongly upregulated average expression levels of *CYP24a1* compared to all other groups (Figure 5D).

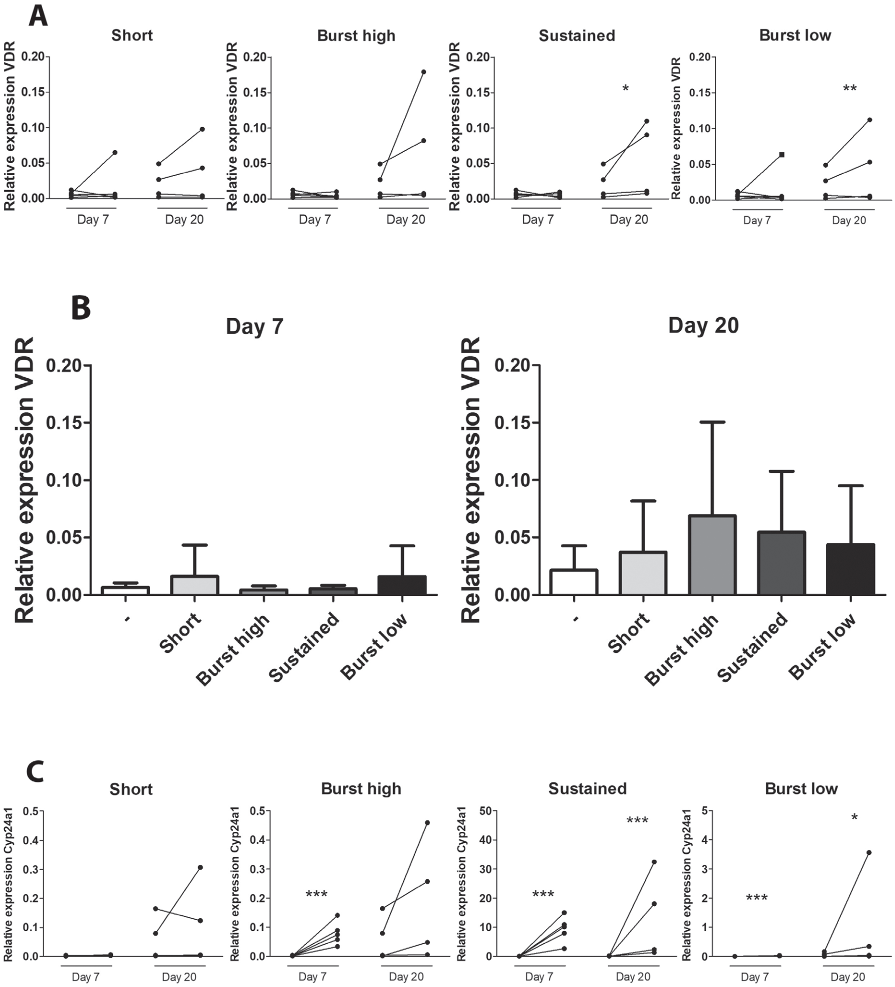

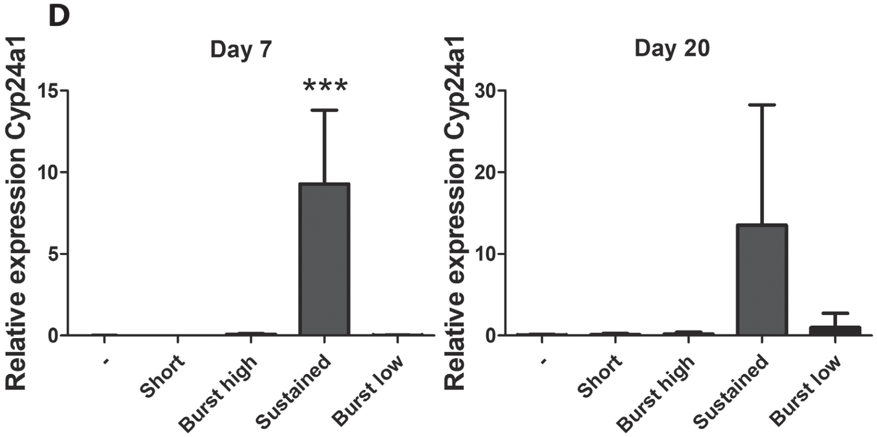

Figure 5. Gene expression of *VDR* and *CYP24a1***.** (**A**) *VDR* expression. Data of controls (left) and vitD_3 treated cells (right) from the same donor are connected with a line. (**B**) Average relative expression of *VDR* at Days 7 and 20. Data represent four or five independent donors (mean + SD). (**C**) Burst high, Sustained, and Burst low application of vitD_3 significantly increased *CYP24a1* (note the 10-fold differences in axis scale). Data of controls (left) and vitD_3 treated cells (right) from the same donor are connected with a line. (**D**) Average relative expression of *CYP24a1* at Days 7 and 20. Data represent four or five independent donors (mean + SD). All gene expression data were normalized to *HPRT*. (A, C) * Significant difference ($p < 0.05$) between control and vitD_3 treatment at the same time point; *** $p < 0.001$. (D) * Significant difference ($p < 0.001$) between Sustained vitD_3 treatment and all other groups.

Discussion

In this study, we evaluated which $vitD_3$ application (Short, Burst, or Sustained) to hASCs seeded on BCP particles, leads to optimal osteogenic differentiation of hASCs in cell culture. We did this because we wished to mimic the effect of different release kinetics of $vitD_3$ from biomaterials in vivo. Our results may help to design scaffolds with bioactive components for bone tissue engineering in a more targeted manner, and suggest that applying a daily dose of $vitD_3$ in vitro (Sustained application), thereby mimicking a sustained release of $vitD_3$ in vivo, stimulates ALP activity of hASCs, where other applications do not, even when the same total amount of $vitD_3$ (124 ng) was applied.

In this study, we mimicked short, burst, and sustained release from a scaffold. The same total amount of $vitD_3$ was used for short, burst high, and Sustained applications (i.e., 124 ng), but delivered over different time spans, thereby leading to different concentrations. The concentration of 10 nM thus obtained for the Sustained application is a widely used concentration to induce osteogenic differentiation of MSCs[7,25,27]. Adding the same 124 ng $vitD_3$ in two days (Burst high) or 30 min (Short) led to concentrations of 100 and 200 nM respectively. For Burst low, we applied the same concentration of $vitD_3$ as the Sustained application (10 nM) but adhered to the same two-day timeframe as burst high, which means that the total amount of $vitD_3$ added to the ASCs over the total culture period was only 6.4 ng.

Our method of mimicking release from scaffolds has a limitation. The medium was refreshed every day to mimic a steady sustained release of bioactive components more accurately. This means the cells got a “shock” from the medium refreshment every day. This might have influenced the responses of the cells to $vitD_3$ compared to more regular treatment regimens, where it is customary that cells are replenished two or three times a week. It could explain our relative lack of differentiation induced by $vitD_3$, where we did not observe an obvious effect of $vitD_3$ on ASC differentiation. Despite this downside, we were still able to discern clear effects of $vitD_3$ on *RUNX2*, *VDR*, and *CYP24* expression and ALP activity, and the cells used in the present study proliferated as normal (Figure 3). If our results are indeed somewhat “blunted” by the daily medium refreshments, it is to be expected that the observed differences of our in vitro investigation are *more* pronounced in vivo. In addition, the ASCs seemed to show an increased *BCL-2* expression over time, while *BAX* expression remained level, indicating that the frequent medium refreshments did not induce apoptosis. Importantly, since all our groups were treated in exactly the same manner, we can readily compare the effects of our $vitD_3$ applications between groups.

One of the first prerequisites for successful tissue engineering approaches is the availability of sufficient numbers of cells. Cell number increases through proliferation or decreases through cell death. VitD_3 (1–100 nM) shows an inverse linear relation with proliferation in human osteoblasts and C_2C_{12} cells [28,29]. Whether vitD_3 decreases proliferation in hASCs is unknown. A similar inhibition of proliferation of hASCs by vitD_3 could have adverse effects on bone healing by limiting available cell numbers, unless perhaps the reduction in proliferation is explained by strong stimulation of differentiation. Unfortunately, the use of calcium-containing biomaterials did not permit us to use DNA as a measure for cell number, but we used the following surrogates for cell number: the Alamar blue assay (Figure 3A; which unfortunately also takes metabolic activity into account), histology (Figure 2A–D), and total protein (Figure 3C). In Figure 3C, it is clearly visible that the total protein content is highly similar between groups at Day 7. This is supported by the Alamar blue data from Day 2 and 7, which show no differences. Based on these data, and the results from histology from Day 2, we can assume that the initial seeding of the particles was homogeneous. Our Alamar blue results, in combination with protein measurements, show that cell numbers varied very little between vitD_3-treated conditions. Together, this indicates that the different vitD_3 applications (Sustained (10 nM), Burst high (100 nM), Burst low (10 nM), or Short (200 nM)) neither reduced nor enhanced proliferation of ASCs (Figure 3). This was confirmed by gene expression of *Ki67*, a marker for proliferation, which also showed no reduction.

Cell number can be affected by cell death, through necrosis or apoptosis. In large tissue engineering constructs, low oxygen tension in the center of the construct can lead to rapid loss of stem cells. Notably, vitD_3 can cause apoptosis in mouse adipocytes (3T3-L1) at a concentration of 77.4 nM ± 23.20 at Day 3 and 61.7 nM ± 20.5 at Day 6 [30] and breast cancer cells (MCF-7) at a concentration of 100 nM [31]. The results of the live-dead staining at day 2 show that even the highest concentration of vitD_3 (Short, 200 nM) did not cause immediate cell death of hASCs. However, this does not guarantee that vitD_3 does not induce cell death at later time points. We therefore, quantified gene expression of *BAX* and *BCL-2* as a measure for apoptosis. Interestingly, the relative expression of *BCL-2*, an inhibitor of pro-apoptotic proteins, seemed to increase at Day 20 compared to Day 7 (not tested), regardless of whether vitD_3 was added, which suggests that inhibition of pro-apoptotic proteins increased over culture time. This general increase in BCL-2 has also been observed in human osteoblasts cultured on plastic with or without treatment of 10 nM vitD_3 [32,33]. By Day 7, the gene expression of *BAX*, a pro-apoptotic molecule, had been upregulated in the condition mimicking sustained-release (10 nM per day for 20 days) and, by Day 20, the expression of *BAX* was upregulated by the condition mimicking burst release (100 nM per day for two days;

Figure 2E). The increase in *BAX* expression in these conditions may indicate initiation of apoptosis, but this also depends on the expression of *BCL-2*. Gene expression of *BCL-2* was not significantly increased for any of the vitD$_3$ treatments. Interestingly, total protein and Alamar blue did not show a decrease for Sustained and Burst high at any time point (Figure 3), suggesting that, if increased *BAX* expression was indeed translated into an increased balance between *BAX* and *BCL-2* protein, then the impact on hASC apoptosis was minor. Our results together show that none of our vitD$_3$ applications seems harmful for hASCs.

Against expectations, expression of the early osteogenic marker *RUNX2* appeared to be higher at Day 20 than at day 7, in both the presence and absence of vitD$_3$. This trend was not statistically tested, but was striking, as the same pattern was observed for all treatment groups. As it has already been shown that calcium phosphate materials can induce the upregulation of *RUNX2* [34] and that Ca^{2+} ions can play a role in the differentiation of stem cells/osteoblasts [35], we suspect that the apparent upregulation of *RUNX2* over time is due to the BCP particles, which likely released ions in the medium, as they are known to do [35,36]. Burst high and Sustained application of vitD$_3$ significantly reduced *RUNX2* expression. This is in line with other studies [37,38] However, the average gene expression levels of *RUNX2* did not significantly differ between treatment groups, suggesting that Burst high and Sustained had no superior effect on hASC differentiation with respect to *RUNX2* expression.

Our results suggest that for the osteogenic differentiation of adipose stem cells cultured in 3D in vitro, continuous exposure to vitD$_3$ or “Sustained release” might be preferable compared to shorter applications, but we are extremely careful with this conclusion, as it is based on ALP activity only. *OPN* expression was unaffected by vitD$_3$ application, and, due to the use of BCP particles (containing calcium and phosphate), it was not possible to perform analyses such as alizarin red staining. However, at days 7 and 20, we found that the early osteogenic marker ALP had been significantly increased by the Sustained application. Mokhtari-Jafari et al. showed that a short (30 min) incubation of hASCs with vitD$_3$ led to higher ALP expression than sustained incubation [25]. The contradictions between their findings and ours might be explained by a difference in concentration of the 30-min pre-incubation, as we used a 20´ higher concentration. Although the concentration they used for the sustained application is the same as in this study, the total amount of vitD$_3$ sensed by our cells is higher, due to daily rather than twice-weekly refreshment of the medium. This indicates that for short incubation, the concentration of vitD$_3$ may be important for the osteogenic differentiation of hASCS, while for sustained application the total amount applied may play a role as well, at least in vitro. This information could be valuable for the development of scaffolds releasing bioactive components, assuming that our results translate to the in vivo situation.

A potential problem with the application of high amounts of active factors, or long durations of application of such factors, is that cells may respond less to further stimulation by those factors, through altered expression of receptors or inhibitors. *VDR* is the main receptor through which vitD$_3$ regulates biological responses [36]. The expression of *VDR* in this study was quite stable, and, overall, the expression was not downregulated, indicating that the various vitD$_3$ applications as used in the current study did not make the cells become less sensitive for vitD$_3$. *CYP24a1* converts the active vitD$_3$ to an inactive form [39] and in our study, it was highly upregulated by Sustained application of vitD$_3$. The rapid inactivation of vitD$_3$ may have reduced the effect of Sustained vitD$_3$ application on hASC differentiation, thereby explaining why the early osteogenic differentiation marker ALP was still upregulated at Day 20. On the other hand, ALP might still be upregulated at Day 20 because of the 3D culture system we used. ALP is an early marker when cells are cultured on plastic, but cultured in 3D the ALP expression increases slowly over time [40–42]. For future research, it is interesting to mimic a sustained release with even lower concentrations, since we speculate that this will decrease the inactivation of vitD$_3$ by *CYP24a1*.

Sustained application stimulated ALP activity, where other applications of vitD$_3$ did not, without inhibition of proliferation or reduction in cell number. This suggests that tissue engineering solutions in which an active compound such as vitD$_3$ is released over a long period of time may be more beneficial for stimulating osteogenic differentiation than shorter durations of application. In line with these results, Faßbender et al. showed that sustained release of a low amount of BMP-2 had a similar positive effect on bone healing as higher BMP-2 amounts released with a burst [43]. On the other hand, a short application—if it works—can be clinically relevant as no exogenous ligands are placed in the body, thereby preventing potential adverse side effects. In the case of vitD$_3$, this could be osteoclastogenesis. VitD$_3$ can induce *RANKL*, which can induce the formation of osteoclasts as shown in a murine monocyte/macrophage cell line at doses as low as 10 nM, which is comparable to the concentration we used in the sustained application [44]. We do not expect these kinds of adverse effects of sustained-release from a biomaterial at lower concentrations, yet each patient reacts differently, and factors such as race and gender may affect the response to vitD$_3$, therefore patient-specific treatment designs might be a good option to consider [45]. The clear donor to donor variability in the response to vitD$_3$ treatment is visible in our data. This is most visible in the qPCR data (Figures 4 and 5) where in some cases the effect of vitD$_3$ on gene expression is higher in two out of the five donors. The race of our donors is unknown, which is unfortunate, as 25-hydroxyvitamin D_3 serum levels and *VDR* expression vary between white and black people, possibly affecting the response to vitD_3 [46]. Importantly, the donors that respond strongly to viD_3 differ from gene to gene analysis, and there are no two individuals that can be designated as “high responders” vs. “low responders”. It is theoretically possible that hASCs from male donors react differently than those of females, but in our study at least four out of five of our donors are female.

In summary, although the effects of vitD_3 on osteogenic differentiation were limited to ALP activity and *RUNX2* expression, the results of this present study are still convincing enough to prompt us to reject our hypothesis that a short incubation with vitD_3 would be more beneficial for osteogenic differentiation than other durations of applications. Adding vitD_3 for a longer period did not lead to apoptosis, and induced the ALP expression at both Days 7 and 20. In addition, it affected gene expression of *RUNX2*, *VDR*, and *CYP24a1*. Short application did none of these things. Overall, a Sustained application seems to have more effect on hASCs compared to shorter applications, and therefore it would be wise to further investigate the effect of sustained release of vitamin D_3 on proliferation and osteogenic differentiation of stem cells, taking into account factors such as donor-to-donor variability, broad dose-response studies, and possible side effects.

Supplementary Figures

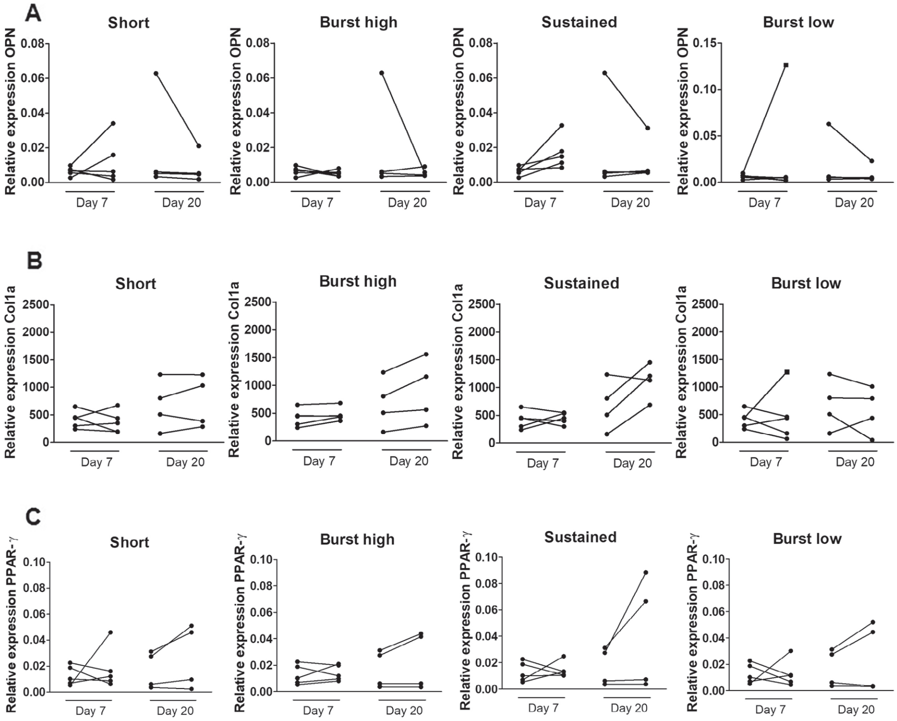

Figure S1. Relative gene expression of OPN, Col1a, and PPAR- γ (**A**) OPN expression was not affected by vitD$_3$ at both day 7 and day 20. (**B**) Col1A expression was not affected by vitD$_3$ at both day 7 and day 20. (**C**) PPAR-γ expression was upregulated at day 20 by sustained application of vitD3 but this is not significant. All genes were normalized to HPRT. The significant difference between control and treatment at each time point was measured using a paired t-test. Significance was considered when $p<0.05$.

References

1. Azi, M.L.; Aprato, A.; Santi, I.; Kfuri Jr., M.; Masse, A.; Joeris, A. Autologous bone graft in the treatment of post-traumatic bone defects: a systematic review and meta-analysis. *BMC Musculoskelet. Disord.* **2016**, *17*, 465.
2. Myeroff, C.; Archdeacon, M. Autogenous Bone Graft: Donor Sites and Techniques. *J. Bone Jt. Surgery-American Vol.* **2011**, *93*, 2227–2236.
3. Lin, H.; Tang, Y.; Lozito, T.P.; Oyster, N.; Kang, R.B.; Fritch, M.R.; Wang, B.; Tuan, R.S. Projection Stereolithographic Fabrication of BMP-2 Gene-activated Matrix for Bone Tissue Engineering. *Sci. Rep.* **2017**, *7*, 11327.
4. Amini, A.R.; Laurencin, C.T.; Nukavarapu, S.P. Bone tissue engineering: recent advances and challenges. *Crit. Rev. Biomed. Eng.* **2012**, *40*, 363–408.
5. Kim, B.S.; Choi, M.K.; Yoon, J.H.; Lee, J. Evaluation of bone regeneration with biphasic calcium phosphate substitute implanted with bone morphogenetic protein 2 and mesenchymal stem cells in a rabbit calvarial defect model. *Oral Surg. Oral Med. Oral Pathol. Oral Radiol.* **2015**, *120*, 2–9.
6. Des Rieux, A.; Ucakar, B.; Mupendwa, B.P.K.; Colau, D.; Feron, O.; Carmeliet, P.; Préat, V. 3D systems delivering VEGF to promote angiogenesis for tissue engineering. *J. Control. Release* **2011**, *150*, 272–278.
7. Song, I.; Kim, B.-S.; Kim, C.-S.; Im, G.-I. Effects of BMP-2 and vitamin D_3 on the osteogenic differentiation of adipose stem cells. *Biochem. Biophys. Res. Commun.* **2011**, *408*, 126–131.
8. Liu, P.; Oyajobi, B.O.; Russell, R.G.G.; Scutt, A. Regulation of Osteogenic Differentiation of Human Bone Marrow Stromal Cells: Interaction Between Transforming Growth Factor-β and 1,25(OH)2 Vitamin D3In Vitro. *Calcif. Tissue Int.* **1999**, *65*, 173–180.
9. Lou, Y.-R.; Toh, T.C.; Tee, Y.H.; Yu, H. 25-Hydroxyvitamin D_3 induces osteogenic differentiation of human mesenchymal stem cells. *Sci. Rep.* **2017**, *7*, 42816.
10. Suliman, S.; Xing, Z.; Wu, X.; Xue, Y.; Pedersen, T.O.; Sun, Y.; Døskeland, A.P.; Nickel, J.; Waag, T.; Lygre, H.; et al. Release and bioactivity of bone morphogenetic protein-2 are affected by scaffold binding techniques in vitro and in vivo. *J. Control. Release* **2015**, *197*, 148–157.
11. Kawa, S.; Nikaido, T.; Aoki, Y.; Zhai, Y.; Kumagai, T.; Furihata, K.; Fujii, S.; Kiyosawa, K. Vitamin D analogues up-regulate p21 and p27 during growth inhibition of pancreatic cancer cell lines. *Br. J. Cancer* **1997**, *76*, 884–889.
12. Skjødt, H.; Gallagher, J.A.; Beresford, J.N.; Couch, M.; Poser, J.W.; Russell, R.G.G. Vitamin D metabolites regulate osteocalcin synthesis and proliferation of human bone cells in vitro. **1985**, *105*, 391.
13. Tannoury, C.A.; An, H.S. Complications with the use of bone morphogenetic protein 2 (BMP-2) in spine surgery. *Spine J.* **2014**, *14*, 552–559.

14. Sukul, M.; Nguyen, T.B.L.; Min, Y.-K.; Lee, S.-Y.; Lee, B.-T. Effect of Local Sustainable Release of BMP2-VEGF from Nano-Cellulose Loaded in Sponge Biphasic Calcium Phosphate on Bone Regeneration. *Tissue Eng. Part A* **2015**, *21*, 1822–36.
15. Poldervaart, M.T.; Wang, H.; van der Stok, J.; Weinans, H.; Leeuwenburgh, S.C.G.; Öner, F.C.; Dhert, W.J.A.; Alblas, J. Sustained Release of BMP-2 in Bioprinted Alginate for Osteogenicity in Mice and Rats. *PLoS One* **2013**, *8*, e72610.
16. Rahman, C. V.; Ben-David, D.; Dhillon, A.; Kuhn, G.; Gould, T.W.A.; Müller, R.; Rose, F.R.A.J.; Shakesheff, K.M.; Livne, E. Controlled release of BMP-2 from a sintered polymer scaffold enhances bone repair in a mouse calvarial defect model. *J. Tissue Eng. Regen. Med.* **2014**, *8*, 59–66.
17. Gazzerro, E.; Gangji, V.; Canalis, E. Bone morphogenetic proteins induce the expression of noggin, which limits their activity in cultured rat osteoblasts. *J. Clin. Invest.* **1998**, *102*, 2106–2114.
18. Zhu, W.; Kim, J.; Cheng, C.; Rawlins, B.A.; Boachie-Adjei, O.; Crystal, R.G.; Hidaka, C. Noggin regulation of bone morphogenetic protein (BMP) 2/7 heterodimer activity in vitro. *Bone* **2006**, *39*, 61–71.
19. Armbrecht, H.J.; Hodam, T.L.; Boltz, M.A.; Partridge, N.C.; Brown, A.J.; Kumar, V.B. Induction of the Vitamin D 24-Hydroxylase (CYP24) by 1,25-Dihydroxyvitamin D $_3$ Is Regulated by Parathyroid Hormone in UMR106 Osteoblastic Cells [1]. *Endocrinology* **1998**, *139*, 3375–3381.
20. Omdahl, J.L.; Morris, H.A.; May, B.K. H YDROXYLASE E NZYMES OF THE V ITAMIN D P ATHWAY : Expression, Function, and Regulation . *Annu. Rev. Nutr.* **2002**, *22*, 139–166.
21. Bahney, C.S.; Zondervan, R.L.; Allison, P.; Theologis, A.; Ashley, J.W.; Ahn, J.; Miclau, T.; Marcucio, R.S.; Hankenson, K.D. Cellular biology of fracture healing. *J. Orthop. Res.* **2019**, *37*, 35–50.
22. Tchetina, E.; Mwale, F.; Poole, A.R. Distinct Phases of Coordinated Early and Late Gene Expression in Growth Plate Chondrocytes in Relationship to Cell Proliferation, Matrix Assembly, Remodeling, and Cell Differentiation. *J. Bone Miner. Res.* **2003**, *18*, 844–851.
23. Lu, Z.; Wang, G.; Dunstan, C.R.; Zreiqat, H. Short-term exposure to tumor necrosis factor-alpha enables human osteoblasts to direct adipose tissue-derived mesenchymal stem cells into osteogenic differentiation. *Stem Cells Dev.* **2012**, *21*, 2420–2429.
24. Overman, J.R.; Farré-Guasch, E.; Helder, M.N.; Ten Bruggenkate, C.M.; Schulten, E.A.J.M.; Klein-Nulend, J. Short (15 minutes) bone morphogenetic protein-2 treatment stimulates osteogenic differentiation of human adipose stem cells seeded on calcium phosphate scaffolds in vitro. *Tissue Eng. - Part A* **2013**, *19*, 571–581.
25. Mokhtari-Jafari, F.; Amoabediny, G.; Dehghan, M.M.; Helder, M.N.; Zandieh-Doulabi, B.; Klein-Nulend, J. Short pretreatment with calcitriol is far superior to continuous treatment in stimulating proliferation and osteogenic differentiation of human adipose stem cells. *Cell J.* **2020**, *22*, 293–301.
26. Jones, G.; Prosser, D.E.; Kaufmann, M. Cytochrome P450-mediated metabolism of vitamin D. *J. Lipid Res.* 2014, *55*, 13–31.

27. Ji, Y.; Zhang, P.; Xing, Y.; Jia, L.; Zhang, Y.; Jia, T.; Wu, X.; Zhao, B.; Xu, X. Effect of 1α, 25-dihydroxyvitamin D_3 on the osteogenic differentiation of human periodontal ligament stem cells and the underlying regulatory mechanism. *Int. J. Mol. Med.* **2019**, *43*, 167–176.
28. van der Meijden, K.; Lips, P.; van Driel, M.; Heijboer, A.C.; Schulten, E.A.J.M.; Heijer, M. den; Bravenboer, N. Primary Human Osteoblasts in Response to 25-Hydroxyvitamin D3, 1,25-Dihydroxyvitamin D_3 and 24R,25-Dihydroxyvitamin D3. *PLoS One* **2014**, *9*, e110283.
29. Girgis, C.M.; Clifton-Bligh, R.J.; Mokbel, N.; Cheng, K.; Gunton, J.E. Vitamin D Signaling Regulates Proliferation, Differentiation, and Myotube Size in C2C12 Skeletal Muscle Cells. *Endocrinology* **2014**, *155*, 347–357.
30. Sergeev, I.N. 1,25-Dihydroxyvitamin D_3 induces Ca2+-mediated apoptosis in adipocytes via activation of calpain and caspase-12. *Biochem. Biophys. Res. Commun.* **2009**, *384*, 18–21.
31. Sergeev, I.N. Calcium as a mediator of 1,25-dihydroxyvitamin D3-induced apoptosis. *J. Steroid Biochem. Mol. Biol.* **2004**, *89–90*, 419–425.
32. Montecino, M.A.; Lian, J.B.; Stein, J.L.; Stein, G.S.; van Wijnen, A.J.; Cruzat, F. Biological and Molecular Effects of Vitamin D on Bone. In *Vitamin D*; Humana Press: Totowa, NJ, 2010; pp. 189–209.
33. Duque, G.; El Abdaimi, K.; Henderson, J.E.; Lomri, A.; Kremer, R. Vitamin D inhibits Fas ligand-induced apoptosis in human osteoblasts by regulating components of both the mitochondrial and Fas-related pathways. *Bone* **2004**, *35*, 57–64.
34. Müller, P.; Bulnheim, U.; Diener, A.; Lüthen, F.; Teller, M.; Klinkenberg, E.-D.; Neumann, H.-G.; Nebe, B.; Liebold, A.; Steinhoff, G.; et al. Calcium phosphate surfaces promote osteogenic differentiation of mesenchymal stem cells. *J. Cell. Mol. Med.* **2007**, *12*, 281–291.
35. Chai, Y.C.; Carlier, A.; Bolander, J.; Roberts, S.J.; Geris, L.; Schrooten, J.; Van Oosterwyck, H.; Luyten, F.P. Current views on calcium phosphate osteogenicity and the translation into effective bone regeneration strategies. *Acta Biomater.* 2012, *8*, 3876–3887.
36. Haussler, M.R.; Whitfield, G.K.; Kaneko, I.; Haussler, C.A.; Hsieh, D.; Hsieh, J.-C.; Jurutka, P.W. Molecular Mechanisms of Vitamin D Action. *Calcif. Tissue Int.* **2013**, *92*, 77–98.
37. Drissi, H.; Pouliot, A.; Koolloos, C.; Stein, J.L.; Lian, J.B.; Stein, G.S.; Van Wijnen, A.J. 1,25-(OH)2-vitamin D_3 suppresses the bone-related Runx2/Cbfa1 gene promoter. *Exp. Cell Res.* **2002**, *274*, 323–333.
38. Garimella, R.; Tadikonda, P.; Tawfik, O.; Gunewardena, S.; Rowe, P.; Van Veldhuizen, P. Vitamin D impacts the expression of Runx2 target genes and modulates inflammation, oxidative stress and membrane vesicle biogenesis gene networks in 143B osteosarcoma cells. *Int. J. Mol. Sci.* **2017**, *18*.
39. Yu, O.B.; Arnold, L.A. Calcitroic Acid–A Review. *ACS Chem. Biol.* **2016**, *11*, 2665–2672.
40. Gurumurthy, B.; Bierdeman, P.C.; Janorkar, A. V. Spheroid model for functional osteogenic evaluation of human adipose derived stem cells. *J. Biomed. Mater. Res. - Part A* **2017**, *105*, 1230–1236.

41. Castrén, E.; Sillat, T.; Oja, S.; Noro, A.; Laitinen, A.; Konttinen, Y.T.; Lehenkari, P.; Hukkanen, M.; Korhonen, M. Osteogenic differentiation of mesenchymal stromal cells in two-dimensional and three-dimensional cultures without animal serum. *Stem Cell Res. Ther.* **2015**, *6*, 167.
42. He, J.; Genetos, D.C.; Yellowley, C.E.; Leach, J.K. Oxygen tension differentially influences osteogenic differentiation of human adipose stem cells in 2D and 3D cultures. *J. Cell. Biochem.* **2010**, *110*, n/a-n/a.
43. Faßbender, M.; Minkwitz, S.; Strobel, C.; Schmidmaier, G.; Wildemann, B. Stimulation of bone healing by sustained bone morphogenetic protein 2 (BMP-2) delivery. *Int. J. Mol. Sci.* **2014**, *15*, 8539–8552.
44. Gu, J.; Tong, X.S.; Chen, G.H.; Wang, D.; Chen, Y.; Yuan, Y.; Liu, X.Z.; Bian, J.C.; Liu, Z.P. Effects of 1α,25-(OH)2D3 on the formation and activity of osteoclasts in RAW264.7 cells. *J. Steroid Biochem. Mol. Biol.* **2015**, *152*, 25–33.
45. Vogenberg, F.R.; Barash, C.I.; Pursel, M. Personalized medicine - Part 1: Evolution and development into theranostics. *P T* 2010, *35*, 560.
46. Powe, C.E.; Evans, M.K.; Wenger, J.; Zonderman, A.B.; Berg, A.H.; Nalls, M.; Tamez, H.; Zhang, D.; Bhan, I.; Karumanchi, S.A.; et al. Vitamin D-binding protein and vitamin D status of black Americans and white Americans. *N. Engl. J. Med.* **2013**, *369*, 1991–2000.
47. Prins, H.-J.; Rozemuller, H.; Vonk-Griffioen, S.; Verweij, V.G.M.; Dhert, W.J.A.; Slaper-Cortenbach, I.C.M.; Martens, A.C.M. Bone-forming capacity of mesenchymal stromal cells when cultured in the presence of human platelet lysate as substitute for fetal bovine serum. *Tissue Eng. Part A* **2009**, *15*, 3741–51.
48. Bastidas-Coral, A.P.; Hogervorst, J.M.A.; Forouzanfar, T.; Kleverlaan, C.J.; Koolwijk, P.; Klein-Nulend, J.; Bakker, A.D. IL-6 counteracts the inhibitory effect of IL-4 on osteogenic differentiation of human adipose stem cells. *J. Cell. Physiol.* **2019**, *234*, 20520–20532.
49. Lowry, H.O. Micromethods for the assay of enzyme II. Specofic procedures. Alkaline phosphatase. *Methods Enzymol.* **1955**, *4*, 371–372.**Chapter 3**

3

Cells Derived from Human Long Bone Appear More Differentiated and More Actively Stimulate Osteoclastogenesis Compared to Alveolar Bone-Derived Cells

International journal of molecular sciences (2020)

Abstract

Osteoblasts derived from mouse skulls have increased osteoclastogenic potential compared to long bone osteoblasts when stimulated with 1,25$(OH)_2$ vitamin D_3 (vitD_3). This indicates that bone cells from specific sites can react differently to biochemical signals, e.g., during inflammation or as emitted by bioactive bone tissue-engineering constructs. Given the high turn-over of alveolar bone, we hypothesized that *human* alveolar bone-derived osteoblasts have an increased osteogenic and osteoclastogenic potential compared to the osteoblasts derived from long bone. The osteogenic and osteoclastogenic capacity of alveolar bone cells and long bone cells were assessed in the presence and absence of osteotropic agent vitD_3. Both cell types were studied in osteogenesis experiments, using an osteogenic medium, and in osteoclastogenesis experiments by co-culturing osteoblasts with peripheral blood mononuclear cells (PBMCs). Both osteogenic and osteoclastic markers were measured. At day 0, long bones seem to have a more late-osteoblastic/preosteocyte-like phenotype compared to the alveolar bone cells as shown by slower proliferation, the higher expression of the matrix molecule *Osteopontin* (*OPN),* and the osteocyte-enriched cytoskeletal component *Actin alpha 1* (*ACTA1)*. This phenotype was maintained during the osteogenesis assays, where long bone-derived cells still expressed more *OPN* and *ACTA1*. Under co-culture conditions with PBMCs, long bone cells also had a higher *Tumor necrose factor-alfa* (*TNF*-α) expression and induced the formation of osteoclasts more than alveolar bone cells. Correspondingly, the expression of osteoclast genes *dendritic cell-specific transmembrane protein* (*DC-STAMP*) and *Receptor activator of nuclear factor kappa-B ligand (RankL)* was higher in long bone co-cultures. Together, our results indicate that long bone-derived osteoblasts are more active in bone-remodeling processes, especially in osteoclastogenesis, than alveolar bone-derived cells. This indicates that tissue-engineering solutions need to be specifically designed for the site of application, such as defects in long bones vs. the regeneration of alveolar bone after severe periodontitis.

Introduction

One of the great challenges of periodontal treatment is the regeneration of the tooth-anchoring degraded alveolar bone. Surprisingly, little is known about both the osteogenic and osteoclastogenic capacity of the cells retrieved from this skeletal site. Bone tissue-engineering approaches using scaffolds are mostly based on research on long bones, whereas the restoration of alveolar bone between teeth after periodontal treatment is promoted by the cells derived from these unique alveolar bone structures. Ideally, the cells in the bone surrounding a tissue engineering construct are instructed by the signals emitted by the constructs to form bone, and also send cues to recruit stem cells, which can differentiate into cells that form bone. Cells from different skeletal sites may react differently to biological signals, e.g., as released by tissue-engineering constructs, such as vitD$_3$ [1]. Furthermore, communication with other cell types might also be different. The reason why these cells may behave differently might lie in their origin, as alveolar bone originates from neural crest cells while long bone originates from the mesoderm [2].

An indication that cells from different skeletal sites may be different is shown by the in vitro comparison of orofacial and iliac crest *human* bone marrow stromal cells (hMSCs), where orofacial stromal cells were shown to have a higher proliferation and express higher levels of alkaline phosphatase (ALP), while the cells from the iliac crest responded more to osteogenic and adipogenic cues [3]. Another indication that there are differences between the cells from different skeletal sites is the cells' responsiveness to biological components and drugs. In response to bone morphogenetic protein 2 (BMP-2), orofacial hMSCs have a higher expression of osteogenic markers such as ALP and *OPN* than the cells from adult iliac crest [4]. Lastly, bisphosphonates are used to prevent the loss of bone density by reducing osteoclastic bone resorption and are therefore prescribed for patients with osteoporosis [5]. The fact that longer and higher treatment with bisphosphonates can lead to the necrosis of the jaw [6,7] and atypical femoral fractures [8,9] indicate that their effect on long bone differs from that on alveolar bone. These different responses indicate that for the most optimal effect, bone tissue-engineering constructs need to be developed site specifically.

For the remodeling of bone, both osteoblast and osteoclast are needed, where the osteoblasts form bone and osteoclasts resorb bone [10]. Several studies also show that osteoclasts differ between skeletal sites. Mouse osteoblasts from calvaria lead to a higher number of osteoclasts compared to osteoblast derived from long bones [1], and De Souza Faloni et al. show that marrows from mice, derived from the jaw and long bone, have different osteoclastogenic potential [11].

This indicates that for optimal bone remodeling, the different effects of constructs on oseoclastogenesis also need to be considered and may also differ per skeletal site. Knowledge of local cells, such as the stem cells of the oral cavity [12], will ultimately lead to better healing and osseointegration of implants [13].

Biological components can be used to enhance bone tissue-engineering constructs. Moreover, vitD$_3$ is such a biological component often used in bone tissue engineering as it can promote the osteogenic differentiation of hMSCs [14]. Moreover, vitD$_3$ also affects the osteoclastogenic differentiation of osteoblasts in vitro by inducing the *RankL* expression [15]. We recently demonstrated that the way vitD$_3$ is administered, mimicking release from tissue-engineering constructs, and affecting the osteogenic capacity of adipose tissue-derived mesenchymal stem cells [16].

In the present study, we compared the degree of differentiation of bone cells derived from *human* alveolar and long bones, their production of signaling molecules, and their ability to stimulate osteoclast formation in the presence or absence of the biological component vitD$_3$. We hypothesize that alveolar bone cells have an increased osteogenic and osteoclastogenic potential compared to long bone cells, as alveolar bone cells seem to have a higher turnover, and therefore, we expect less differentiated cells.

Materials and Methods

Bone Cell Cultures

In this study, we used two types of cells: cells derived from alveolar bone and long bones, in this case, the tibia. Both cell types were obtained by the outgrowth of cells from pieces of bone. In short, bone fragments were transported in Dulbecco's modified Eagle's medium (DMEM, Gibco, Paisley, UK) supplemented with 2% antibiotic antimycotic solution 100× (Sigma, St. Louis, MO, USA) and then cut into small pieces, washed with PBS and were incubated for 2 h in 2 mg/mL collagenase II (Sigma, St. Louis, MO, USA) in DMEM at 37 –C in a shaking water bath. The bone fragments were washed with a medium containing 10% fetal calf serum (FCS) and transferred to 25 cm2 flasks. Bone fragments were cultured in DMEM with 1% antibiotic antimycotic solution 100× and 10% FCS. When the cells reached confluency, the cells were harvested using 0.25% trypsin and 0.1% EDTA in PBS. For each cell type, we used cells from 5 different donors. Cells were not from the same donors and are from passage 2–4. The donors for the long bone cells were all female and were between 69-86 years of age. Of the alveolar bone cell donors, two were male and three were female with an age between 37 and 60.

Alveolar Bone Cells

Cells were derived from human interdental alveolar crest bone. Patients who were referred for multiple adjacent tooth extractions and immediate denture placement were asked to participate. Interdental alveolar crestal bone was regarded as surgical waste since this bony rim has to be smoothened before wound closure. Treatments took place at the Department of Oral and Maxillofacial Surgery at the hospital OLVG in Amsterdam, The Netherlands. Prior to the treatment, written informed consent was signed by the patienst, and the study protocol was approved by the research ethics committee of the OLVG (protocol-ID: WO17.194).

Long Bone Cells

Cells were derived from surgical waste from *human* bone from the knee, after surgery performed at the VU University Medical Center, Amsterdam, The Netherlands. This in agreement with The Ethical Review Board of the VU Medical Center, Amsterdam, The Netherlands, under protocol number 2016/105.

Osteogenesis Experiments

For the osteogenesis experiments, cells either derived from long bone or alveolar bone were seeded at 3 × 104 cells/well in a 48-well plate and cultured in a basic medium, one day before the start of the experiment (day–1). At day 0, the medium was refreshed and the cells were cultured in basic medium, osteogenic medium, or osteogenic medium supplemented with vitD$_3$. The basic culture medium consisted of the D modification of Dulbecco's modified Eagle's medium (DMEM, Gibco BRL, Paisley, Scotland), 5% fetal clone I serum (FCI, HyClone, Logan, UT), 5% fetal clone III serum (FCIII, HyClone) and 1% Antibiotic Antimycotic Solution, 100× (Sigma, St. Louis, MO, USA). Osteogenic medium is a basic medium supplemented with 50 µM ascorbic acid-2-phosphate (Sigma, St. Louis, MO, USA) and 50 µM β-Glycerophosphate (Sigma). In some cultures, osteogenic medium was supplemented with 10 nM vitD$_3$ (osteogenic + vitD$_3$). The medium was refreshed twice a week for 3 weeks.

Alkaline Phosphatase (ALP) Activity

Cells were lysed with 200 µL of Milli-Q water at day 0, day 7, day 14, and day 21 and frozen at -20 –C. Samples were collected by scraping after 3 freeze-thaw cycles for ALP measurement. ALP was measured using 4-nitrophenyl phosphate disodium salt at pH 10.3 as a substrate for ALP, a method described by Lowry [34]. Absorbance was measured at 405 nm with Synergy HT® spectrophotometer. ALP levels were corrected for DNA content and expressed as µmol/ng. DNA was measured using a Cyquant cell proliferation assay kit (Molecular probes, Eugene, OR, USA) according to the manufacturers' instructions.

Mineralization

Cells were cultured for 21 days to test for mineralization of the cells. All the samples were washed with deionized water and fixed with 4% formaldehyde for 10 min. After rinsing with deionized water, 300 µL of 2% Alizarin red S (Sigma-Aldrich) staining with a pH of 4.3 was added to each well. After a 15-min incubation, the cells were washed and air-dried.

Quantitative Polymerase Chain Reaction (qPCR)

At day 0, and after 14 days and 21 days of culture, the total RNA was isolated with TRIzol® reagent (Invitrogen) following the manufacturer's protocol. The quality and concentration of the RNA were measured using a Synergy HT® spectrophotometer. Then, 750 ng RNA was reverse-transcribed to cDNA using the RevertAid™ First Strand cDNA Synthesis Kit 1612 (Fermentas, St. Leon-Rot, Germany) according to the manufacturer's protocol. For the qPCR reaction, cDNA was diluted 5× and 1 µL was used, together with 3 µL PCR-H_2O, 0.5 µL (20 µM) forward primer, 0.5 µL (20 µM) reverse primer, and 5 µl LightCycler® 480 SYBR Green I Mastermix (Roche Diagnostics, Mannheim, Germany). All the measurements with a Ct value higher than 36 were considered unreliable and discarded. The values of all the genes were normalized to hypoxanthine phosphoribosyl transferase (HPRT) or glyceraldehyde 3-phosphate dehydrogenase (GAPDH) following the comparative cycle threshold (Ct) method and presented as the mean relative fold expression (2–ΔCt). All the primer sequences for osteogenesis experiments are listed in Table 1.

Table 1. *Primer sequences osteogenesis.*

Gene (Human)	Forward Sequence	Reverse Sequence
COL1	*5′ GCATGGGCAGAGGTATAATG 3′*	*5′ GGTCCTTTGGGTCCTACAA 3′*
RUNX2	*5′ CCAGAAGGCACAGACAGAAGCT 3′*	*5′ AGGAATGCGCCCTAAATCACT 3′*
OPN	*5′ TTCCAAGTAAGTCCAACGAAAG 3′*	*5′ GTGACCAGTTCATCAGATTCAT 3′*
DMP-1	*5′ TAGGCTAGCTGGTGGCTTCT 3′*	*5′ AACTCGGAGCCGTCTCCAT 3′*
ACTA1	*5′ CTGGCA′CCACACCTTCTACA 3′*	*5′ CACGCTCAGTGAGGATCTT 3′*
IL-6	*5′ ACAGCCACTCACCTCTTCA 3′*	*5′ ACCAGGCAAGTCTCCTCAT 3′*
COX2	*5′ GCATTCTTTGCCCAGCACTT 3′*	*5′ AGACCAGGCACCAGACCAAAGA 3′*
CYR6	*5′ TCCGAGGTGGAGTTGACGAGAA3′*	*5′ TTCACAAGGCGGCACTCAGG 3′*
HPRT	*5′ GCTGACCTGCTGGATTACAT 3′*	*5′ CTTGCGACCTTGACCATCT 3′*
GAPDH	*5′ TGGGTGTGAACCATGAGAAGTATG 3′*	*5′ GGTGCAGGAGGCATTGCT 3′*

Osteoclastogenesis Experiments

To analyze the capacity of alveolar bone and long bone-derived cells to contribute to osteoclast formation, these cells were seeded at 1.5 × 104 cells/well in a 48-well plate and allowed to spread overnight (day –1). The next day (day 0), 0.5 × 106 peripheral blood mononuclear cells (PBMCs) were seeded on top. The PBMCs were isolated from the buffy coat (Sanquin, Amsterdam, The Netherlands) by a standard density gradient centrifugation with Ficoll-Paque [35]. Co-cultures of bone cells and PBMCs were cultured for up to 21 days in basic medium (same composition as the basic medium in the osteogenesis experiments) or the basic medium supplemented with 10 nM vitD$_3$. The medium was refreshed twice a week. As a control, the PBMCs on plastic, also without the supplementation of RankL and the macrophage colony-stimulating factor (M-CSF), were used.

ELISA

After 7 days of culture, the supernatant of the osteoclastogenesis plate was collected and the Enzyme Linked Immunosorbent Assays were performed with the DuoSet ELISA kits (R&D systems, Abington, United Kingdom) for the human TNF-α, and IL-1β, following the manufacturer's protocol.

Osteoclast Quantification

After 21 days of culture, the cells were fixed with 4% formaldehyde for 10 min and stained with leukocyte acid phosphatase kit (Sigma) to identify the TRAcP activity. The nuclei were stained with diamidino-2phenylindole dihydrochloride (DAPI). The whole culture well was analyzed for the number of osteoclasts. Osteoclasts were considered as TRAcP+ multinucleated cells (MNCs) containing three or more nuclei. Two groups were counted, cells with 3–5 nuclei and cells with more than 5 nuclei.

qPCR

At day 0, and after 14 days and 21 days of culture, the total RNA was isolated with TRIzol® reagent (Invitrogen) following the manufacturer's protocol. The quality and concentration of the RNA were measured using a Synergy HT® spectrophotometer. Then, 750 ng RNA was reverse-transcribed to cDNA using the RevertAid™ First Strand cDNA Synthesis Kit 1612(Fermentas, St. Leon-Rot, Germany) according to the manufacturer's protocol. For the qPCR reaction, cDNA was diluted 5× and 1 µL was used, together with 3 µL PCR-H$_2$O, 0.5 µl (20 µM) forward primer, 0.5 µL (20 µM) reverse primer, and 5 µL LightCycler® 480 SYBR Green I Mastermix (Roche Diagnostics, Mannheim, Germany). All the measurements with a Ct value higher than 36 were considered unreliable and discarded. The values of all the genes were normalized to HPRT or GAPDH following the comparative cycle threshold (Ct) method and presented as the mean relative fold expression (2–ΔCt). All the primer sequences for osteoclastogenesis experiments are listed in Table 2.

Table 2. *Primer sequences osteoclastogenesis.*

Gene (Human)	Forward Sequence	Reverse Sequence
DC-STAMP	*5’ ATTTTCTCAGTGAGCAAGCAGTTTC 3’*	*5’ AGAATCATGGATAATATCTTGAGTTCCTT 3’*
Tracp	*5’ CACAATCTGCAGTACCTGCAAGGAT 3’*	*5’ CCCATAGTGGAAGCGCAGATA 3’*
IL-6	*5’ ACAGCCACTCACCTCTTCA 3’*	*5’ ACCAGGCAAGTCTCCTCAT 3’*
RankL	*5’CATCCCATCTGGTTCCCATAA 3’*	*5’ GCCCAACCCCGATCATG 3’*
OPG	*5’ TGGAATAGATGTTACCCTGTGTG 3’*	*5’ GCTGCTCGAAGGTGAGGTTA 3’*
COX2	*5’ GCATTCTTTGCCCAGCACTT 3’*	*5’ AGACCAGGCACCAGACCAAAGA 3’*
HPRT	*5’ GCTGACCTGCTGGATTACAT 3’*	*5’ CTTGCGACCTTGACCATCT 3’*
GAPDH	*5’ TGGGTGTGAACCATGAGAAGTATG 3’*	*5’ GGTGCAGGAGGCATTGCT 3’*

Statistics

Data were obtained from the cultures of 5 independent donors ($n = 5$) for each cell type. Data are presented as mean + standard deviation (SD). A t-test was conducted to test for the statistical differences between the alveolar bone cells and the long bone cells at day 0 (Figure 1). The differences between the groups in the number of osteoclasts are measured with a one-way ANOVA with a Tukey post hoc test. Statistical comparisons of the experiments with multiple

time points were done using a 2-way ANOVA with Bonferroni post-tests. With time and ‘cell type’ used as the dependent variables, the P values of < 0.05 were considered significantly different. The analyses were performed using GraphPad Prism 5.0 (GraphPad Software, San Diego, CA, USA).

Results

Alveolar Bone Cells and Long Bone Cells Differ in Basic Appearance, Proliferation, and Expression of Mature Bone Cell Markers

To identify the differences between the alveolar-derived bone cells and the long bone-derived cells, it is first of all important to know the baseline characteristics of the cells derived from both skeletal sites. We tested the differences in appearance, proliferation, and bone markers. In Figure 1A, B, representative micrographs of the cells derived from bone harvested at both sites, cultured on tissue culture plastic on day 7, are shown. At confluence, alveolar bone cells (Figure 1A) had a fibroblastic appearance, while the appearance of long bone cells was more cuboidal (Figure 1B). The proliferation of the cells was measured with the total DNA content (Figure 1C). At both days 14 and 21, there was significantly more DNA in the alveolar bone samples, indicating the higher proliferation for the cells derived from the alveolar bone. At day 14, there was 2.9-fold more DNA in the samples derived from alveolar bone cells compared to the long bone cells, and at day 21 there was 1.6-fold more DNA in the alveolar bone samples compared to the long bone samples. The gene expression of several bone markers (Figure 1D–H) was measured at day 0. The relative expression of extracellular matrix protein *Collagen type I* (*Col1A*) (Figure 1D) and the differentiation marker *Runt-related transcription factor 2* (*RUNX2*) (Figure 1E) seemed higher in the cells derived from the long bones but this was not significant. In contrast, all the relatively late markers, *OPN* (Figure 1F), *Dentine matrix protein 1* (*DMP-1*) (Figure 1G), and *ACTA1* (Figure 1H) were significantly higher expressed in long bone cells than in alveolar bone cells.

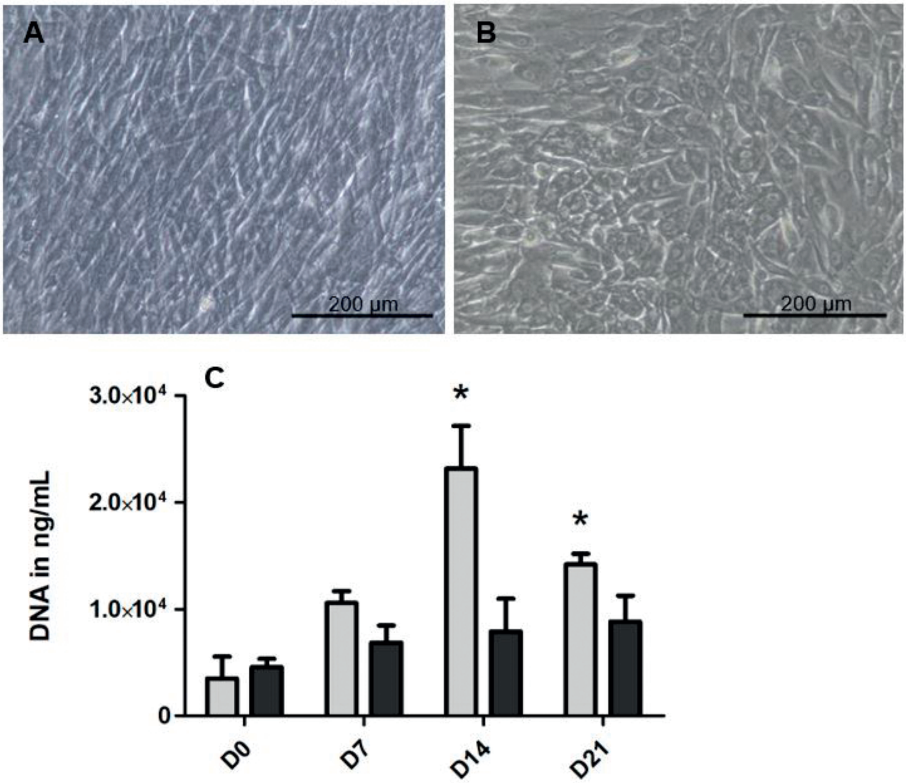
A
200 µm
B
200 µm
C
DNA in ng/mL
3.0×10⁴
2.0×10⁴
1.0×10⁴
0
*
*
D0
D7
D14
D21

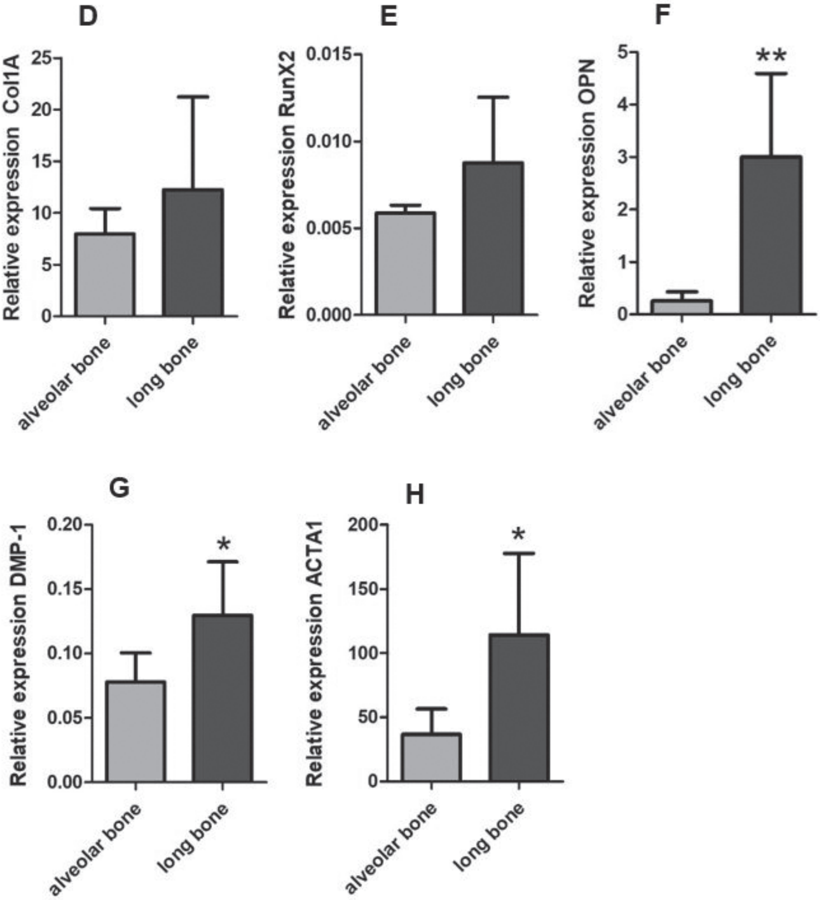

Figure 1. Basic differences between the cells from the alveolar bone and long bones. Light microscopy of (**A**) the alveolar bone cells and (**B**) the long bone cells at day 7. (**C**) DNA content, as a measure of the number of cells at a given time point, of both cells derived from alveolar bone and the long bone at day 0, day 7, day 14, and day 21. To gain insight into the osteogenic lineage of both cell types, the gene expression of osteogenic genes was assessed at day 0 (**D**–**H**) The relative expression of both (**D**) *Col1a* and (**E**) *RUNX2* was comparable in both the alveolar bone cells and the long bone cells. The relative expression of (**F**) *OPN*, (**G**) *DMP-1,* and (**H**) *ACTA1* was significantly higher at day 0, in long the bone cells compared to the alveolar bone cells. Significance for DNA was measured using 2-way ANOVA with Bonferroni post-tests. For the relative gene expression, significance was measured using a t-test.
* $p < 0.05$, ** $p < 0.01$.

Cells Derived from Long Bone Have a Higher Expression of Late Osteogenic Markers Compared to Alveolar Bone Cells

Having determined the basic differences between alveolar bone cells and long bone cells, we then assessed the osteogenic potential of both cell types. We tested this potential with an osteogenic medium and an osteogenic medium supplemented with vitD$_3$. Cellular ALP activity levels (Figure 2A) were similar in alveolar bone and the long bones under all conditions. The differentiation marker *RUNX2* was under basic circumstances, significantly higher expressed by the alveolar bone cells than by long bone cells at day 21. This difference was not present when vitD$_3$ was added. VitD$_3$ upregulated the gene expression of *RUNX2* of long bone cells (Supplementary Materials Figure S1A). The relative expression of *Col1a* was similar in all conditions (Figure 2C). *OPN* expression appeared higher in the long bone samples compared to the alveolar bone samples for all conditions, but was only significantly higher at day 14 in a basic condition and day 21 in the condition with vitD$_3$. Over time, the expression of *DMP-1* significantly increased in alveolar bone cell cultures in basic condition (Figure 2E). The osteogenic medium led to a significant increase in *DMP-1* expression when comparing day 14 with day 21, in both alveolar bone cells and long bone-derived cells. The expression of *DMP-1* was upregulated by the supplementation of vitD$_3$ in long bone cells, specifically at day 21 (Supplementary Materials Figure S1B). At this time point, it was also significantly higher than the *DMP-1* expression in alveolar bone cells. The *ACTA1* expression was higher in the long bone cells than in the alveolar bone cells both in the basic and osteogenic conditions (Figure 2F). The addition of vitD$_3$ seemed to lower the expression for both cell types at day 14. At day 21, the expression was significantly upregulated for both cell types and there was a significant difference between the alveolar bone cells and the long bone cells. The calcium deposits as a measure for mineralization were assessed using alizarin red staining. At day 21, there were no calcium deposits visible in both cell types (Supplementary Materials Figure S1C).

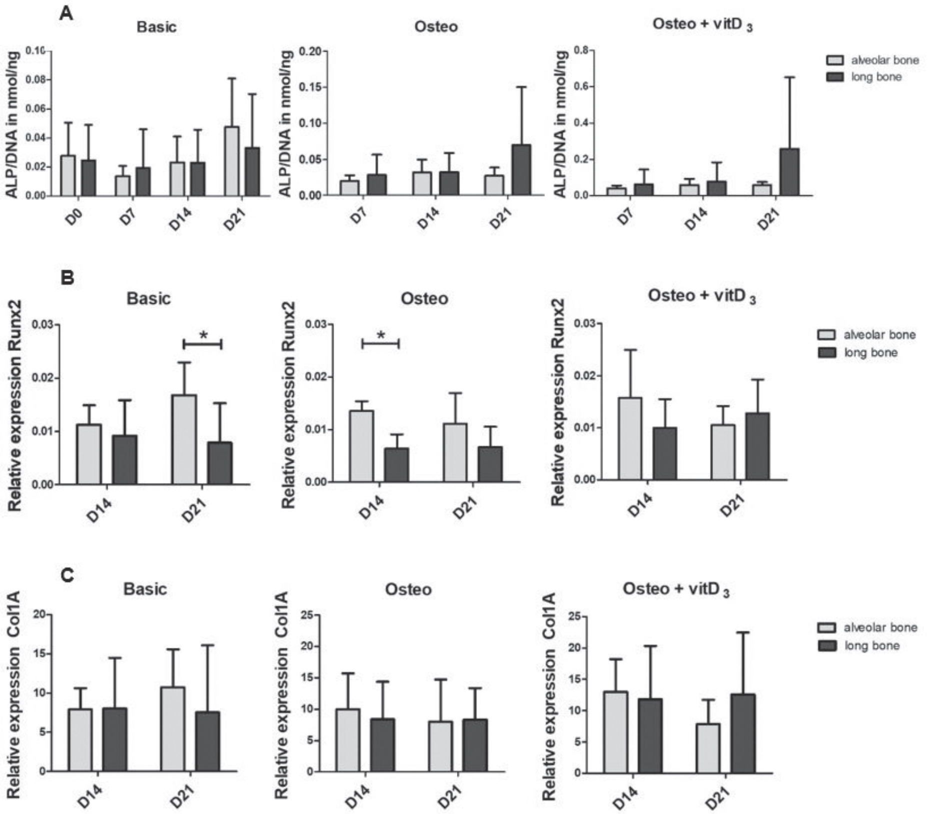
A
Basic
Osteo
Osteo + vitD 3
ALP/DNA in nmol/ng
0.10
0.08
0.06
0.04
0.02
0.00
0.20
0.15
0.10
0.05
0.00
0.8
0.6
0.4
0.2
0.0
D0
D7
D14
D21
alveolar bone
long bone
B
Basic
Osteo
Osteo + vitD 3
Relative expression Runx2
0.03
0.02
0.01
0.00
*
D14
D21
alveolar bone
long bone
C
Basic
Osteo
Osteo + vitD 3
Relative expression Col1A
20
15
10
5
0
25
D14
D21
alveolar bone
long bone

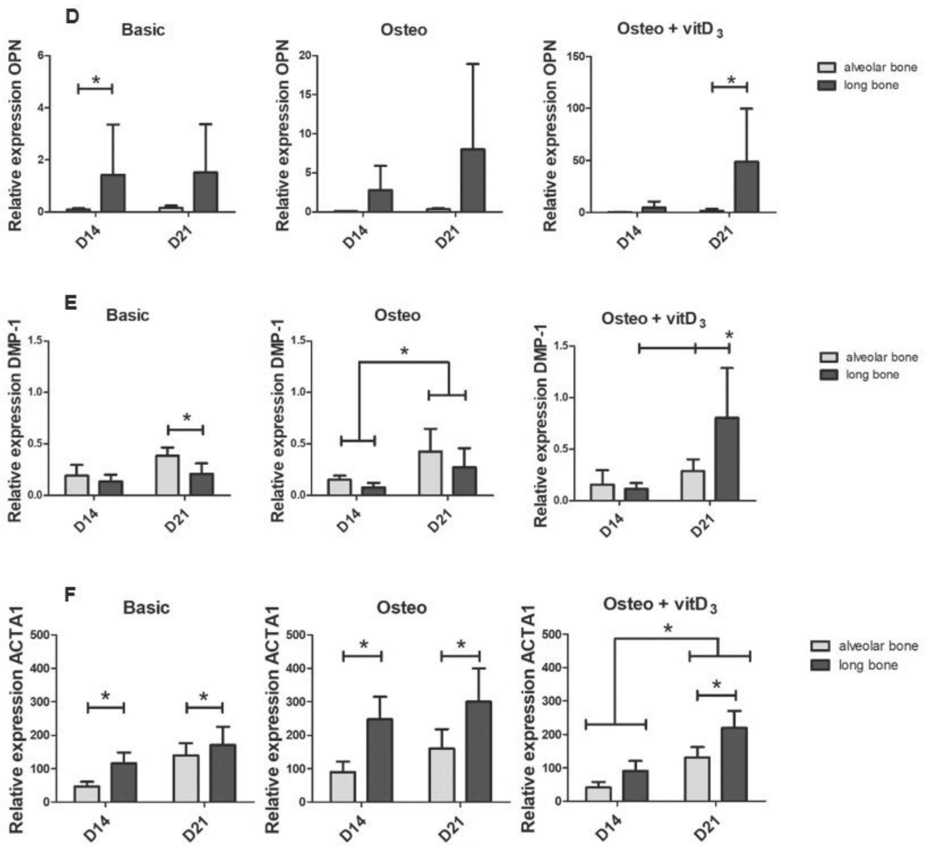

Figure 2. The osteogenic potential of the alveolar bone cells and the long bone cells in the osteogenic medium and the osteogenic medium supplemented with vitD_3. Graphs depict the relative expression in the basic, osteogenic, and osteogenic + vitD_3 conditions of the cells derived from the alveolar bone and the long bone. Since the osteogenic differentiation is usually assessed at 14 and 21 days, the expression was measured at day 14 and day 21. (**A**) Cellular alkaline phosphatase (ALP) expression corrected for the DNA levels. (**B**) *RUNX2* expression. (**C**) *Col1a* expression. (**D**) *OPN* expression. (**E**) *DMP-1* expression. (**F**) *ACTA1* expression. Significance was measured using 2-way ANOVA with Bonferroni post-tests. * $p < 0.05$.

Communication Genes in Osteogenic Conditions of Alveolar Bone Cells and Long Bone Cells

After assessing the osteogenic potential for both cell types, we next wanted to determine if the alveolar bone cells and long bone cells differed in the expression of molecules that are associated with communication. The expression of *Interleukin 6* (*IL-6*) (Figure 3A), *Cyclo-oxygenase-2* (*COX2*) (Figure 3B), and *Cysteine-rich angiogenic inducer 61* (*CYR61*) (Figure 3C) were measured. *IL-6* can be secreted by osteoblasts to stimulate the formation of osteoclasts, but *IL-6* also stimulates the differentiation of osteoblasts. At day 0, the relative expression of *IL-6* was significantly higher in long bone cells (Figure 3A). The osteogenic medium influenced the expression of *IL-6* differently in the two cell types. In the alveolar bone cells, it seems to be inhibited while it induced the expression in long bone cells. The expression was significantly higher in the long bone cells compared to the alveolar-derived bone cells (Supplementary Materials Figure S2A). The supplementation of vitD$_3$ induced the expression of *IL-6* both in the cells derived from alveolar bone and long bone, but there was no difference in the gene expression between the cells (Supplementary Materials Figure S2A). *COX2* is needed for normal fracture healing [17]. The relative expression of *COX2* was 3.3-fold higher in the long bone cells at day 0. At day 14 and day 21, the expression levels were similar between long bone and alveolar bone cells. The osteogenic medium upregulated the *COX2* expression, particularly in alveolar bone cells, leading to a 5-fold difference in the expression between the two cell types at day 21. Interestingly, supplementation with vitD$_3$ induced the expression of *COX2* in long bone cells, especially on day 21 (Supplementary Materials Figure S2B). Besides being a matrix protein, *CYR61* promotes osteogenic differentiation [18]. Long bone cells expressed more *CYR61* than alveolar bone cells, in almost all conditions, but only significantly at day 21 under basic and osteogenic conditions.

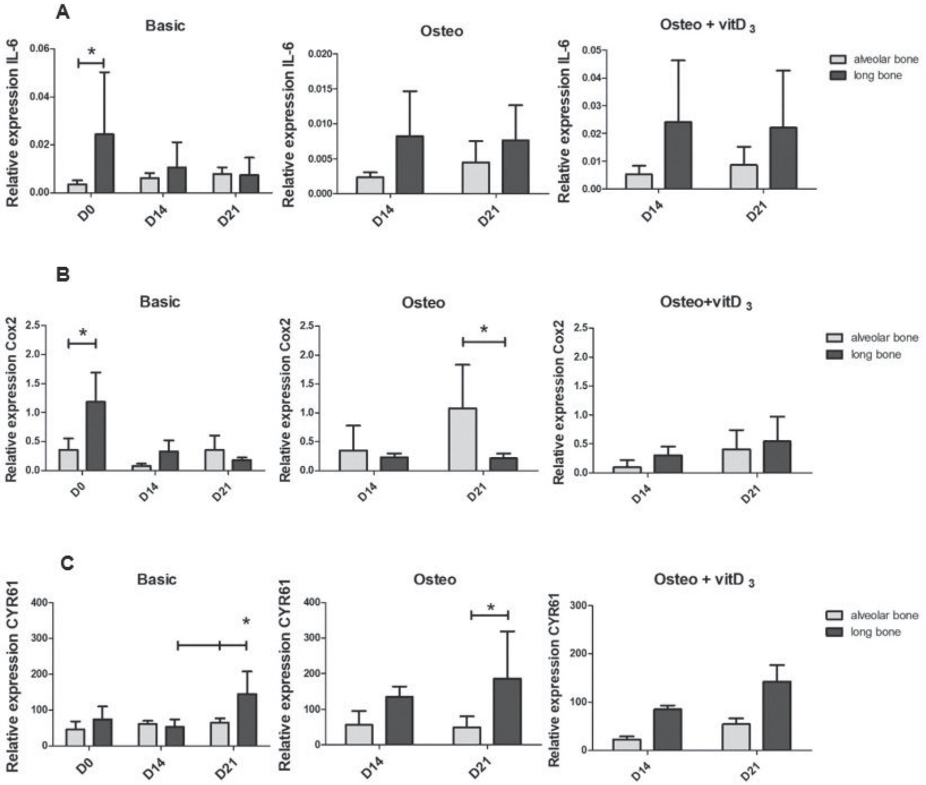

Figure 3. Differences in the expression of mRNAs associated with communication in the osteogenic conditions of the alveolar bone cells and the long bone cells. Graphs depict the relative expression in the basic, osteogenic, and osteogenic + vitD_3 conditions of the cells derived from the alveolar bone and the long bone. Relative expression was measured at day 0, day 14, and day 21. (**A**) Relative expression of *IL-6*. (**B**) Relative expression of *COX2*. (**C**) Relative expression of *CYR61*. The significance of the relative gene expression was measured using a 2-way ANOVA with Bonferroni post-tests. * $p < 0.05$.

Long Bone Cells Induce More Osteoclast Formation than Alveolar Bone Cells

Besides the osteogenic potential of both cell types, we also assessed the osteoclastogenic potential of the cell types. After 21 days of culture, the total number of osteoclasts was counted (Figure 4A). A distinction was made between the osteoclasts with 3–5 nuclei and 6+ nuclei, but only the total number of osteoclasts was shown since low numbers of larger osteoclasts were counted. On average, 19.2 ± 20.4 large osteoclasts were found in long bone, 2.9 ± 4.3 in alveolar bone, and 0.8 ± 0.5 in peripheral blood mononuclear cells (PBMCs) only (no bone) cultures. There were significantly more osteoclasts induced by long bone cells than by alveolar bone cells and PBMCs only, as a control condition. In the condition with vitD$_{3,}$ the same trend is visible although not significantly. Interestingly, similar numbers of osteoclasts were counted in alveolar bone-PBMC co-cultures as in the PBMCs alone control cultures. In this control condition, without bone-derived cells, this was 93.8 ± 51 and 100 ± 25 osteoclasts, respectively, and in the condition supplemented with vitD$_3$, it was 145.4 ± 114.8 and 104.3 ± 17.1 osteoclasts, respectively. In line with the increased osteoclast counts in long bone-PBMC co-cultures, the relative expression of osteoclast marker *DC-STAMP* was significantly higher in long bone at day 14 and day 21 (Figure 4B). At day 14, the average expression was 4.3-fold higher and 4.6-fold higher at day 21. In the condition with vitD$_{3,}$ the expression of *DC-STAMP* was higher in long bones, which was significant at day 14. The relative expression of *Tartrate-resistant acid phosphatase* (*TRAcP*) was significantly higher in the control condition in the long bone cells at day 21 (Figure 4C). In the condition with vitD$_{3,}$ there were no differences.

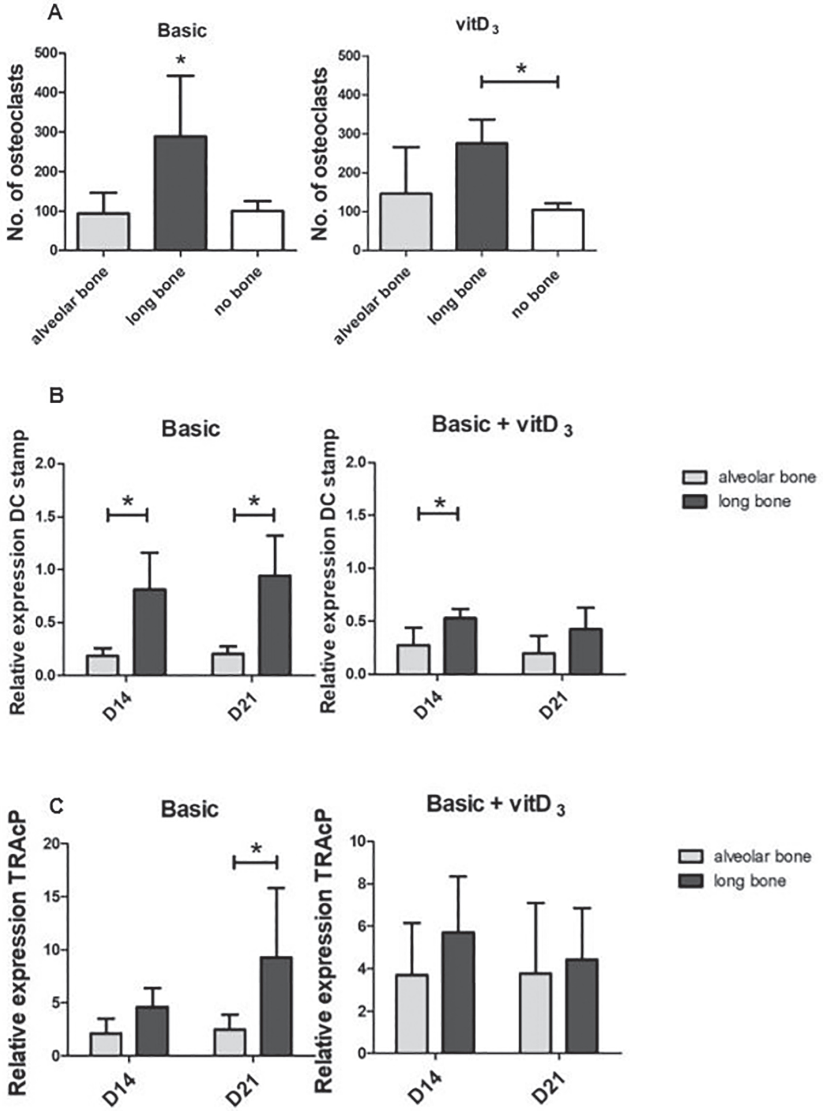

Figure 4. The osteoclastogenic potential of the alveolar bone cells and the long bone cells in the basic medium and the basic medium supplemented with vitD$_3$. The osteoclastogenic potential of the co-cultures with the PBMCs and long bone cells and the PBMCS and alveolar bone cells. Graphs depict the basic medium and the basic medium + vitD$_3$. (**A**) The total number of osteoclasts induced by the Alveolar bone cells, long bone cells, and the PBMCs alone at 21 days. Differentiation was further assessed with qPCR for osteoclast-specific genes (**B**, **C**). (**B**) The relative expression of DC-STAMP. (**C**) Relative expression of TRAcP. Significance for the number of osteoclasts was measured using a one-way ANOVA with a Tukey post-hoc test and the significance of the relative gene expression was measured using 2-way ANOVA with Bonferroni post-tests. * $p < 0.05$.

Expression of Pro-Osteoclastogenesis Proteins and mRNAs

To explain the higher numbers of osteoclasts formed during the co-culture with long bone cells, compared to the alveolar bone-derived cells, we then assessed TNF-α and Interleukin-1 beta (IL-1β) in the supernatant of the osteoclastogenesis experiments (Figure 5A). The concentrations were determined at day 7, the time point with the peak expression of TNF-α [19]. The concentration of TNF-α was significantly lower in the co-cultures with alveolar bone cells (24 pg/mL) than in the co-cultures with long bone cells (114 pg/mL) and PBMSc alone (102 pg/mL). The concentration seemed lower when vitD$_3$ was added in all groups. The concentration of IL-1β was too low to detect in all conditions. The relative expression of *IL-6* in the basic condition increased after day 0 for both cell types (Figure 5B). In the condition with vitD$_3$, no differences were present. The expression of *IL-6* in the osteoclastogenesis experiments was on average 369-fold higher at day 14 and 395-fold higher at day 21 than the *IL-6* expression in the osteogenesis experiments under basic culture conditions. The relative expression of *RankL* was higher in the long bone cells than in alveolar bone cells, significantly so at day 14 (Figure 5C). Although adding vitD$_3$ caused a significantly higher expression of *RankL* in the long bones cultures at day 14 compared to the alveolar bone co-cultures, it decreased at day 21. Osteoprotegerin (*OPG*) is an important negative regulator of osteoclast differentiation. Under basic conditions, its expression decreased at day 14 in long bone-PBMC co-cultures (Figure 5D). Supplementation with vitD$_3$ did not lead to a difference between the long bone cells and alveolar bone cells. The ratio of *RankL* and *OPG* is generally used as an indication of osteoclast differentiation. At day 14, this ratio is significantly higher (19.6-fold) in the long bone cells than in alveolar bone cells (Figure 5E), concomitant with the increased osteoclastogenesis by long bones. VitD$_3$ lowers this ratio. In alveolar bone cells, the expression of *COX2* was on average 9.2-fold higher than in long bones at day 14 and 5.6-fold at day 21 (Figure 5F). At day 14, the supplementation of vitD$_3$ led to the inhibition of *COX2* expression and induced its expression in long bone cells (Supplementary Materials Figure S3).

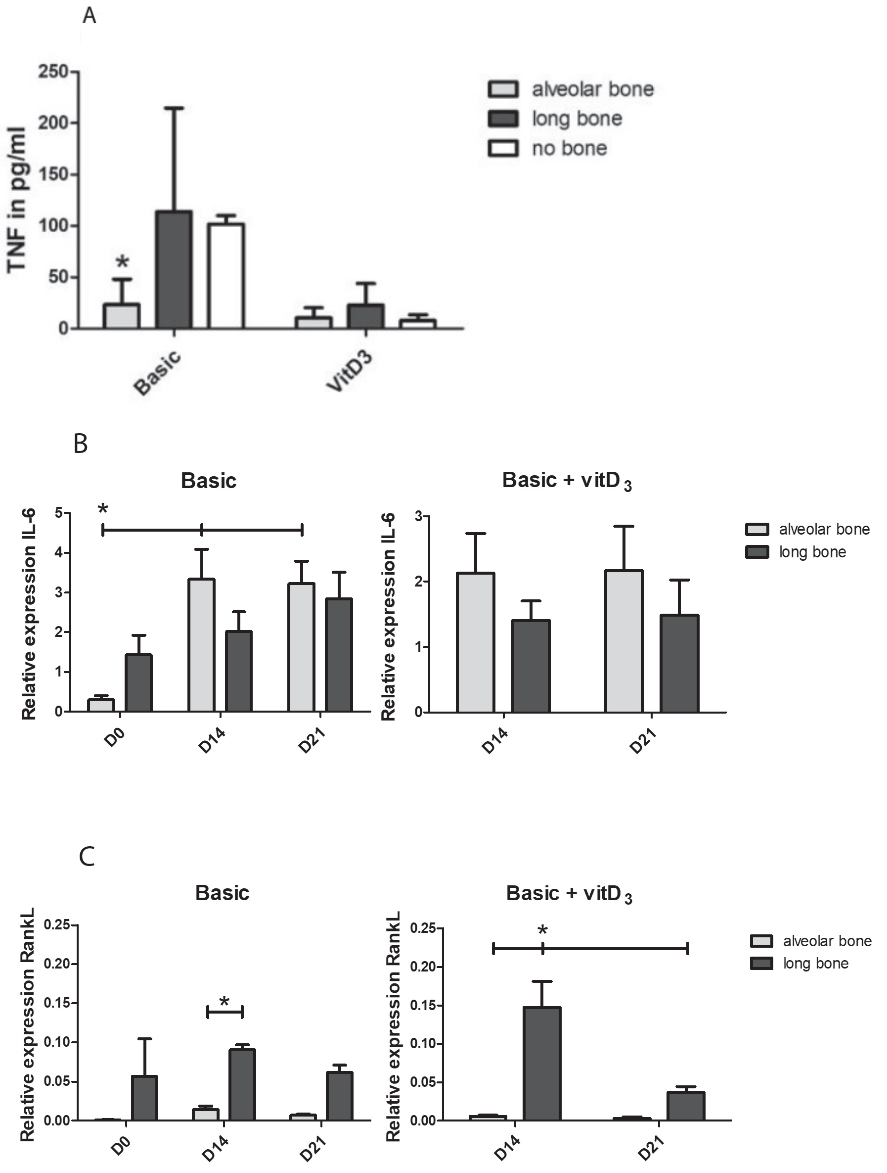
A
TNF in pg/ml
250
200
150
100
50
0
*
Basic
VitD3
alveolar bone
long bone
no bone
B
Basic
Relative expression IL-6
5
4
3
2
1
0
*
D0
D14
D21
Basic + vitD$_3$
Relative expression IL-6
3
2
1
0
D14
D21
alveolar bone
long bone
C
Basic
Relative expression RankL
0.25
0.20
0.15
0.10
0.05
0.00
*
D0
D14
D21
Basic + vitD$_3$
Relative expression RankL
0.25
0.20
0.15
0.10
0.05
0.00
*
D14
D21
alveolar bone
long bone

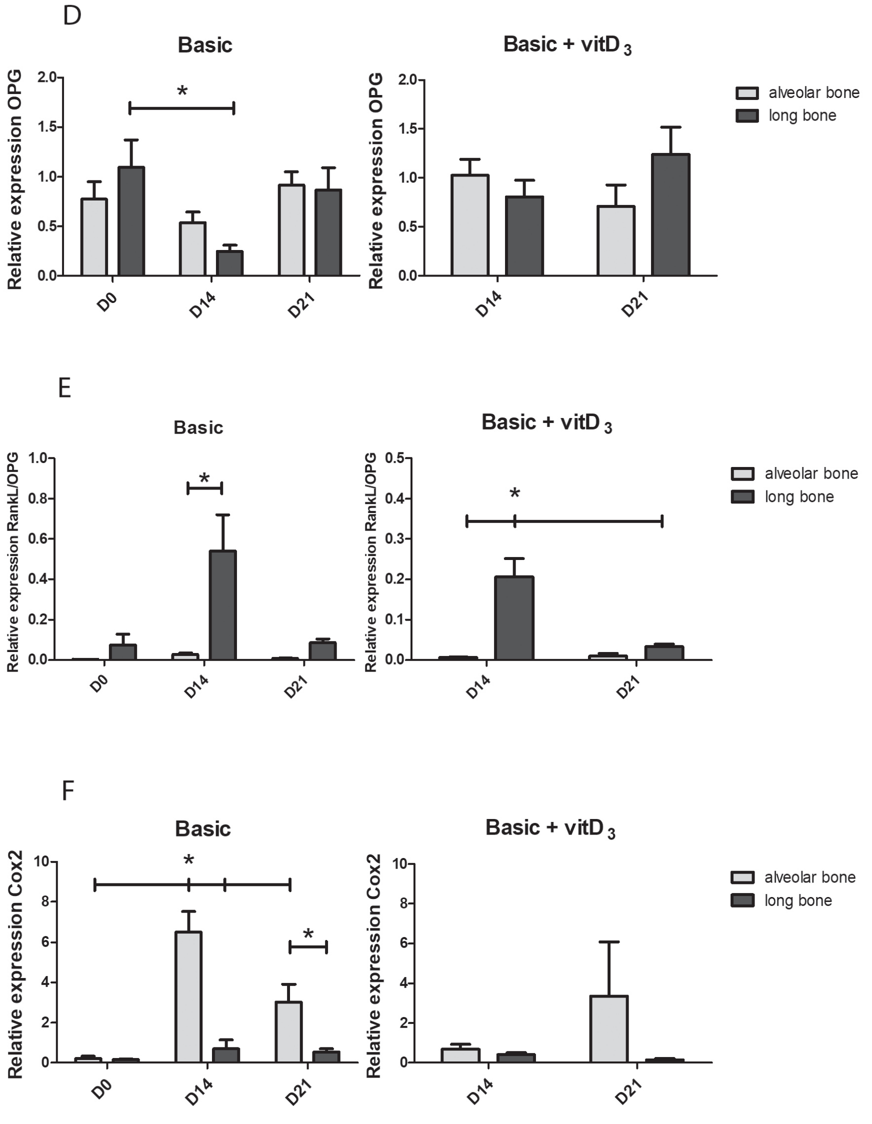

Figure 5. Differences in the proteins and the genes involved with osteoclastogenic differentiation in the alveolar bone cells and the long bone cultures. Graphs depict the basic medium and the basic medium + vitD$_3$ (**A**) Concentration of TNF-α in media at day 7. (**B**) Relative expression of *IL-6*. (**C**) Relative expression of *RankL*. (**D**) Relative expression of osteoprotegerin *(OPG)*. (**E**) The ratio *RankL/OPG* gives an indication for osteoclast activation. (**F**) Relative expression of *COX2*. Significance was measured using a 2-way ANOVA with Bonferroni post-tests. * $p < 0.05$.

Discussion

In this study, we compared the ability of bone cells derived from human alveolar and long bones to differentiate towards mature bone-forming osteoblasts, and their ability to stimulate osteoclast formation. These experiments were performed in the presence and absence of vitD$_{3,}$ since vitD$_3$ could stimulate differentiation when incorporated in tissue-engineering constructs as we have recently proposed [16]. We found that under basic conditions without VitD$_{3,}$ long bone cells seemed to be more differentiated than alveolar bone cells, both at baseline and over time. Furthermore, long bone-derived cells induced more osteoclasts than alveolar bone cells. Taken together, our results suggest that long bone-derived cells are more differentiated, more actively communicate with osteoclast precursors, and have a stronger osteoclastogenic potential than alveolar bone cells.

Although the cells derived from both skeletal locations were isolated using the same protocol, the cells differed in their basic appearance, proliferation, and expression of bone markers. The long bone cells in our study had a more cuboidal appearance at day 7, while alveolar bone cells had a fibroblastic appearance. This indicates that long bone cells have a more osteoblastic appearance from the start, as osteoblasts are cuboidal-shaped cells. In vivo, this cuboidal appearance is required for tightly connecting to neighboring cells, needed for the consort deposition of osteoid [20,21]. Alveolar bone-derived cells proliferate faster than the cells derived from long bones, and this might have to do with the higher bone turnover in the jaw [22] and is also in line with a less differentiated state. Several late to very-late bone differentiation markers (*OPN, DMP-1,* and *ACTA1*) were higher expressed in long bone cells than in alveolar bone cells (Figure 1), underscoring their more mature, differentiated phenotype. *OPN* is a protein used as a marker for osteogenic differentiation. *DMP-1* is a bone mineralization marker and is expressed in early and mature osteocytes [23]. Furthermore, *ACTA1* is highly expressed in osteocytes [24]. Taken together, our data suggest that long bone cells have a more late-osteoblastic/preosteocyte-like phenotype than alveolar bone-derived cells.

Besides the basic differences, we also compared the osteogenic differentiation of both cell types. Again, the cells derived from long bones showed a higher degree of differentiation, as *OPN* and *ACTA1* expression was higher and vitD$_3$ induced the expression of *RUNX2* and *DMP-1* more in long bone cells than in alveolar bone cells (Figure 2). This is in contrast with the stronger osteogenic potential described by Aghaloo et al. in mandibular MSCs compared to the MSCs from long bones [25]. This difference might lie in the cell source; they used cells derived from rats, we used cells from human donors.

Rats continue to grow throughout their lifespan, whereas humans do not. Moreover, alveolar bone-derived cells might differ from the cells derived elsewhere from the mandibula. Differences in the effect of vitD$_3$ on osteoblasts were also found in murine osteoblasts, where vitD$_3$ had no effect on the osteoblast derived from long bones while inhibiting mineralization by calvarial osteoblasts [26]. In this study, both the cells derived from alveolar bone and long bone did not mineralize at day 21. Ruppeka-Rupeika et al. showed that alveolar bone-derived cells are capable of forming mineralizing nodules at day 21 [27]. One of the differences between the study by Ruppeka-Rupeika and our study is the serum that was used to culture the cells. They only used FC1, while for the current comparison we used a combination of FC1 and FC3 for both cell types, since in our laboratory, the alveolar bone cells were routinely cultured in FC1 and the long bone cells in FC3. This difference indicates that the lack of nodule formation in both alveolar bone cells and long bone cells in the present study might be a result of the serum used. In any case, the cells from both origins showed an equal lack of bone nodule formation.

We also investigated the osteoclastogenic potential of the cells derived from alveolar bone and long bone. Long bone-derived bone cells stimulated the formation of osteoclasts, while alveolar bone-derived cells did not, since numbers were comparable to the control condition without the bone cells added (Figure 4). Jaw and long bone-derived cells from the bone marrow of mice have different osteoclastogenic potential, mostly due to the differences in the cellular composition of the bone marrow [11]. This might also be true for the population of cells isolated by the outgrowth of cells. In line with the increased osteoclast formation induced by long bone cells is the higher expression of *RANKL*, TNF-α, and *IL-6* in long bone-PBMC co-cocultures, as well as in the increased *RANKL/OPG* ratio that favors osteoclast formation. Moreover, DC-STAMP is needed for cell-cell fusion [28] and was significantly higher expressed in the long bone-PBMC co-cultures in basic conditions, supporting our finding that the cells derived from long bones induced the formation of more osteoclasts. Interestingly, the supplementation of vitD$_3$ seemed to downregulate the expression of DC-STAMP in both co-cultures of PBMCs with long bone cells and with alveolar bone cells (Supplementary Materials Figure S4), which correlates with a lower number of osteoclasts counted in the condition with vitD$_3$. *COX2* expression was significantly higher expressed in alveolar bone cells. *COX2* is very important for fracture healing and plays a role in both osteoblast and osteoclast differentiation [29]. The inhibition of COX2 inhibits osteoclast formation [30], and this would suggest that the higher expression of *COX2* would induce osteoclast formation, which is in contrast with our data.

VitD_3 is a biological component used in bone regeneration because it promotes the osteogenic differentiation of hMSCs by the upregulation of ALP and enhancing mineralization [31]. In the present study, the addition of vitD_3 did not upregulate the cellular ALP, neither in alveolar bone cells nor in long bone cells. This might be because these cells are already in the osteogenic lineage and ALP is in general an early marker. Supplementation with vitD_3 did enhance the expression of other osteogenic markers, such as *OPN* and *DMP-1*. VitD_3 affects osteoclast formation by upregulating *RANKL* expression in human SaOS2 osteoblastic cells [32]. In contrast, supplementation with vitD_3 to our human primary osteoblasts did not upregulate *RANKL* expression, and thereby did not enhance osteoclast formation.

Our results are measured in the absence of mechanical loading, which is not representative of the in vivo situation, wherein both the jaw as in the tibia, mechanical loading is present. Mechanical loading is known to have an enhancing effect on osteoblasts and a restrained effect on osteoclasts [33]. Adding mechanical loading to the cells would be interesting for further research on the differences in skeletal sites.

Due to donor to donor variability, some results had high SDs, which is observed more often when using human primary cells from multiple donors [16]. This high variance is inevitable, due to a higher degree of genetic differences between human individuals when compared to e.g., cells from inbred mouse or rat strains. Despite the variance between donors, many striking differences were observed in the present study. On the one hand, we would like to advocate such a comparison using cells from actual human donors, since it is likely closer to clinical reality when compared to using laboratory animals. On the other hand, and unfortunately, the cells derived from alveolar bone were not from the same donor as the cells derived from long bones, which would have made this study stronger. However, we can still see clear statistically significant differences between the cells derived from alveolar bone and long bone, which suggests that the two populations of cells are different. Many results were confirmed using different techniques, for instance, the osteoclasts were higher in long bone cultures, which was confirmed with the qPCRs of osteoclast genes expressed in these cultures.

In conclusion, the results of this present study showed that the cells derived from alveolar bone and long bone differ in their expression of osteogenic markers and their ability to induce osteoclast formation. We have to reject our hypothesis, as the results show that long bone cells instead of alveolar bone cells are more differentiated within the osteogenic lineage, and have increased osteoclastogenic potential. We show that cells from different skeletal sites, in this case, alveolar bone, and long bone, are different and react differently to osteotropic agent vitD_3. These differences show that skeletal sites give rise to site-specific differences between the cells and indicate, that for the regeneration of specific sites, such as the alveolar bone, more research on site-specific tissue-engineering constructs is necessary.

Acknowledgments

We want to thank Behrouz Zandieh Doulabi and Jolanda M.A. Hogervorst from the department of Oral Cell Biology, ACTA for performing qPCR analysis.

Supplementary Figures

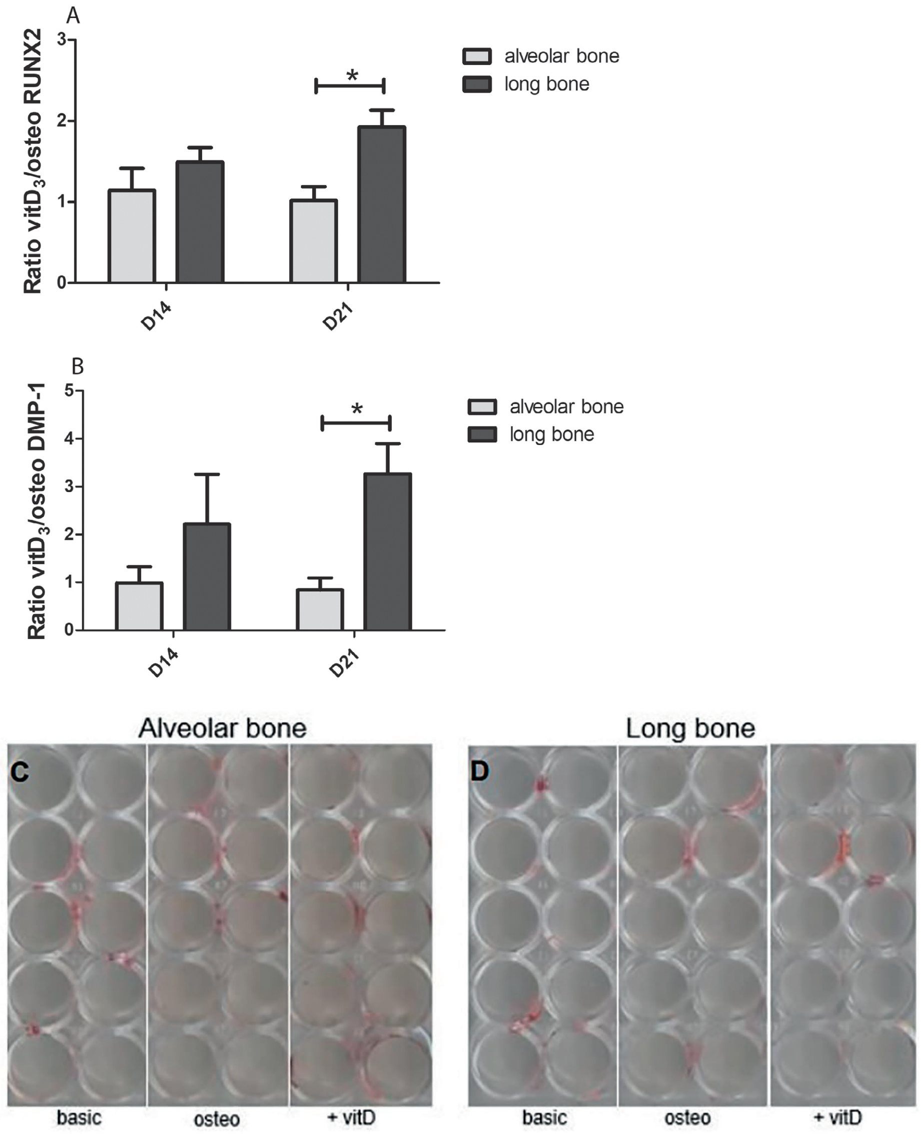

Figure S1. Graphs depict the osteogenic medium + vitD$_3$ over the osteogenic medium at day 14 and day 21. (**A**) Effect of vitD$_3$ on the *RUNX2* expression. vitD$_3$ had more effect on the long bone cells, which is significantly different on day 21. (**B**) Effect of vitD$_3$ on the *DMP-1* expression. vitD$_3$ had more effect on long bone cells, which is significantly different on day 21. (**C**) Alizarin red staining for the calcium deposits. No calcium deposits were visible for both the alveolar bone cells and the long bone cells. Significance was measured using a 2-way ANOVA with Bonferroni post-tests. * = $p < 0.05$.

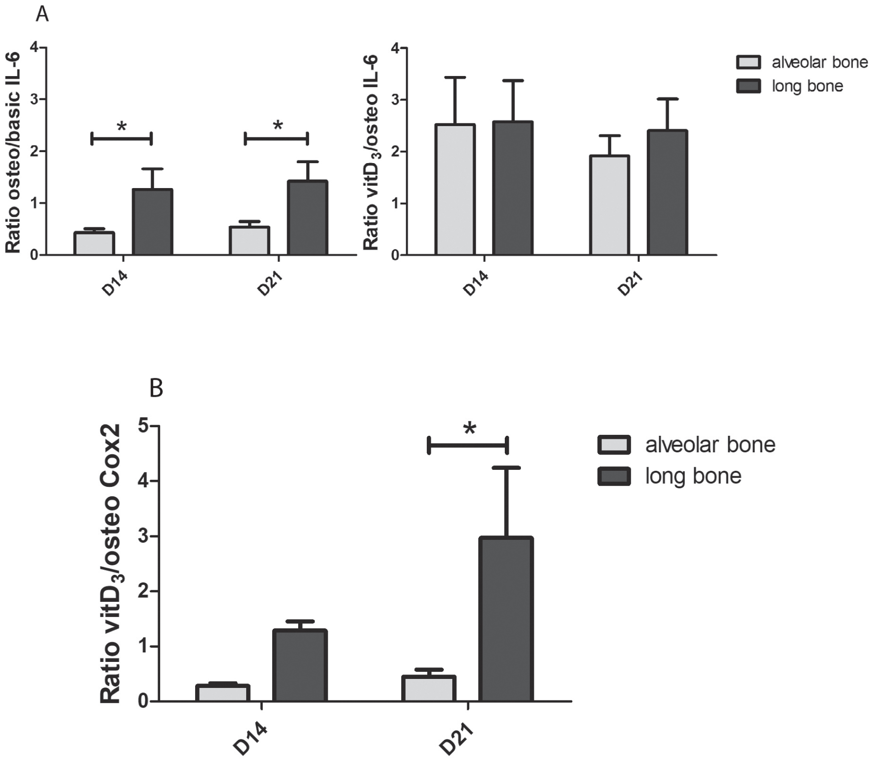

Figure S2. Graphs depict osteogenic medium over the basic or the osteogenic medium + vitD$_3$ over the osteogenic medium. (**A**) Osteogenic medium significantly increased the expression of *IL-6* in the long bone cells. Supplementation of vitD$_3$ upregulated the *IL-6* expression in both the alveolar bone cells and the long bone cells. (**B**) Effect of vitD$_3$ on the *COX2* expression. VitD$_3$ had more effect on the long bone cells, which is significantly different on day 21. Significance was measured using 2-way ANOVA with Bonferroni post-tests. * = $p < 0.05$.

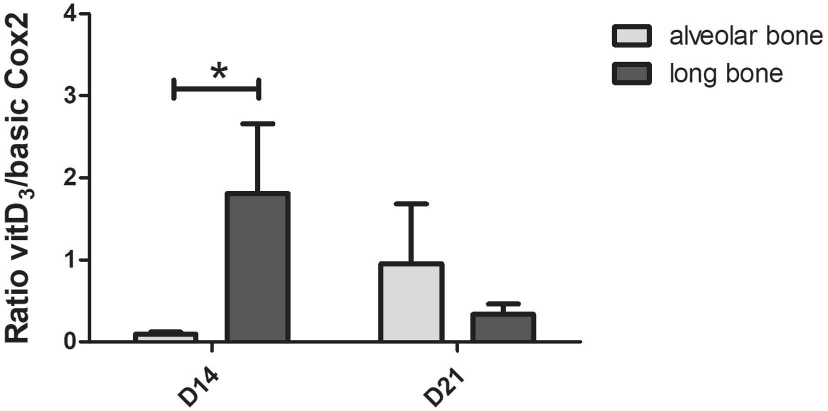

Figure S3. Graphs depicts the basic medium + vitD$_3$ over the basic medium. Effect of vitD$_3$ on the *COX2* expression. On day 14, vitD$_3$ significantly upregulated the *COX2* expression. Significance was measured using 2-way ANOVA with Bonferroni post-tests. * = $p < 0.05$.

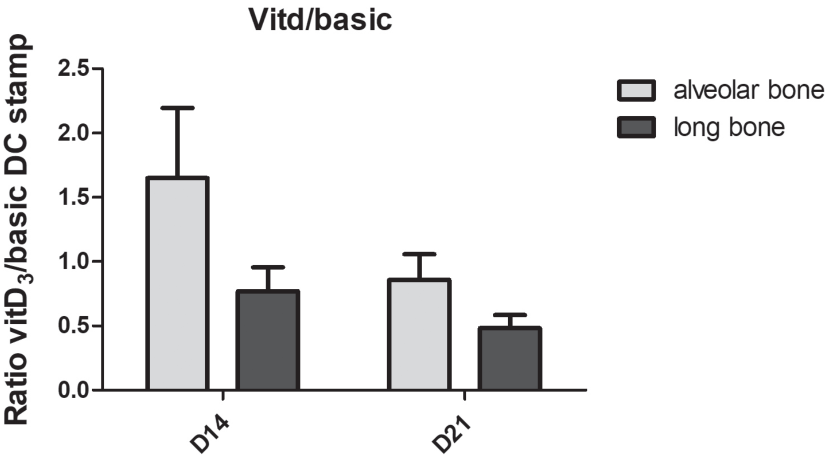

Figure S4. Graphs depict the basic medium + vitD$_3$ over the basic medium. (A) Effect of vitD$_3$ on the *DC stamp* expression. Significance was measured using 2-way ANOVA with Bonferroni post-tests.

References

50. Wan, Q.; Schoenmaker, T.; Jansen, I.D.C.; Bian, Z.; de Vries, T.J.; Everts, V. Osteoblasts of calvaria induce higher numbers of osteoclasts than osteoblasts from long bone. *Bone* **2016**, *86*, 10–21.
51. Anderson, D.J. Cellular and molecular biology of neural crest cell lineage determination. *Trends Genet*. **1997**, *13*, 276–280.
52. Akintoye, S.O.; Lam, T.; Shi, S.; Brahim, J.; Collins, M.T.; Robey, P.G. Skeletal site-specific characterization of orofacial and iliac crest human bone marrow stromal cells in same individuals. *Bone* **2006**, *38*, 758–768.
53. Osyczka, A.M.; Damek-Poprawa, M.; Wojtowicz, A.; Akintoye, S.O. Age and Skeletal Sites Affect BMP-2 Responsiveness of Human Bone Marrow Stromal Cells. *Connect. Tissue Res.* **2009**, *50*, 270–277.
54. Watts, N.B.; Diab, D.L. Long-Term Use of Bisphosphonates in Osteoporosis. *J. Clin. Endocrinol. Metab.* **2010**, *95*, 1555–1565.
55. Ruggiero, S.L.; Mehrotra, B.; Rosenberg, T.J.; Engroff, S.L. Osteonecrosis of the Jaws Associated with the Use of Bisphosphonates: A Review of 63 Cases. *J. Oral Maxillofac. Surg.* **2004**, *62*, 527–534.
56. Shane, E.; Goldring, S.; Christakos, S.; Drezner, M.; Eisman, J.; Silverman, S.; Pendrys, D. Osteonecrosis of the jaw: More research needed. *J. Bone Miner. Res.* **2006**, *21*, 1503–1505.
57. Saita, Y.; Kaneko, K.; Ishijima, M. Atypical femoral fractures and bisphosphonate use: Current evidence and clinical implications. *Ther. Adv. Chronic Dis.* **2015**, *6*, 185–193.
58. Schilcher, J.; Michaëlsson, K.; Aspenberg, P. Bisphosphonate use and atypical fractures of the femoral shaft. *N. Engl. J. Med.* **2011**, *364*, 1728–1737.
59. Crockett, J.C.; Rogers, M.J.; Coxon, F.P.; Hocking, L.J.; Helfrich, M.H. Bone remodelling at a glance. *J. Cell Sci.* **2011**, *124*, 991–998.
60. De Souza Faloni, A.P.; Schoenmaker, T.; Azari, A.; Katchburian, E.; Cerri, P.S.; De Vries, T.J.; Everts, V. Jaw and long bone marrows have a different osteoclastogenic potential. *Calcif. Tissue Int.* **2011**, *88*, 63–74. [CrossRef] [PubMed]
61. Trubiani, O.; Marconi, G.D.; Pierdomenico, S.D.; Piatelli, A.; Diomede, F.; Pizzicannella, J. Human oral stem cells, biomaterials and extracellular vesicles: A promising tool in bone tissue repair. *Int. J. Mol. Sci.* **2019**, *20*, 4987.
62. Marconi, G.D.; Diomede, F.; Pizzicannella, J.; Fonticoli, L.; Merciaro, I.; Pierdomenico, S.D.; Mazzon, E.; Piatelli, A.; Trubiani, O. Enhanced VEGF/VEGF-R and RUNX2 Expression in human periodontal ligament stem cells cultured on sandblasted/etched titanium disk. *Front. Cell Dev. Biol.* **2020**, *14*, 315.
63. Liu, P.; Oyajobi, B.O.; Russell, R.G.G.; Scutt, A. Regulation of Osteogenic Differentiation of Human Bone Marrow Stromal Cells: Interaction Between Transforming Growth Factor-β and 1,25(OH)2 Vitamin D3In Vitro. *Calcif. Tissue Int.* **1999**, *65*, 173–180.

64. Haussler, M.R.; Whitfield, G.K.; Kaneko, I.; Haussler, C.A.; Hsieh, D.; Hsieh, J.C.; Jurutka, P.W. Molecular mechanisms of vitamin D action. *Calcif. Tissue Int.* **2013**, *92*.
65. Kelder, C.; Hogervorst, J.M.A.; Wismeijer, D.; Kleverlaan, C.J.; de Vries, T.J.; Bakker, A.D. Burst, short, and sustained vitamin D_3 applications differentially affect osteogenic differentiation of human adipose stem cells. *Int. J. Mol. Sci.* **2020**, *21*, 3202.
66. Simon, A.M.; Manigrasso, M.B.; O'Connor, J.P. Cyclo-oxygenase 2 function is essential for bone fracture healing. *J. Bone Miner. Res.* **2002**, *17*, 963–976.
67. Su, J.L.; Chiou, J.; Tang, C.H.; Zhao, M.; Tsai, C.H.; Chen, P.S.; Chang, Y.W.; Chien, M.H.; Peng, C.Y.; Hsiao, M.; et al. CYR61 regulates BMP-2-dependent osteoblast differentiation through the αvβ3 integrin/integrin-linked kinase/ERK pathway. *J. Biol. Chem.* **2010**, *285*, 31325–31336.
68. de Vries, T.J.; Yousovich, J.; Schoenmaker, T.; Scheres, N.; Everts, V. Tumor necrosis factor-α antagonist infliximab inhibits osteoclast formation of peripheral blood mononuclear cells but does not affect periodontal ligament fibroblast-mediated osteoclast formation. *J. Periodontal Res.* **2016**, *51*, 186–195.
69. Florencio-Silva, R.; Sasso, G.R.D.S.; Sasso-Cerri, E.; Simões, M.J.; Cerri, P.S. Biology of Bone Tissue: Structure, Function, and Factors That Influence Bone Cells. *Biomed Res. Int.* **2015**, *2015*, 421746.
70. Wrobel, E.; Leszczynska, J.; Brzoska, E. The Characteristics Of Human Bone-Derived Cells (HBDCS) during osteogenesis in vitro. *Cell. Mol. Biol. Lett.* **2016**, *21*, 26.
71. Huja, S.S.; Fernandez, S.A.; Hill, K.J.; Li, Y. Remodeling dynamics in the alveolar process in skeletally mature dogs. *Anat. Rec. Part A Discov. Mol. Cell. Evol. Biol.* **2006**, *288*, 1243–1249.
72. Gluhak-Heinrich, J.; Ye, L.; Bonewald, L.F.; Feng, J.Q.; MacDougall, M.; Harris, S.E.; Pavlin, D. Mechanical Loading Stimulates Dentin Matrix Protein 1 (DMP1) Expression in Osteocytes In Vivo. *J. Bone Miner. Res.* **2003**, *18*, 807–817.
73. Paic, F.; Igwe, J.C.; Nori, R.; Kronenberg, M.S.; Franceschetti, T.; Harrington, P.; Kuo, L.; Shin, D.G.; Rowe, D.W.; Harris, S.E.; et al. Identification of differentially expressed genes between osteoblasts and osteocytes. *Bone* **2009**, *45*, 682–692.
74. Aghaloo, T.L.; Chaichanasakul, T.; Bezouglaia, O.; Kang, B.; Franco, R.; Dry, S.M.; Atti, E.; Tetradis, S. Osteogenic potential of mandibular vs. Long-bone marrow stromal cells. *J. Dent. Res.* **2010**, *89*, 1293–1298.
75. Yang, D.; Atkins, G.J.; Turner, A.G.; Anderson, P.H.; Morris, H.A. Differential effects of 1,25-dihydroxyvitamin D on mineralisation and differentiation in two different types of osteoblast-like cultures. *J. Steroid Biochem. Mol. Biol.* **2013**, *136*, 166–170.
76. Ruppeka-Rupeika, E.; Hogervorst, J.; Wouters, F.; Schoenmaker, T.; Forouzanfar, T.; de Vries, T.J. Osteogenic and osteoclastogenic potential of jaw bone-derived cells—A case study. *J. Cell. Biochem.* **2018**, *119*, 5391–5401.
77. Vignery, A. Macrophage fusion: The making of osteoclasts and giant cells. *J. Exp. Med.* **2005**, *202*, 337–340.

78. Kellinsalmi, M.; Parikka, V.; Risteli, J.; Hentunen, T.; Leskelä, H.V.; Lehtonen, S.; Selander, K.; Väänänen, K.; Lehenkari, P. Inhibition of cyclooxygenase-2 down-regulates osteoclast and osteoblast differentiation and favours adipocyte formation in vitro. *Eur. J. Pharmacol.* **2007**, *572*, 102–110.
79. Kawashima, M.; Fujikawa, Y.; Itonaga, I.; Takita, C.; Tsumura, H. The effect of selective cyclooxygenase-2 inhibitor on human osteoclast precursors to influence osteoclastogenesis in vitro. *Mod. Rheumatol.* **2009**, *19*, 192–198.
80. Lou, Y.-R.; Toh, T.C.; Tee, Y.H.; Yu, H. 25-Hydroxyvitamin D_3 induces osteogenic differentiation of human mesenchymal stem cells. *Sci. Rep.* **2017**, *7*, 42816.
81. Kitazawa, S.; Kajimoto, K.; Kondo, T.; Kitazawa, R. Vitamin D_3 supports osteoclastogenesis via functional vitamin D response element of human RANKL gene promoter. *J. Cell. Biochem.* **2003**, *89*, 771–777.
82. Guo, Y.; Wang, Y.; Liu, Y.; Wang, H.; Guo, C.; Zhang, X.; Bei, C. Effect of the same mechanical loading on osteogenesis and osteoclastogenesis in vitro. *Chin. J. Traumatol.* **2015**, *18*, 150–156.
83. Lowry, H.O. Micromethods for the assay of enzyme II. Specofic procedures. Alkaline phosphatase. *Methods Enzymol.* **1955**, *4*, 371–372.
84. Moonen, C.G.J.; Karlis, G.D.; Schoenmaker, T.; Forouzanfar, T.; Loos, B.G.; de Vries, T.J. T cell proliferation is induced by chronically tlr2-stimulated gingival fibroblasts or monocytes. *Int. J. Mol. Sci.* **2019**, *20*, 6134.

4

The 3D-Printing of Calcium Phosphate with K-Carrageenan under Conditions Permitting the Incorporation of Biological Components—A Method

Journal of functional biomaterials (2018)

Abstract

Critical-size bone defects are a common clinical problem. The golden standard to treat these defects is autologous bone grafting. Besides the limitations of availability and co-morbidity, autografts have to be manually adapted to fit in the defect, which might result in a sub-optimal fit and impaired healing. Scaffolds with precise dimensions can be created using 3-dimensional (3D) printing, enabling the production of patient-specific, 'tailor-made' bone substitutes with an exact fit. Calcium phosphate (CaP) is a popular material for bone tissue engineering due to its biocompatibility, osteoconductivity, and biodegradable properties. To enhance bone formation, a bioactive 3D-printed CaP scaffold can be created by combining the printed CaP scaffold with biological components such as growth factors and cytokines, e.g., vascular endothelial growth factor (VEGF), bone morphogenetic protein-2 (BMP-2), and interleukin-6 (IL-6). However, the 3D-printing of CaP with a biological component is challenging since production techniques often use high temperatures or aggressive chemicals, which hinders/inactivates the bioactivity of the incorporated biological components. Therefore, in our laboratory, we routinely perform extrusion-based 3D-printing with a biological binder at room temperature to create porous scaffolds for bone healing. In this method paper, we describe in detail a 3D-printing procedure for CaP paste with K-carrageenan as a biological binder.

Introduction

Critical size bone defects caused by trauma, bone cancer, congenital defects, and overloading are a common clinical problem for which the standard treatment is autologous bone grafts [1,2]. These grafts are used in dentistry, oral and maxillofacial surgery, and orthopaedic surgery to stimulate the formation of new bone. However, current treatment options have significant limitations, i.e., autologous bone grafts are only available in limited volume, and a second surgery is needed for the harvesting procedure which is often associated with co-morbidity [3]. Importantly, autografts have to be manually adapted to fit the defect area. Unfortunately, the achieved fit is not precise, leaving lacunae in the contact area between the autograft and the defect border, which may impair bone healing and prolong the healing period. 3D-printing offers a solution to this problem by enabling the reproducible production of clinically relevant scaffolds of precise dimensions, tailor-made to fit the defect, thereby facilitating bone regeneration.

CaP in scaffolds is often used for bone regeneration since the crystals in CaP-containing scaffolds resemble the hydroxyapatite in natural bone, and the scaffolds are biocompatible. In addition, most forms of CaP dissolve chemically or are resorbed by osteoclasts in the human body, rendering the scaffolds bioresorbable [4]. Subsequently, the CaP can re-precipitate thereby transforming the scaffold surface, which stimulates the formation of bone [5,6].

3D-printing is a term that describes techniques that create objects in a layered fashion. Additive manufacturing techniques used in the medical field today include SLA, selective laser sintering, selective laser melting, and extrusion-based printing. 3D-printing is based on computer-aided planning and 3D-design by using digital modeling and imaging technology (i.e., computer-aided design, or CAD). Therefore, shapes, geometries, and internal structures can be precisely defined. In addition, this method allows for the layer-by-layer build-up of the construct with proteins, drugs, and/or peptides, enabling localized characteristics to fit explicit functions of the construct at a specific site.

Several 3D-printing techniques can be used to fabricate CaP scaffolds. The two major types of printing used to print CaP are powder printing and extrusion-based printing. In extrusion-based printing, materials are extruded from a nozzle. This technique is gaining more and more interest as it can be carried out at room temperature and allows for the incorporation of biological components and/or cells [7–10]. Extrusion-based printing of CaP is often based on the combination of particles with a polymer.

For example, hydroxyapatite particles can be combined with PCL and polylactic-co-glycolic acid (PLGA) [11].

In powder printing, a layer is created by binding particles in a powder bed, either by sintering with a laser (SLS) or binding by drops of liquid (3D-powder printing) [12,13]. Both SLS and 3D-powder printing are used to bind CaP particles together, thereby creating porous and interconnected scaffolds. Unfortunately, these types of scaffolds are often not very strong, and need additional treatment, such as sintering or chemical treatment, to improve the strength of the scaffold [12,14].

Most CaP scaffolds have very good osteoconductive properties, i.e., they allow the bone to grow along their surfaces. To speed up the bone healing process, the scaffold should actively stimulate de novo bone formation and vascularization throughout the defect. Active stimulation can be achieved by adding biological components, such as bone morphogenetic protein-2 (BMP-2) and vascular endothelial growth factor (VEGF), to scaffolds to enhance vascularization and bone formation [15,16]. The prime method to add biological components to a scaffold is adhesion to the scaffold's surface. However, this method results in a burst release of the biomolecules in the first hours after incorporation into a defect site [17]. Such a burst release is often disadvantageous since high levels of biological factors are released following an uncontrolled release pattern during a short period of time, thereby possibly causing complications. A solution to this problem might be provided by the incorporation of components into the scaffold, resulting in a more sustained release pattern [18].

The printing of CaP for drug and growth factor delivery is challenging. Techniques using high temperatures or aggressive chemicals, such as SLS and 3D-powder printing, hinder the bioactivity of the incorporated biological components since cells and proteins that are active at body temperature lose their bioactivity at these high temperatures or are denatured by the chemicals. Extrusion-based printing is an option for achieving the incorporation of active growth factors, as this type of printing can operate at room temperature and use biological binders such as collagen and carrageenan. Carrageenan is derived from red seaweed and resembles the glycosaminoglycans (GAGs) in the extracellular matrix [19]. Other desirable properties are the interconnected porous network, elastic behaviour, and the ability to encapsulate cells [20,21]. The 3D-printing of CaP allows the incorporation of the biological component in the CaP and/or in the biological binder when it is performed at room temperature. Although several studies show printing methods for CaP at mild conditions [11,22–25], only a few studies show the incorporation of biological components such as growth factors [26,27]. Therefore, in our laboratory, we have developed a method to print CaP at room temperature, permitting the incorporation of biologically active factors. The aim of the current methods paper is to describe a method to perform 3D-printing with CaP paste combined with the biological binder K-carrageenan under mild conditions in sufficient detail to serve as a basis for experiments by other laboratories.

Material and Methods

Production of Calcium Phosphate Paste

The CaP paste is produced by a precipitation reaction according to a modified version of a coating protocol described earlier [18,28]. In brief, a supersaturated CaP solution containing 684 mM NaCl (31434-1KG-M, Sigma-Aldrich, St Louis, MO, USA), 20 mM $CaCl_2{\cdot}2H_2O$ (102382, Merck Millipore, Darmstadt, Germany), 10.1 mM $Na_2HPO_4{\cdot}2H_2O$ (106580, Merck Millipore, Darmstadt, Germany), and 200 mM HCl (100317, Merck Millipore, Darmstadt, Germany) is made.

The pH is increased from approximately 0.83 to 7.4 (range: 7.35–7.45) by adding TRIS (252859-500G, Sigma-Aldrich, St Louis, MO, USA). After adjusting the pH of the solution, incubation is performed overnight in a shaking water bath at 37 °C to allow CaP precipitation. After incubation, the precipitate (Figure 1A) is retrieved by removing (careful pouring) as much as possible of the supernatant. This precipitate is poured into sterile 50 mL tubes and centrifuged at 1000× *g* for 10 min. The supernatant is removed and discarded. Then PBS (14200-067, Thermo Fisher Scientific, Waltham, MA, USA) is added and the solution is mixed by shaking to wash the precipitate. After five repetitions of washing, centrifuging, and pouring off the supernatant, the last supernatant is removed. The result is a layer of CaP precipitate, from which the remaining moisture is removed by filtering with a 0.22 µm PES bottle top filter (431161, Corning Incorporated, Corning, New York, NY, USA) and an air pump until cracks appear in the CaP (Figure 1B, C). Before water removal with the filter, the CaP 'slurry' obtained from 1 L CaP solution is approximately 13.87 g. After water removal, approximately 7.52 g of CaP paste remains (Figure 1D). After preparation, the CaP paste is stored in a syringe with a cap at room temperature. It is advised to use the paste within one week, as water evaporation will occur, thereby significantly influencing the structure of the paste.

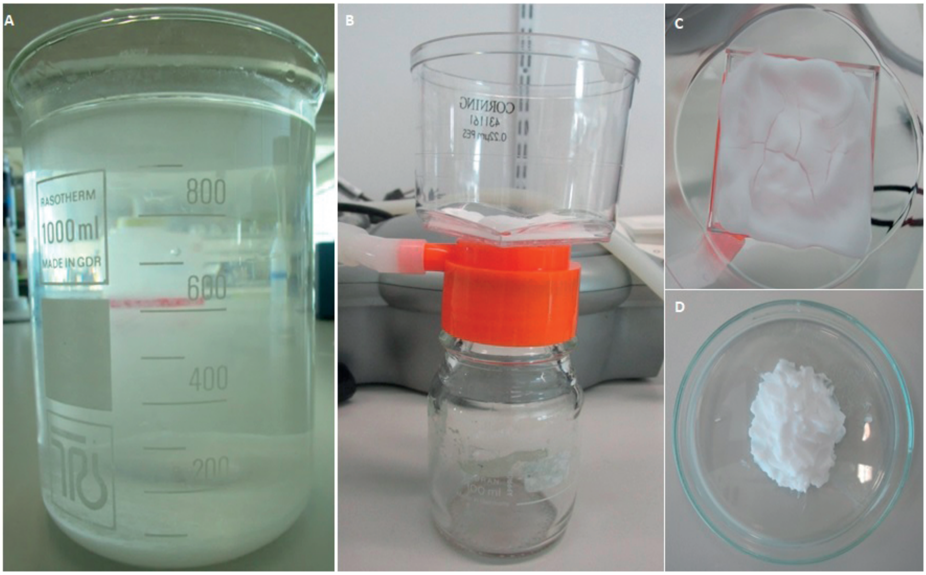

Figure 1. The calcium phosphate precipitation and calcium phosphate paste preparation. (**A**) CaP precipitate after overnight incubation; (**B**) Remaining moisture is removed from the CaP precipitate with a bottle top filter; (**C**) Cracks are formed in the CaP paste, indicating that water removal is sufficient to allow for printing; (**D**) CaP paste is ready to be used for 3D-printing.

Mixing

To print the CaP (with/without biological factors), a K-carrageenan (C1804, TCI, Tokyo, Japan) solution with a K-carrageenan concentration of 2.8% (wt/vol; kindly provided by Prof. S. Matsukawa, Tokyo) is mixed with the earlier prepared CaP paste in a 1:1.9 (wt/vol) ratio. The K-carrageenan solution is weighed and heated to 37 ◦C in a water bath. The amount of CaP paste is determined with a 5- or 10-mL syringe and added to the K-carrageenan in a 7 mL plastic container. To a homogeneous mixture, sonication is performed using a sonicator (Vibra cell™, VCX 400, Sonics, Newtown, CT, USA) with the following settings: amplitude: 20%; pulse: alternating 1.0 s 'on' and 1.0 s 'off' for 90 s. The mixture is then loaded into a printing cartridge, and ready to be printed.

Incorporation and Release of Biological Factors

To show the incorporation of biological factors in our scaffolds, bovine serum albumin, fluorescein conjugate (BSA-FITC; Molecular Probes, Eugene, OR, USA) is used as a model biological factor. To incorporate the model factor in the CaP paste, the BSA-FITC is added to the precipitate after the washing steps. A total of 100 µL of a 10 mg/mL BSA-FITC solution is added to approximately 10 mL precipitate and mixed with a spatula. Thereafter the standard protocol can be followed by drying the precipitate. To incorporate BSA-FITC in K- carrageenan, 10 µL of 10 mg/mL BSA-FITC is added to the warm (37 –C) K-carrageenan solution and mixed with a spatula. The standard protocol can be followed by adding the appropriate amount of CaP paste and mixing it with sonication. After 3D-printing, images are made with a Leica fluorescence microscope (Leica Microsystems, Wetzlar, Germany). For each condition (BSA-FITC in CaP paste, BSA-FITC in K-carrageenan, and control without BSA-FITC), a scaffold is placed in 2 mL of PBS to measure the release of BSA-FITC from the scaffold. Per condition, the release from 3 scaffolds is measured. At day 3, a 200 µL sample is taken and assayed, in duplicate, for fluorescence intensity at 520 nm with a Synergy HT® spectrophotometer (BioTek Instruments, Winooski, VT, USA).

Three-Dimensional Printing

For 3D-printing, a pneumatic-driven printing head of a 3D-Discovery printer (RegenHU, Fribourg, Switzerland) is used. Before placing the printing cartridge in the printhead, a 23 G (inner diameter: 0.33 mm) blunt needle (Cellink®, Gothenburg, Sweden) is attached to the cartridge. Scaffolds are designed using BioCad software (RegenHU, Fribourg, Switzerland), and a circular grid design with a diameter of 15 mm is used. Optimization of the system has resulted in the determination of optimal printing parameters as listed in Table 1. After scaffold printing, the K-carrageenan in the scaffold is cross-linked with an excess of 1 M KCl (104936, Merck Millipore, Darmstadt, Germany) for 30 min.

Table 1. *The printing parameters used for the 3D-printing of CaP scaffolds with K-carrageenan as a binder.*

Parameter	Value
Initial height (mm)	*0.5–0.80 (range)*
Thickness (mm) *(range) Speed rate (mm/s)*	*0.25–0.40* *7*
Pressure [1] (Bar)	*0.5–2.0 (range)*
Line space 2 (mm)	*2.50*

[1] 'Pressure' is an adaptable parameter. When printing multiple scaffolds in a row, the pressure might have to be increased; 2 'Line space' is the amount of space between the lines of the grid. Line space influences the number of lines used to fill up the grid.

Scanning Electron Microscope Imaging

For scanning electron microscope (SEM) imaging, samples are fixated overnight with a solution containing 4% paraformaldehyde, 1% glutaraldehyde, and 0.1 M sodium cacodylate. Samples are washed with distilled water, dehydrated with ethanol series, and dried overnight at room temperature. Samples are coated with gold using an Edwards Sputter Coater S150B (Edwards, Burgess Hill, England) and the images are made with a Zeiss EVO LS-15 scanning electron microscope (Zeiss, Oberkochen, Germany) with an accelerating voltage of 7 kV.

Results and Discussion

3D-printing is used with increasing frequency to create patient-specific constructs based on computer-aided planning and 3D-design by using digital modeling and imaging technology. In this method paper, we describe a protocol for the printing of CaP at room temperature with the possibility of incorporating biological components.

The first step of the process entails the production of the CaP paste. We tested whether the sequence in which the salts are dissolved during the CaP production process affects the precipitation process. This appeared not to be the case. To estimate CaP mineral maturation in the precipitate, the Ca/P ratio was analyzed. The CaP ratio in 3 samples is 1.46 ± 0.1 (mean ± SD). In the study by Leeuwenburgh et al. (2001), different layers are precipitated as coatings. One of these coatings uses the same salts in the supersaturated solution as we do in our study, and is described as an octacalcium phosphate coating [29]. In our protocol, higher ion concentrations are used, i.e., 5 times higher Na+ and Cl– ion concentration, 5.4 times higher $HPO_4$2– ion concentration, and 6.5 times higher Ca2+ concentration. The Ca/P ratio in our study is slightly higher compared to the Ca/P ratio of octacalcium phosphate, indicating the presence of calcium-deficient hydroxyapatite [30].

To characterize the CaP material, we used a scanning electron microscope (SEM). Under SEM, dried CaP particles appear as irregular microspheres with plate-like crystals (Figure 2A). When the K-carrageenan is mixed with the CaP paste and dried (Figure 2B), fewer plate-like crystals are present. The exact crystal structure of the CaP after printing with K-carrageenan remains to be determined, but the crystal structure is likely amorphous [31]. We use CaP paste rather than dry particles for printing and do not dry the 3D-printed scaffolds after printing, as this causes excessive shrinking and possibly structural damage to the constructs. From 1 L ion solution, 7.5 g of CaP paste is produced. When all the water is evaporated from 7.5 g paste, approximately 1.4 g of CaP particles is obtained. The paste thus contains approximately 4.4 g of water per gram of CaP precipitate.

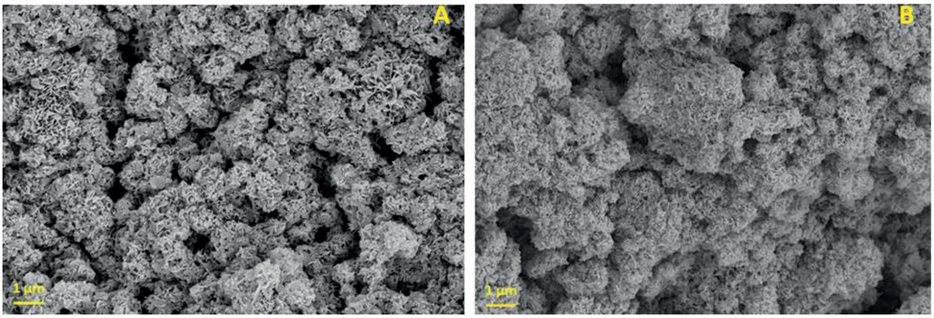

Figure 2. Scanning electron microscopy. (**A**) CaP; (**B**) CaP with K-carrageenan. Magnification: 5000×, Scalebar: 1 µm.

Here K-carrageenan is used as a biological binder. Other materials, e.g., bioink from Cellink® or a silanized hydroxypropylmethylcellulose hydrogel, can be used as well. The bioink from Cellink® is composed of nanofibrillated cellulose and alginate. The nanofibrils are morphologically similar to collagen [32], one of the main components in the bone matrix. The bioink is optimized for extrusion-based printing. Silanized hydroxypropylmethylcellulose hydrogels can be mixed with BCP granules [33] and, therefore, can be mixed with CaP. Moussa et al. (2017) show that adipose stem cells are viable inside these hydrogels [34]. We use K-carrageenan because of its resemblance to native glycosaminoglycans and proven biocompatibility [35,36].

We routinely print scaffolds with a diameter of 1.5 cm and strands of 1–1.5 mm in width (Figure 3). Scaffolds printed in consecutive order vary somewhat in dimensions. We measured the strand width of 3 scaffolds printed in one experiment. The width of the strands varied from 0.8 to 1.6 mm. The average strand width (measured at 10 different points: 5 vertical and 5 horizontal) of the 3 scaffolds was respectively 1.3, 1.2, and 1.0 mm. The average pore size was also measured, which was respectively 0.31, 0.39, and 0.55 mm2. In our experience, scaffolds printed on consecutive days had the same dimensions. The maximum printing volume is 130 mm × 90 mm × 60 mm.

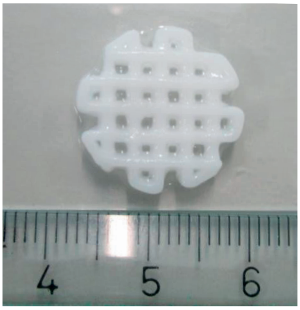

Figure 3. The 3D-printed scaffold. Scale in centimeters.

For the printing of viscous composites, optimization steps are needed. For example, the nozzle can penetrate the previously printed layers, which is unfavourable. This problem may be solved by adopting the printing parameters. When the layer thickness (setting of the printer) is increased, the distance the nozzle goes up with every layer increases, thereby solving the problem. Small incremental steps (0.01 mm) are used until the needle stops penetrating the previous layers. In addition, increasing the parameter initial height can also help solve the problem. We tend to print at a pressure of 1 Bar, which creates strands between 1 and 1.5 mm as described above. By decreasing the pressure, it is possible to create thinner strands, although this might lead to a disruption of the continuity of the printing process. Another option to decrease the strand thickness is to increase the initial height of the nozzle, as the strands are more stretched while being printed. The advantage of using thinner strands is that it provides increased scaffold porosity, but the disadvantage is that the strands might be mechanically weaker. The thinnest strands that we have obtained using CaP paste and K-carrageenan have a thickness of 0.75 mm.

The 3D-printing method described in this paper is performed at room temperature and without aggressive solvents, allowing biological components to be incorporated into the CaP and/or in the K-carrageenan. BSA-FITC is used as a model to show the incorporation of biological components in CaP. In Figure 4, a fluorescent signal is visible when BSA-FITC is incorporated into the CaP paste (A), and in the K-carrageenan (B). The materials are not autofluorescent as no fluorescent signal is visible in the control sample (C). The release of BSA-FITC from the scaffolds is measured after 3 days. The cumulative BSA-FITC release from the scaffolds incorporated in the CaP paste and, in the K-carrageenan is determined (Figure 5). The BSA-FITC release from K-carrageenan is less than that from CaP paste. This might be explained by the fact that the total amount of BSA-FITC incorporated in CaP paste was 10 times higher than in K-carrageenan. This difference in the amount used was based on the expectation that more BSA-FITC would be lost during its incorporation in CaP paste. We show that biological factors can be incorporated in both CaP paste and, in a K-carrageenan solution and that these factors are released from the scaffolds. We estimate that approximately 0.02% of the incorporated BSA-FITC is released from CaP/K-carrageenan scaffolds after 3 days.

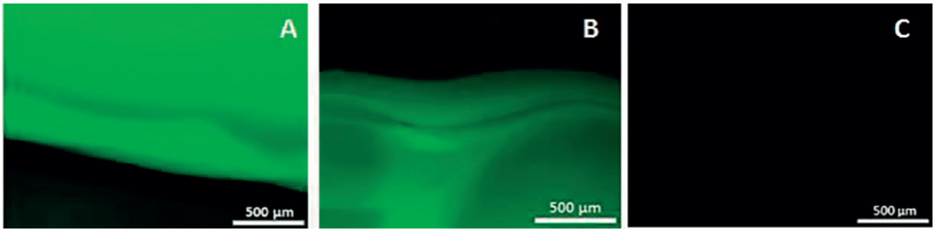

Figure 4. The fluorescent images of incorporated bovine serum albumin, fluorescein conjugate.

*(**A**) CaP/K-carrageenan scaffold with BSA-FITC incorporated in the CaP paste; (**B**) Scaffold with BSA-FITC incorporated in the K-carrageenan solution; (**C**) Control scaffold without BSA-FITC incorporated. Magnification: 4×.*

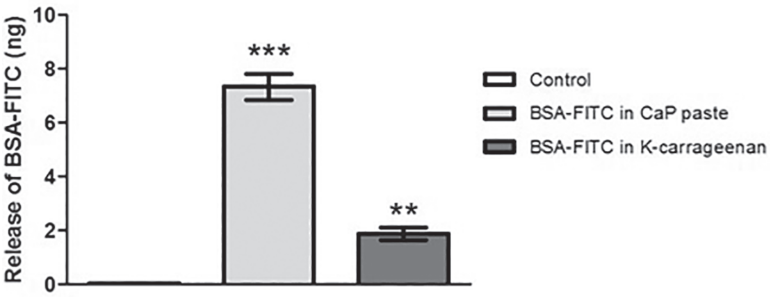

Figure 5. The release of incorporated BSA-FITC. From a CaP scaffold with BSA-FITC incorporated in the CaP paste, a scaffold with BSA-FITC incorporated in the K-carrageenan solution, and a control scaffold without BSA-FITC incorporated. Normalized for the volume of the scaffolds. The significance is compared to the control scaffold, ** is $p < 0.01$ and *** is $p < 0.001$.

Liu et al. (2001) have tested the release of co-precipitated BSA from CaP particles. They found that only 0.3% of the incorporated BSA was released during the first 4 h, which increased to 0.85% after 6 days [18]. It has been reported that the release of BMP-2 increases due to the resorption of the material by cells [28]. Our precipitation protocol is based on the protocol of Liu et al. but the release of biological factors from the printed end product is likely to be different from the particles as described by Liu et al. (2001) as we use the precipitated CaP as a paste rather than as dry particles, and we combine the CaP with carrageenan. By experimenting with incorporating biological components in the K-carrageenan and/or in CaP paste, favorable release kinetics can be tailored.

For eventual clinical purposes, it is important that the whole scaffold production process can be performed under sterile conditions. The CaP paste can be produced in a sterile manner since a CaP solution and a TRIS solution can be made separately and filtered with a Millipore filter unit of 0.22 µm. After filtering, the solutions are mixed and incubated overnight in a shaking water bath at 37 °C. The K-carrageenan can be sterilized by heating till 85 °C for 3 h and both the mixing and the 3D-printing can be done under sterile conditions, for example, in a cleanroom. Taken together, we have provided a detailed protocol for the printing of CaP-carrageenan hybrid scaffold which can be used as a base by other labs to establish their own 3D-printing protocol.

Acknowledgments

We want to thank Lester Geonzon from the Department of Food Science and Technology and Professor Shingo Matsukawa at the Tokyo University of Marine Science and Technology for providing us with 2.8% K-carrageenan solution.

References

1. Burg, K.J.L.; Porter, S.; Kellam, J.F. Biomaterial developments for bone tissue engineering. *Biomaterials* **2000**, *21*, 2347–2359.
2. Enneking, W.F.; Eady, J.L.; Burchardt, H.A. Autogenous cortical bone grafts in the reconstruction of segmental skeletal defects. *J. Bone Jt. Surg.* **1980**, *62*, 1039–1058.
3. Pape, H.C.; Evans, A.; Kobbe, P. Autologous bone graft: Properties and techniques. *J. Orthop. Trauma* **2010**, *24*, S36–S40.
4. Ducheyne, P.; Radin, S.; King, L. The effect of calcium phosphate ceramic composition and structure on in vitro behavior. I. Dissolution. *J. Biomed. Mater. Res.* **1993**, *27*, 25–34.
5. Radin, S.R.; Ducheyne, P. The effect of calcium phosphate ceramic composition and structure on in vitro behavior. II. Precipitation. *J. Biomed. Mater. Res.* **1993**, *27*, 35–45.
6. Barrère, F.; van Blitterswijk, C.A.; de Groot, K. Bone regeneration: Molecular and cellular interactions with calcium phosphate ceramics. *Int. J. Nanomed.* **2006**, *1*, 317–332.
7. Levato, R.; Visser, J.; Planell, J.A.; Engel, E.; Malda, J.; Maleos-Timoneda, M.A. Biofabrication of tissue constructs by 3D bioprinting of cell-laden microcarriers. *Biofabrication* **2014**, *6*, 035020.
8. Chung, J.H.Y.; Naficy, S.; Yue, Z.; Kapsa, R.; Quigley, A.; Moulton, S.E.; Wallace, G.G. Bio-ink properties and printability for extrusion printing living cells. *Biomater. Sci.* **2013**, *1*, 763–773.
9. Gao, G.; Schilling, A.F.; Hubbell, K.; Yonezawa, T.; Truong, D.; Hong, Y.; Dai, G.; Cui, X. Improved properties of bone and cartilage tissue from 3D inkjet-bioprinted human mesenchymal stem cells by simultaneous deposition and photocrosslinking in peg-gelma. *Biotechnol. Lett.* **2015**, *37*, 2349–2355.
10. Ozbolat, I.T.; Hospodiuk, M. Current advances and future perspectives in extrusion-based bioprinting. *Biomaterials* **2016**, *76*, 321–343.
11. Jakus, A.E.; Rutz, A.L.; Jordan, S.W.; Kannan, A.; Mitchell, S.M.; Yun, C.; Koube, K.D.; Yoo, S.C.; Whiteley, H.E.; Richter, C.-P.; et al. Hyperelastic "bone": A highly versatile, growth factor–free, osteoregenerative, scalable, and surgically friendly biomaterial. *Sci. Transl. Med.* **2016**, *8*, 358ra127.
12. Gbureck, U.; Hölzel, T.; Klammert, U.; Würzler, K.; Müller, F.A.; Barralet, J.E. Resorbable dicalcium phosphate bone substitutes prepared by 3D powder printing. *Adv. Funct. Mater.* **2007**, *17*, 3940–3945.
13. Berry, E.; Brown, J.M.; Connell, M.; Craven, C.M.; Efford, N.D.; Radjenovic, A.; Smith, M.A. Preliminary experience with medical applications of rapid prototyping by selective laser sintering. *Med. Eng. Phys.* **1997**, *19*, 90–96.
14. Vella, J.B.; Trombetta, R.P.; Hoffman, M.D.; Inzana, J.; Awad, H.; Benoit, D.S.W. Three dimensional printed calcium phosphate and poly(caprolactone) composites with improved mechanical properties and preserved microstructure. *J. Biomed. Mater. Res. Part A* **2018**, *106*, 663–672.
15. Wernike, E.; Montjoven, M.O.; Liu, Y.; Wismeijer, D.; Hunziker, E.B.; Siebenrock, K.A.; Hofstetter, W.; Klenke, F.M. Vegf incorporated into calcium phosphate ceramics promotes vascularisation and bone formation in vivo. *Eur. Cells Mater.* **2010**, *19*, 30–40.

16. Amirian, J.; Linh, N.T.B.; Min, Y.K.; Lee, B.-T. Bone formation of a porous gelatin-pectin-biphasic calcium phosphate composite in presence of BMP-2 and VEGF. *Int. J. Biol. Macromol.* **2015**, *76*, 10–24.
17. Ziegler, J.; Mayr-Wohlfart, U.; Kessler, S.; Breitig, D.; Günther, K.P. Adsorption and release properties of growth factors from biodegradable implants. *J. Biomed. Mater. Res.* **2002**, *59*, 422–428.
18. Liu, Y.; Layrolle, P.; de Bruijn, J.; van Blitterswijk, C.; de Groot, K. Biomimetic coprecipitation of calcium phosphate and bovine serum albumin on titanium alloy. *J. Biomed. Mater. Res.* **2001**, *57*, 327–335.
19. Vignesh, S.; Gopalakrishnan, A.; Poorna, M.R.; Nair, S.V.; Jayakumar, R.; Mony, U. Fabrication of micropatterned alginate-gelatin and k-carrageenan hydrogels of defined shapes using simple wax mould method as a platform for stem cell/induced pluripotent stem cells (iPSC) culture. *Int. J. Biol. Macromol.* **2018**, *112*, 737–744.
20. Liu, J.; Zhan, X.; Wan, J.; Wang, Y.; Wang, C. Review for carrageenan-based pharmaceutical biomaterials: Favourable physical features versus adverse biological effects. *Carbohydr. Polym.* **2015**, *121*, 27–36.
21. Mihaila, S.M.; Gaharwar, A.K.; Reis, R.L.; Marques, A.P.; Gomes, M.E.; Khademhosseini, A. Photocrosslinkable kappa-carrageenan hydrogels for tissue engineering applications. *Adv. Healthc. Mater.* **2013**, *2*, 895–907.
22. Lode, A.; Meissner, K.; Lou, Y.; Sonntag, F.; Glorius, S.; Nies, B.; Vater, C.; Despang, F.; Hanke, T.; Gellinsky, M. Fabrication of porous scaffolds by three-dimensional plotting of a pasty calcium phosphate bone cement under mild conditions. *J. Tissue Eng. Regen. Med.* **2014**, *8*, 682–693.
23. Maazouz, Y.; Montufar, E.B.; Guillem-Marti, J.; Fleps, I.; Ohman, C.; Persson, C.; Ginebra, M.P. Robocasting of biomimetic hydroxyapatite scaffolds using self-setting inks. *J. Mater. Chem. B* **2014**, *2*, 5378–5386.
24. Maazouz, Y.; Montufar, E.B.; Malbert, J.; Espanol, M.; Ginebra, M.-P. Self-hardening and thermoresponsive alpha tricalcium phosphate/pluronic pastes. *Acta Biomater.* **2017**, *49*, 563–574.
25. Barba, A.; Diez-Escudero, A.; Maazouz, Y.; Rappe, K.; Espanol, M.; Montufar, E.B.; Bonany, M.; Sadowska, J.M.; Guillem-Marti, J.; Öhman-Mägi, C.; et al. Osteoinduction by foamed and 3D-printed calcium phosphate scaffolds: Effect of nanostructure and pore architecture. *ACS Appl. Mater. Interfaces* **2017**, *9*, 41722–41736.
26. Trombetta, R.; Inzana, J.A.; Schwarz, E.M.; Kates, S.L.; Awad, H.A. 3D printing of calcium phosphate ceramics for bone tissue engineering and drug delivery. *Ann. Biomed. Eng.* **2017**, *45*, 23–44.
27. Akkineni, A.R.; Luo, Y.; Schumacher, M.; Nies, B.; Lode, A.; Gelinsky, M. 3D plotting of growth factor loaded calcium phosphate cement scaffolds. *Acta Biomater.* **2015**, *27*, 264–274.
28. Liu, T.; Wu, G.; Zheng, Y.; Wismeijer, D.; Everts, V.; Liu, Y. Cell-mediated BMP-2 release from a novel dual-drug delivery system promotes bone formation. *Clin. Oral Implants Res.* **2014**, *25*, 1412–1421.

29. Leeuwenburgh, S.; Layrolle, P.; Barrère, F.; de Bruijn, F.; Schoonman, J.; van Blitterswijk, C.A.; de Groot, K. Osteoclastic resorption of biomimetic calcium phosphate coatings in vitro. *J. Biomed. Mater. Res.* **2001**, *56*, 208–215.
30. Mavropoulos, E.; Rossi, A.M.; Da Rocha, N.C.C.; Soares, G.A.; Moreira, J.C.; Moure, G.T. Dissolution of calcium-deficient hydroxyapatite synthesized at different conditions. *Mater. Charact.* **2003**, *50*, 203–207.
31. Wu, G.; Liu, Y.; Iizuka, T.; Hunziker, E.B. Biomimetic coating of organic polymers with a protein- functionalized layer of calcium phosphate: The surface properties of the carrier influence neither the coating characteristics nor the incorporation mechanism or release kinetics of the protein. *Tissue Eng. Part C Methods* **2010**, *16*, 1255–1265.
32. Martínez Ávila, H.; Schwarz, S.; Rotter, N.; Gatenholm, P. 3D bioprinting of human chondrocyte-laden nanocellulose hydrogels for patient-specific auricular cartilage regeneration. *Bioprinting* **2016**, *1–2*, 22–35.
33. Struillou, X.; Rakic, M.; Badran, Z.; Macquigneau, L.; Colombeix, C.; Pilet, P.; Verner, C.; Gauthier, O.; Weiss, P.; Soueidan, A. The association of hydrogel and biphasic calcium phosphate in the treatment of dehiscence-type peri-implant defects: An experimental study in dogs. *J. Mater. Sci. Mater. Med.* **2013**, *24*, 2749–2760.
34. Moussa, L.; Pattappa, G.; Doix, B.; Benselama, S.L.; Demaraquay, C.; Benderitter, M.; Sémont, A.; Tamarat, R.; Guicheux, J.; Weiss, P.; et al. A biomaterial-assisted mesenchymal stromal cell therapy alleviates colonic radiation-induced damage. *Biomaterials* **2017**, *115*, 40–52.
35. Yegappan, R.; Selvaprithiviraj, V.; Amirthalinam, S.; Jayakumar, R. Carrageenan based hydrogels for drug delivery, tissue engineering and wound healing. *Carbohydr. Polym.* **2018**, *198*, 385–400.
36. Goonoo, N.; Khanbabaee, B.; Steuber, M.; Bhaw-Luximon, A.; Jonas, U.; Pietsch, U.; Jhurry, O.; Schönherr, H. κ-Carrageenan Enhances the Biomineralization and Osteogenic Differentiation of Electrospun Polyhydroxybutyrate and Polyhydroxybutyrate Valerate Fibers. *Biomacromolecules* **2017**, *18*, 1563–1573.

5

Physical and Biological Aspects of 3D Calcium Phosphate Scaffolds Containing Vitamin D_3

Abstract

Recently we described a method for the 3D-printing of a bioink consisting of a calcium phosphate paste and κ-carrageenan, with the possibility to incorporate active biological components, for the healing of critical-sized bone defects. In this study, we assessed whether bioinks made of this mixture, either or not enhanced with 1,25$(OH)_2$vitD_3 (vitD_3), are likely to be clinically relevant. To do this, printability, compressive stiffness, and bioactivity of CaP-based bioinks mixed with 2.8%, 3.8%, or 4.8% (wt/vol) κ-carrageenan were measured. Furthermore, the human osteosarcoma cell line U2OS was cultured in the presence of constructs made with the bioink, either or not containing 125 ng vitD_3, and cytotoxicity, cell viability, and cytokine release were measured up to 7 days. Constructs (15 mm diameter, 3 mm height, 1 mm strand thickness) could be consistently printed with 2.8% and 3.8% κ-carrageenan but not with 4.8% κ-carrageenan solution. The compressive stiffness of solid cylindrical constructs (10.7 mm diameter) made with 2.8% and 3.8% κ-carrageenan was very similar, respectively 170 ± 45 kPA and 212 ± 77 kPA. The bioink was not cytotoxic and did not have a negative effect on the proliferation of U2OS cells. The gene expression of CYP24a1 was upregulated by conditioned medium of constructs with vitD_3, indicating that the vitD_3 is released and bioactive. Furthermore, the bioink led to an increased release of RANKL and reduced OPG released by the cells, independent of adding vitD_3. These results show that constructs made of CaP paste and κ-carrageenan can be consistently produced, are not fragile or cytotoxic, allow the release of active biological factors, and thus show promise for future use in a clinical setting.

Introduction

The intrinsic healing capacity of bone is compromised when a defect is of a critical size. Therefore, critical size bone defects remain a clinical challenge. Often autologous bone grafts, taken from the patient, are used for the treatment of this kind of defects [1,2]. This treatment can have adverse effects, such as donor site morbidity and pain, and especially trauma patients may have limited availability of donor bone [3]. Bone tissue engineering constructs may be used as an alternative treatment option, thereby avoiding these disadvantages. To aid the healing of bone, such constructs would preferably have both osteoconductive properties [4] i.e. conducts bone growth along its surface, and osteoinductive properties [5] i.e. induce de novo bone formation [3].

For bone tissue engineering, calcium phosphate (CaP) containing materials are frequently used for the generation of scaffolds, since CaP-based scaffolds resemble the contents of the apatite in natural bone, and CaP-containing materials generally have osteoconductive properties [6]. To improve the osteoinductive properties, CaP-based constructs can be enhanced with biological components such as *Vascular endothelial growth factor* (VEGF), Bone morphogenetic protein 2 (BMP-2), and 1,25$(OH)_2$ vitamin D_3 (vitD_3), to stimulate bone formation and blood vessel formation[7]. VitD_3 is the active form of vitamin D and holds promise for the use in bone tissue engineering, because it stimulates the osteogenic differentiation of *human* bone marrow stromal cells (hMSCs) [8]. In addition, vitD_3 is relatively safe, works at low doses, and is relatively cheap. Adding vitD_3 to tissue engineering constructs may help the healing of large bone defects.

Tissue engineering constructs based on CaP-containing scaffold can be fabricated in several ways, such as solvent casting/ particulate leaching [9], electrospinning [10], and 3D-printing [11]. Recently, 3D-printing gained more interest for the production of tissue engineering constructs, as it permits the rapid fabrication of patient-specific scaffolds that will fit the defect perfectly, enabling maximum contact area between the construct and the native bone. 3D printed constructs can be locally functionalized with biological components to fit particular requirements at a specific anatomical site. The 3D-printing of CaP-based materials can be performed with several 3D-printing techniques, such as powder printing or extrusion-based printing [12,13]. With the first technique, CaP particles are fused, either by a laser or by a liquid binder, and in the second technique, fluid CaP-containing material is extruded from a nozzle. These techniques often use high temperatures or aggressive chemicals, hindering the incorporation of biological components.

We have previously described a method for the 3D-printing of a bioink consisting of a CaP paste mixed with κ-carrageenan, with the possibility to incorporate active biological components [14]. In the present study, we assessed whether constructs made with this bioink and enhanced with vitD_3 are potentially clinically relevant, by measuring the possibility to consistently print cylindrical objects, quantifying compressive stiffness of cylinders cast with the bioink, and determining the response of human osteoblast-like cells to leachables released from the ink.

Material and Methods

CaP paste production

Production of the CaP paste is achieved by a precipitation reaction described earlier [14]. In short, a sterile supersaturated CaP solution containing 684 mM NaCl (31434, Sigma-Aldrich, St Louis, MO, USA), 20 mM $CaCl_2·2H_2O$ (102382, Merck Millipore, Darmstadt, Germany), 10.1mM $Na_2HPO_4·2H_2O$ (106580, Merck Millipore, Darmstadt, Germany), and 200 mM HCl (100317, Merck Millipore, Darmstadt, Germany) was made and filtered with a 0.22 µm sterivex filter (Millipore, Burlington, MA, USA) for sterilization. The pH was adjusted to 7.4 ± 0.5 by the addition of a sterile TRIS (Sigma-Aldrich, St Louis, MO, USA) solution. Thereafter, the solution was incubated overnight in a shaking water bath at 37°C to allow for precipitation. The precipitate was washed five times with sterile PBS and the remaining moisture was removed by filtering with a 0.22 µm PES bottle top filter (431161, Corning Incorporated, Corning, New York, NY, USA) and an air pump resulting in a CaP paste.

K-carrageenan

K-carrageenan is a compound derived from red seaweed and resembles the glycosaminoglycans (GAGs) in the extracellular matrix [15]. Sodium-type κ-carrageenan (Tokyo Chemical Industry Co., Ltd. Tokyo, Japan) is dialyzed against NaCl solution and subsequently against deionized water to obtain Na^+ type carrageenan solution. The Na+ and K+ concentrations, analyzed by inductively coupled plasma atomic emission, are 0.4% and 0.11%, while no Mg^{2+} or Ca^{2+} are detected in the dialyzed sample. K-carrageenan solutions with concentrations of 2.8%, 3.8%, and 4.8% (wt/vol) were prepared by dissolving freeze-dried κ-carrageenan (kindly provided by Prof. S. Matsukawa, Tokyo) overnight in milliQ in a water bath at 37°C. The solutions were sterilized by boiling in a closed container for 1 hour. The solutions were stored at 4°C and warmed up to 37°C before use.

Production of cylinders

To test the compression modulus, activity of released vitD_3, cytotoxicity of the bioink, and effect of the bioink on human osteoblast-like cells, we used cylinders prepared with the bioink. The cylinders had a diameter of 10.78 ± 0.16 mm and were 4.55 ± 0.19 mm in height, and were prepared as follows: The CaP paste and κ-carrageenan solutions were mixed in a 1:1.9 (wt/vol) ratio. For cylinders containing vitD_3, 125 ng vitD_3 (Sigma, stock: 30µM in 100% ethanol, stored at -80°C, in the absence of light) per cylinder was added to the κ-carrageenan before mixing. One cylinder consists of approximately 0.6 ml of bioink. The sample was sonicated to ensure a homogeneous mixture. Sonication was performed at room temperature using a sonicator (Vibra cell™, VCX 400, Sonics, Newtown, CT, USA) with the following settings: amplitude: 20%; pulse: alternating 1.0 sec 'on' and 1.0 sec 'off' for in total 90 s. The mixture was then collected in a syringe and pushed into polyvinylsiloxane molds with a thickness of 4 mm and 10 mm in diameter. Sterile glass slides are used to equalize the mixture in the molds. Cylinders were crosslinked using an excess of sterile 1M KCl (Merck Millipore, Darmstadt, Germany) for 45 minutes. After this incubation, the KCl was removed and the cylinders were washed with sterile PBS. The cylinders were carefully pressed out of the molds with a spatula and were directly used.

Printability

The printability of bioinks containing 2.8%, 3.8%, or 4.8% κ-carrageenan solutions were compared with respect to the following parameters: consistent strand thickness, consistent pore size, and the number of failed constructs. Scaffolds were printed according to the method described by Kelder et al [14]. In short, CaP paste was mixed with κ-carrageenan in a 1:1.9 (wt/vol) ratio. The mixtures were loaded to a cartridge of a 3D-Discovery printer (RegenHU, Fribourg, Switzerland) and printed with a 23G (inner diameter: 0.33 mm) blunt needle. A simple construct was printed with an intended diameter of 15 mm and a strand thickness of 1 mm. We measured the diameter, strand size, and pore size by counting pixels in digital images of known resolution. The printer settings were fine-tuned for each batch. For each κ-carrageenan concentration, we printed 5-6 scaffolds, on two separate occasions.

Compression modulus

To measure the compression modulus of the bioink we used cylinders that were prepared as described above in "production of cylinders". Cylinders were prepared and then stored in PBS for 24 hours. Compression was measured using a universal testing machine (Instron 6022, Instron, Norwood, MA, USA) with a loading cell of 50 N and a speed of 1.0 mm/sec.

The compression elastic modulus (E) was calculated in the linear area between 30 – 90 sec, using the following equation:

$$\mathrm{E} = \frac{\Delta\sigma}{\Delta\varepsilon} = \frac{\frac{F}{A}}{\frac{\Delta L}{L0}}$$

Where σ= stress; ε= strain; F=Force; A=Area; ΔL= change of length; L0= initial length.

Cytotoxicity of the bioink

To measure the cytotoxicity, 2.0×10^5 human osteosarcoma-derived (U2OS) cells were seeded one day before the experiment (day -1) on the bottom of a 12-well plate, and cultured in basic medium consisting of minimum Essential Medium Alpha (α-MEM; Thermo Fisher Scientific, Waltham, MA, USA) without phenol red, supplemented with 1% fetal clone I serum (FCI, HyClone, Logan, UT, USA), and 1% Antibiotic Antimycotic Solution 100× (PSF; Sigma, St Louis, MO, USA). At day 0, cylinders with and without vitD_3 are placed in inserts (pore size 3.0 µm; Greiner Bio-one, Alphen aan de Rijn, the Netherlands) above the cells with 0.5 ml of medium in the insert and 1.5 ml of medium in the well. After 24 hours, the medium in the inserts was collected and mixed with the medium in the well and the cytotoxicity was measured using ToxiLight™ bioassay kit (Lonza, Bazel, Switzerland) according to the manufacturers' protocol.

Cell viability

The viability of U2OS cells was measured with AlamarBlue™ Cell viability reagent (Invitrogen, Carlsbad, CA, USA). Alamar blue conversion was measured at day 0, day 2, day 5, and day 7. For each time point, 3.0×10^4 cells per well (12-well plate) were seeded one day before the experiment (day -1) in basic medium, consisting of α-MEM (no phenol red) supplemented with 10% FCI and 1% PSF. Tissue culture inserts containing cylinders produced of the bioink (with or without vitD_3) were placed above the cells at day 0 with 0.5 ml of medium in the insert and 1.5 ml of medium in the well. To measure the Alamar blue conversion, the cylinders and medium were removed, and 2 ml of medium containing 10% AlamarBlue reagent was added to the wells and incubated for 4 hours at 37˚C. As a negative control, the same medium with 10% AlamarBlue reagent was incubated in an empty well. After incubation, 100 µl (in duplicate) was taken from each sample, transferred to a black 96-well plate and fluorescence was measured at 530-560 nm with Synergy HT® spectrophotometer (BioTek Instruments, Winooski, VT, USA). Medium without cells and with 10% AlamarBlue reagent was autoclaved to fully reduce the AlamarBlue reagent and used as a positive control. Samples are presented as a percentage of the positive control.

DNA content and Alkaline Phosphatase activity

One day before the experiment 3.0×10^4 U2OS cells were seeded/well in a 12 well plate and cultured in basic medium, consisting of α-MEM (without phenol red) supplemented with 10% FCI and 1% PSF. Tissue culture inserts containing bioink cylinders (with or without vitD_3) were placed above the cells at day 0 with 0.5 ml of medium in the insert and 1.5 ml of medium in the well. At day 0, day 2, day 5, and day 7, cells were washed with PBS and lysed with 200 µl of Milli-Q water and frozen at -20°C for storage. After three freeze-thaw cycles, samples were collected by scraping followed by a centrifuging step to get rid of debris. DNA content was measured using a Cyquant cell proliferation kit (Molecular probes, Eugene, OR, USA) according to manufacturers' protocol. ALP was measured in cell lysate according to the method described by Lowry [16] using 4-nitrophenyl phosphate disodium salt at pH 10.3 as a substrate for ALP. Absorbance was measured at 405 nm with the Synergy HT® spectrophotometer. To correct for cell number, ALP measurements were normalized for DNA content.

Activity of released vitD3

The activity of the released vitD_3 was determined by quantifying the gene expression of CYP24a1 in U2OS cells. CYP24a1 expression is strongly upregulated in osteoblasts when bioactive vitD_3 is available. Cylinders with or without vitD_3 were placed in 2 ml of basic culture medium, as described above, for 24 hours. The conditioned medium was collected and placed on top of U2OS cells seeded at 5.0×10^4 cells per well in a 12 well plate. The next day, total RNA was isolated with TRIzol® reagent (Invitrogen) following the manufacturer's protocol. The concentration and purity of RNA were measured using a Synergy HT® spectrophotometer and 750 ng RNA was reverse-transcribed to cDNA using RevertAid™ First Strand cDNA Synthesis Kit 1612 (Fermentas, St. Leon-Rot, Germany) according to the manufacturer's protocol. For the qPCR reaction, cDNA was diluted 5× and 1 µl was used, together with 3 µl PCR-H_2O, 0.5 µl (20 µM) forward primer (5' CAAACCGTGGAAGGCCTATC 3'), 0.5 µl (20 µM) reverse primer (5' AGTCTTCCCCTTCCAGGATCA 3'), and 5 µl 2x LightCycler® 480 SYBR Green I Mastermix (Roche Diagnostics). The values of Cyp24a1 were normalized to hypoxanthine phosphoribosyl transferase (HPRT, FWRD: 5' GCTGACCTGCTGGATTACAT 3' REV: 5' CTTGCGACCTTGACCATCT 3') following the comparative cycle threshold (ΔCt).

Legendplex

One day before the experiment (day -1), cells were seeded at a density of 3.0×10^4 cells per well in a 12-well plate in basic medium consisting of α-MEM (no phenol red) supplemented with 10% FCI and 1% PSF and cultured up to 7 days. Inserts with cylinders (with or without vitD_3) were placed above the cells at day 0 with 0.5 ml of medium in the insert and 1.5 ml of medium in the well. The medium was collected at day 0, day 2, day 5, and day 7. Secreted Osteoprotegerin (OPG), Osteopontin (OPN), Receptor activator of nuclear factor kappa-B ligand (RANKL), Tumor Necrosis Factor Alpha (TNF-α), and Interleukin-6 (IL-6) were quantified according to manufacturer's protocol in the conditioned mediums using LEGENDplex™ (BioLegend, San Diego, CA, USA) according to the manufacturers' instructions on a BD Accuri™ C6 FACS machine. The settings suggested by BioLegend were used and the analysis was performed with the software provided by the manufacturer.

Statistics

Data were obtained from 6 separate cultures of U2OS cells combined with constructs made of 6 fresh batches of bioink (n=6). Data are presented as mean + standard deviation (SD). A t-test was conducted to test for the statistical differences between 2.8% and 3.8% κ-carrageenan constructs in diameter, strand thickness, pore size, and compressive modulus. For the statistical difference between the 3 groups in cytotoxicity, a one-way ANOVA with a Tukey post hoc test was used. Statistical comparisons of the experiments with multiple time points were done using a 2-way ANOVA with Bonferroni post-tests. With time and 'condition' used as the dependent variables, the *p* values of < 0.05 were considered significantly different. The analyses were performed using GraphPad Prism 5.0 (GraphPad Software, San Diego, CA, USA).

Results

Reproducible constructs can be 3D-printed with 2.8% and 3.8% κ-carrageenan but not with 4.8% κ-carrageenan.

In order to assess the printability of the bioink consisting of a mixture of CaP paste and κ-carrageenan, we printed simple scaffolds and measured the diameter, strand thickness, and pore size (Figure 1). In total 11 constructs were printed per concentration. For both 2.8% and 3.8% κ-carrageenan, 3 out of 11 constructs were incomplete/incorrect and were not included in the measurements. Printing with a mixture made with 4.8% κ-carrageenan was not feasible, due to the lower viscosity of the material, which caused the flowing of the strands. For this reason, only data of scaffolds printed with 2.8% and 3.8% κ-carrageenan are shown. The printing settings were optimized for each batch. There was no difference in diameter between constructs made with 2.8% or 3.8% κ-carrageenan, but the spread of the data seems wider in 3.8% (Figure 1B). Also, the strand thickness is similar between the 2 mixtures, but here the spread seems larger in constructs printed with 2.8% κ-carrageenan (Figure 1C). There are significantly larger pores in the construct printed with 3.8% κ-carrageenan (Figure 1D).

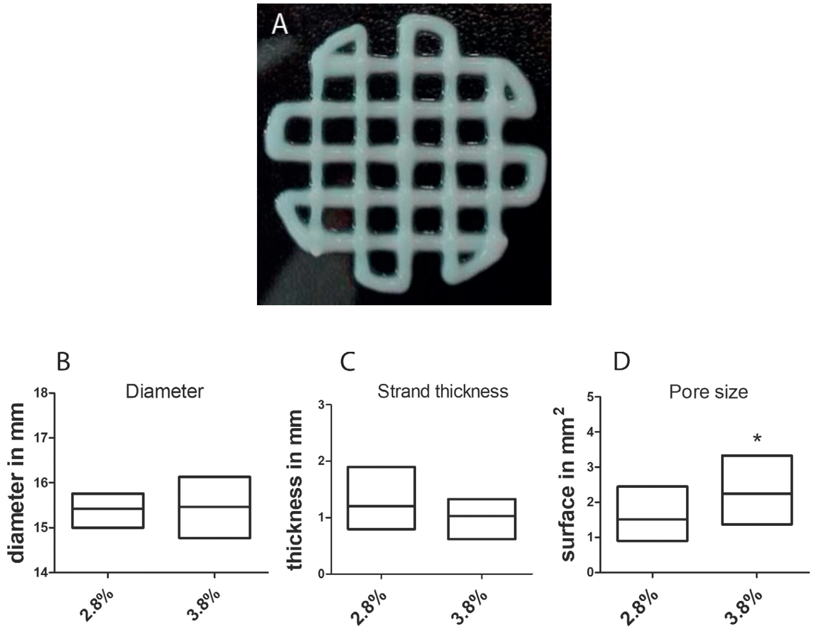

Figure 1. Printability of constructs printed with 2.8% and 3.8% κ-carrageenan. Measurements of diameter, strand thickness, pore size of constructs printed with 2.8% and 3.8% κ-carrageenan. (A) Simple 3D-printed construct. (B)The average diameter of 3D-printed constructs was similar in both groups (C) average strand thickness was also similar in both constructs made with 2.8% κ-carrageenan and 3.8% κ-carrageenan (D) Average pore size was significantly higher in constructs printed with 3.8% κ-carrageenan. Significance was determined using a t-test. * $p<0.05$.

Adding vitD3 to the bioink has an anti-cytotoxic effect.

To be clinically applicable, the mixture of CaP paste and κ-carrageenan should be stiff enough to be placed in non-load bearing defects and should not negatively affect the cells surrounding scaffolds. The apparent compressive stiffness was determined by calculating the apparent compression elastic modulus of the bioink when cast into a solid cylindrical shape (Figure 2A). The compressive modulus was slightly higher in constructs made with 3.8% κ-carrageenan, namely 212 ± 77 kPA compared to 170 ± 45 kPA for 2.8% κ-carrageenan, but this is not significant. Because the strand thickness appears to be more homogeneous and the compressive modulus seems marginally higher, we continued our experiments with constructs made of bioink containing 3.8% carrageenan. When the cytotoxicity was assessed by ToxiLight™ bioassay kit, no differences in relative luminescence were found between the control (cells incubated on plastic only), and those exposed to cylindrical constructs (3.8% κ-carrageenan). Interestingly, relative luminescence was significantly lower in cells exposed to constructs with vitD_3 compared to those exposed to samples without vitD_3 (Figure 2B). Adding vitD_3 reduced the luminescence by an average of 9.7 percent. The morphology of cells cultured in the presence of cylinders with or without vitD$_3$ seems similar to that of cells cultured on plastic without cylinders (Figure 2C,2D, 2E). Interestingly, the wells containing cylinders without vitD$_3$ seemed to contain more round cells, reminiscent of dividing cells, compared to the condition without vitD$_3$. Alamar blue, together with DNA levels, was used to assess cell viability and proliferation (Figure 2F,2G). Between day 0 and day 7, Alamar blue conversion increased 9.5-fold in the control, 8.8-fold in cells cultured with cylinders with vitD$_{3,}$ and 6.6-fold in cells cultured with cylinders without vitD$_3$. At day 5 the cells cultured on plastic convert significantly more Alamar blue than cells cultured together with constructs (with and without vitD$_3$). Also, conversion of Alamar blue was significantly lower in cell cultures grown in the presence of a construct without vitD$_3$ compared to cultures grown with constructs with vitD$_{3.}$ At day 7, the cells cultured on plastic still converted significantly more Alamar blue than the cells cultured together with constructs with no vitD$_3$, but do not differ with the cells cultured together with cylinders with vitD$_{3.}$ DNA levels increased on average 3.2-fold between day 0 and day 7. There are no differences in DNA levels between the conditions at any time point (Figure 2G).

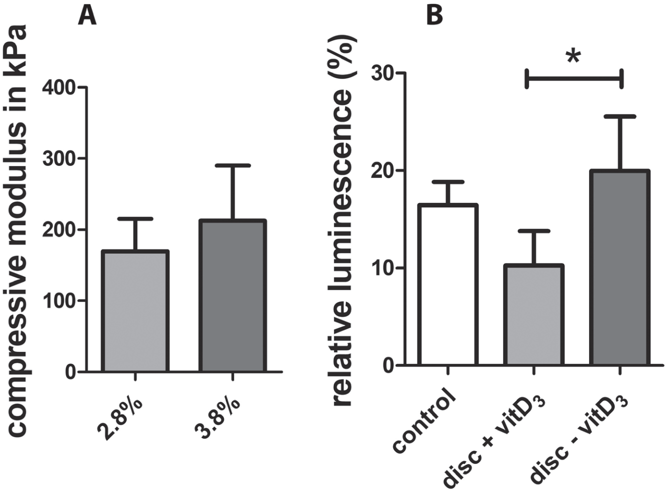

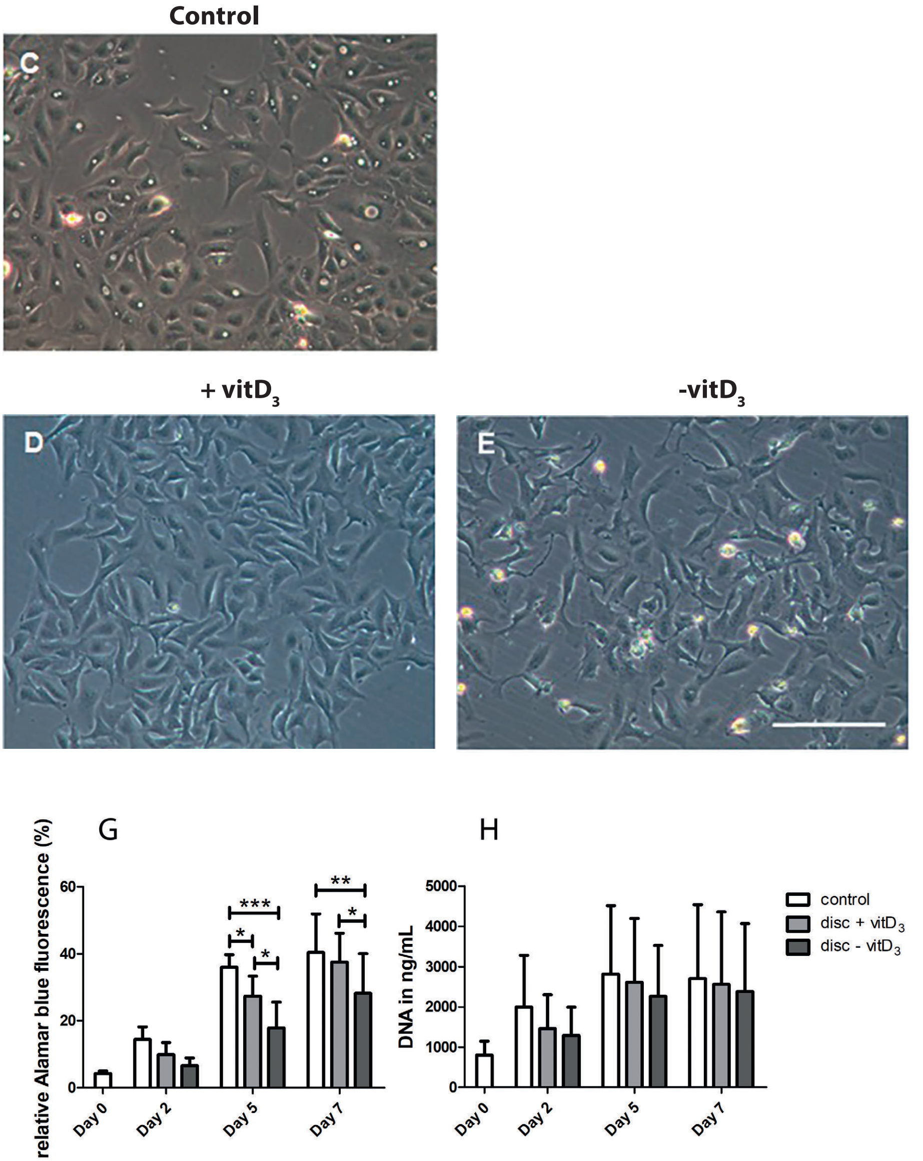

Figure 2. Compressive modulus and cytotoxicity of the bioink.

*(A) Compressive modulus of cylinders made with 2.8% and 3.8% κ-carrageenan was similar in both groups. (B) Cytotoxicity was measured by ToxiLight™ of U2OS cells cultured on plastic and together with cylinders with or without vitD$_3$. (C, D, E) morphology of cells on plastic and together with cylinders with and without vitD$_3$. Cylinders without vitD$_3$ are more cytotoxic than cylinders made with vitD$_3$. Scale bars represent 200 µm (F) Alamar blue levels of cells on plastic and together with cylinders with and without vitD$_3$. (G) DNA levels measured of cells on plastic and together with cylinders with and without vitD$_3$. * $p<0.05$, ** $p<0.01$, *** $p<0.01$*

VitD$_3$ is released from the bioink and is bioactive.

To have a biological effect, the released vitD$_3$ from the cylinders needs to be bioactive. Cells cultured for 1 day with medium incubated with cylinders made from bioink containing vitD$_3$ had on average a 165-fold higher relative gene expression of Cyp24a1 than cells cultured with conditioned medium from cylinders without vitD$_3$ (n=2).

The bioink increased the release of OPN, RANKL, and OPG compared to the control.

To be clinically relevant, the constructs should stimulate the cells adjacent to this material to differentiate towards bone and/or produce factors that stimulate bone remodeling. To measure osteogenic differentiation, cellular ALP activity, and OPN released in the culture medium was measured. The ALP activity (Figure 3A) was very similar at all time points and no differences were apparent between the groups. The released OPN (Figure 3B) increased significantly up to day 5 for all conditions. At day 7 the released OPN was higher in the conditions containing a construct. This apparent effect was significant in the condition with a construct without vitD$_3$. To measure the ability of the cells to contribute to osteoclast formation, the release of IL-6, TNF-α, RANKL, and OPG by the cells was also measured in the medium. The amount of IL-6 released was similar between all the groups except at day 5, where the concentration was significantly higher in the medium taken from cells grown on plastic compared to the conditioned medium taken from cells grown in the presence of constructs (figure 3C). Cells exposed to each of the three culture conditions released a similar amount of TNF-α at all time points (Figure 3D). The amount of RANKL released was higher in conditioned medium taken from cells grown in the presence of constructs than in medium taken from cells grown on plastic (Figure 3E). This was significant for the constructs with vitD$_3$ at day 2 and day 5. At day 7, this was significant for both conditions with a construct. The amount of released OPG was ~ 15-times higher than the amount of released RANKL at day 0, this increased in time. At day 5 and day 7, the amount of OPG released was significantly higher in medium taken from the control than in medium taken from cells grown in the presence of constructs (Figure 3F).

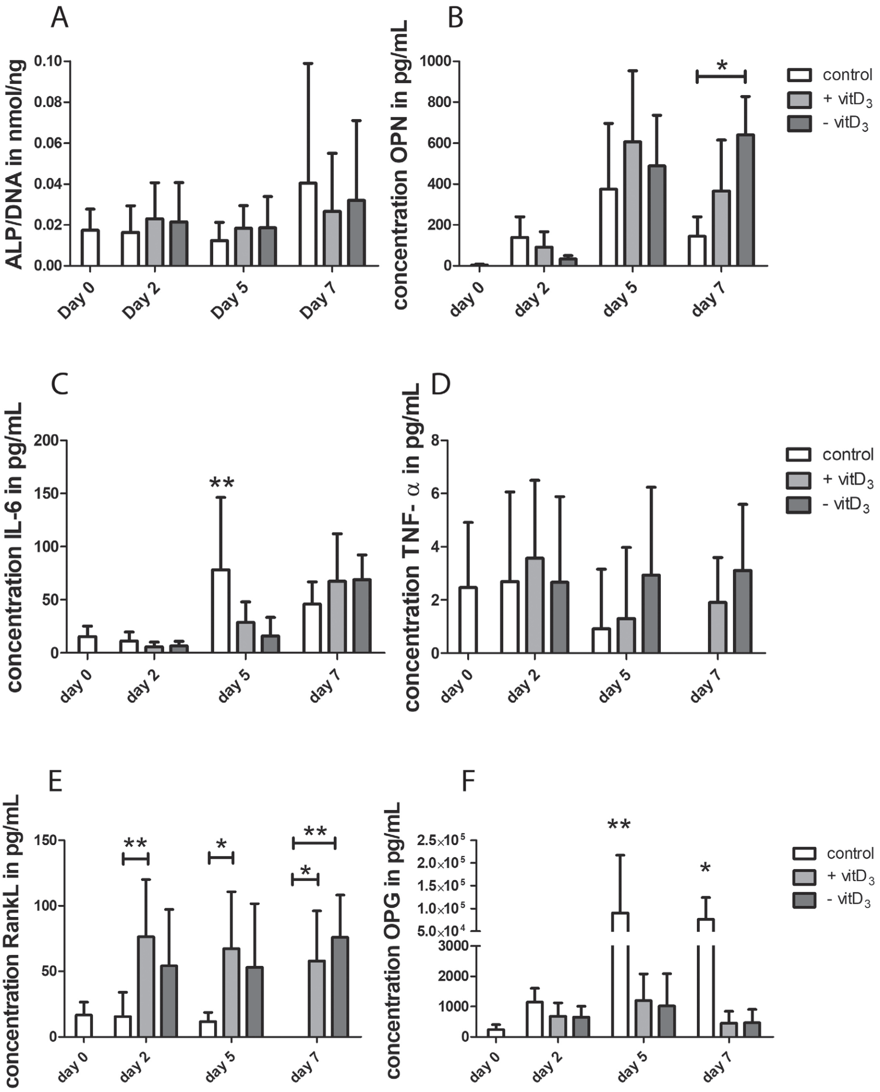

Figure 3. ALP activity and released cytokines of U2OS cells cultured with or without the bioink.

All experiments were done at day 0, day 2, day 5, and day 7 in samples with cells cultured on plastic, and cells cultured on plastic together with cylinders (3.8% κ-carrageenan) with or without vitD$_{3.}$ *(A) Cellular ALP, as a measure for osteogenic differentiation, was corrected for DNA levels and is similar in all conditions. (B) The released OPN was significantly higher in the condition with a construct without vitD*$_3$ *compared to plastic at day 7. (C) Released IL-6 was significantly higher in U2OS cells cultured on plastic at day 5. (D) Released TNF-a was similar in all conditions at all time points. (E) The released RANKL was significantly higher in the condition with a construct with vitD*$_3$ *at all time points. (F) Released OPG was significantly higher when cells were cultured without a 3D construct. Significance was measured using 2-way ANOVA with Bonferroni posttests. * p<0.05, ** p<0.01.*

Discussion

In this study, we evaluated the potential clinical applicability of a bioink consisting of a mixture of CaP paste and k-carrageenan, enhanced with biological component vitD$_3$. We chose vitD$_3$ since vitD$_3$ stimulates osteogenic differentiation of mesenchymal stem cells when released from tissue-engineered constructs, as we have shown recently [17]. We found that bioinks containing 3.8% k-carrageenan were printable, released active vitD$_3$ did not inhibit the proliferation of U2OS cells, and led to increased release of soluble RANKL and strongly reduced OPG released by these cells. Taken together, our results suggest that constructs made of CaP paste and κ-carrageenan could give rise to 3D-printed scaffolds that are clinically relevant.

Although the compression elastic modulus of cylinders cast with the bioink as used in the present study is not in the same range (10^4-times lower) as the compression elastic modulus of bone [18], it is similar to other bioinks used for 3D-bioprinting, e.g. based on alginate and gelatin [19,20]. The bioink is strong enough to contain its shape and can be carefully picked up and handled by a surgeon to be placed in a non-load-bearing defect. Initial stabilization e.g. with metal plates will be necessary. Engler et al., show that stiffer matrices (~ 40 kPa) direct mesenchymal stem cells into the osteogenic lineage compared to softer matrices (between 7- 17 kPa) which direct the cells towards the myogenic lineage and even softer matrices (between 0.1 and 1 kPa) which direct the cells towards the neurogenic lineage [21]. Since the compression elastic modulus of our material is higher than 40 kPa, we speculate that this may direct stem cell differentiation towards the osteogenic lineage.

The construct that contains vitD$_3$ appears to be less toxic for the cells than tissue culture plastic, although this effect is not significant (n=4). We speculate that the adenylate kinase, used as a measure for cytotoxicity, is partly absorbed by the bioink, or that the construct might already be chemically dissolving, thereby somehow interfering with the measurement. This would mean that the release of adenylate kinase from cells in the presence of constructs is underestimated, and the combination of CaP and k-carrageenan may actually be slightly cytotoxic. This would be in line with the results from Lim et al., who show that higher concentrations of κ-carrageenan in gelatin/ κ-carrageenan scaffolds lead to lower cell viability of fibroblasts [22]. In any case, adding vitD$_3$ to the construct seems to have a protective effect on the cells. This is also visible in Alamar blue data. This positive effect of vitD$_3$ on cell viability has been reported for the human cell line HepG2 [23].

$VitD_3$ can induce osteogenic differentiation in stem cells [24]. The results in this study show no differences in ALP activity and no effect of cylinders made of bioink containing $vitD_3$ vs. those without $vitD_3$ on the release of OPN by U2OS cells. It might be that U2OS cells do not respond to the $vitD_3$ with an increase in differentiation. Luo et al. show that U2OS cells have a low basal ALP level and do not respond to BMPs with an increase in osteogenic differentiation [25]. U2OS were capable to detect and respond to $vitD_3$ since CYP24a1 expression did go up by 165-fold. To better assess the effect of the bioink on osteogenic differentiation another cell source might be more suitable, such as hMSCs or primary human bone cells.

Interestingly, the bioink enhanced the release of RANKL by U2OS cells, especially the bioinks containing $vitD_3$. RANKL plays an important role in osteoclastogenesis and can be induced by $vitD_3$ [26]. This could indicate that the bioink enhances the stimulation of osteoclastogenesis by osteoblasts, especially since incubation with cylinders made of the bioink also reduced OPG expression by U2OS cells by almost 100-fold. This shows that the bioink may stimulate osteoclastogenesis to some degree, albeit that the number of soluble OPG molecules (60kDa) still exceeds the number of soluble RANKL molecules (32 kDa) by ~5-fold even in the presence of constructs containing $vitD_3$. In addition, our assays did not allow us to establish changes in membrane-bound RANKL, e.g. as a result of shedding. Future osteoblast-mediated osteoclastogenesis experiments may reveal to what extent scaffolds made of our bioink modulate the formation, and activity, of osteoclasts.

IL-6 is a dual-edged cytokine that can play a role in osteogenesis, by enhancing differentiation of osteoblasts, upregulating ALP, and bone matrix formation [27,28], and play a role in osteoclastogenesis by upregulating RANKL [27,29]. Our results show that the released IL-6 increases in time, especially in the medium taken from cells cultured in the presence of constructs made of the bioink. At day 7, the amount of IL-6 released by cells cultured together with a construct with $vitD_3$ was significantly higher compared to the amount released at day 0 and day 2 and the amount of IL-6 released by cells cultured together with a construct without $vitD_3$ was significantly higher at day 7 compared to all other time points. IL-6 can stimulate the first stages of osteogenic differentiation of osteoblast precursor cells [27], indicating that the bioink might induce osteogenic differentiation by inducing IL-6 release by osteoblasts in the vicinity. On the other hand, it may serve to increase RANKL expression and thereby osteoclastogenesis, although the conditions and time points that showed the highest IL-6 expression by U2OS cells did not correspond to the conditions and time points showing the highest RANKL expression. Finally, once implanted *in vivo*, cells in and near the constructs will be exposed to a cocktail of cytokines produced as part of the wound healing process. More research is needed on the effect of our bioink on the osteogenic and osteoclastogenic differentiation of mesenchymal stem cells before we can conclude whether our construct will positively affect bone formation and remodeling. So far, we have no indication that the construct will *negatively* affect these processes in any way.

To have clinical potential, other aspects such as upscaling of production, the possibility to sterilize, and storage of preprinted materials should be considered. The printability of larger constructs made of CaP paste and κ-carrageenan needs to be tested. The gel is relatively pliable before crosslinking so special care should be taken to maintain the desired shape and porosity. Also, the storage of 3D-printed constructs needs to be considered. As the bioink is partly consisting of a gel structure it is not possible to store 3D-printed constructs in a dry environment because the construct will dry out and shrink. Storage in a wet environment such as PBS or SBF is possible, but when the material is enhanced with biological components, such as the vitD$_3$ as used in the current study, part of the biological component would already be released and lost. For this reason, it would be optimal to directly place the construct after printing. We now only tested the reaction of cells that were not in direct contact with constructs made with the bioink, because we wished to determine the effect of the bioink on cells surrounding the 'scaffold' first. It is also important that stem cells recruited to the defect are able to attach to the material, but others have shown that several cell types are capable of attaching to precipitated CaP and κ-carrageenan.

In conclusion, constructs made of a bioink consisting of a combination of CaP paste and 3.8% κ-carrageenan, enhanced with vitD$_3$, are relatively easy to handle, are bioactive, and are not cytotoxic to cells in the direct vicinity, paving the way for further development in order to create personalized 3D-printed scaffolds suitable for use in tissue engineering of large bone defects.

Acknowledgments

We want to thank RegenHU for supplying us with the 3D-Discovery printer.

References

1. Sakkas, A.; Wilde, F.; Heufelder, M.; Winter, K.; Schramm, A. Autogenous bone grafts in oral implantology—is it still a “gold standard”? A consecutive review of 279 patients with 456 clinical procedures. *Int. J. Implant Dent.* **2017**, *3*, 1–17.
2. Pape, H.C.; Evans, A.; Kobbe, P. Autologous Bone Graft: Properties and Techniques. *J. Orthop. Trauma* **2010**, *24*, S36–S40.
3. Amini, A.R.; Laurencin, C.T.; Nukavarapu, S.P. Bone tissue engineering: Recent advances and challenges. *Crit. Rev. Biomed. Eng.* **2012**, *40*, 363–408.
4. Agrawal, S.; Srivastava, R. Osteoinductive and Osteoconductive Biomaterials. In *Racing for the Surface*; Springer International Publishing, 2020; pp. 355–395.
5. Barradas, A.M.C.; Yuan, H.; van Blitterswijk, C.A.; Habibovic, P. Osteoinductive biomaterials: current knowledge of properties, experimental models and biological mechanisms. *Eur. Cell. Mater.* 2011, *21*.
6. Shepherd, J.H.; Best, S.M. Calcium phosphate scaffolds for bone repair. *JOM* 2011, *63*, 83–92.
7. Liu, T.; Zheng, Y.; Wu, G.; Wismeijer, D.; Pathak, J.L.; Liu, Y. BMP2-coprecipitated calcium phosphate granules enhance osteoinductivity of deproteinized bovine bone, and bone formation during critical-sized bone defect healing. *Sci. Rep.* **2017**, *7*.
8. Song, I.; Kim, B.-S.; Kim, C.-S.; Im, G.-I. Effects of BMP-2 and vitamin D3 on the osteogenic differentiation of adipose stem cells. *Biochem. Biophys. Res. Commun.* **2011**, *408*, 126–131.
9. Thadavirul, N.; Pavasant, P.; Supaphol, P. Development of polycaprolactone porous scaffolds by combining solvent casting, particulate leaching, and polymer leaching techniques for bone tissue engineering. *J. Biomed. Mater. Res. Part A* **2014**, *102*, 3379–3392.
10. Nandakumar, A.; Fernandes, H.; de Boer, J.; Moroni, L.; Habibovic, P.; van Blitterswijk, C.A. Fabrication of Bioactive Composite Scaffolds by Electrospinning for Bone Regeneration. *Macromol. Biosci.* **2010**, *10*, 1365–1373.
11. Huang, Y.H.; Jakus, A.E.; Jordan, S.W.; Dumanian, Z.; Parker, K.; Zhao, L.; Patel, P.K.; Shah, R.N. Three-Dimensionally Printed Hyperelastic Bone Scaffolds Accelerate Bone Regeneration in Critical-Size Calvarial Bone Defects. *Plast. Reconstr. Surg.* **2019**, *143*, 1397–1407.
12. Gbureck, U.; Hölzel, T.; Klammert, U.; Würzler, K.; Müller, F.A.; Barralet, J.E. Resorbable Dicalcium Phosphate Bone Substitutes Prepared by 3D Powder Printing. *Adv. Funct. Mater.* **2007**, *17*, 3940–3945.
13. Ozbolat, I.T.; Hospodiuk, M. Current advances and future perspectives in extrusion-based bioprinting. *Biomaterials* **2016**, *76*, 321–343.
14. Kelder, C.; Bakker, A.; Klein-Nulend, J.; Wismeijer, D.; Kelder, C.; Bakker, A.D.; Klein-Nulend, J.; Wismeijer, D. The 3D Printing of Calcium Phosphate with K-Carrageenan under Conditions Permitting the Incorporation of Biological Components—A Method. *J. Funct. Biomater.* **2018**, *9*, 57.

15. Vignesh, S.; Gopalakrishnan, A.; M.R, P.; Nair, S. V; Jayakumar, R.; Mony, U. Fabrication of micropatterned alginate-gelatin and k-carrageenan hydrogels of defined shapes using simple wax mould method as a platform for stem cell/induced Pluripotent Stem Cells (iPSC) culture. *Int. J. Biol. Macromol.* **2018**, *112*, 737–744.
16. Lowry, H.O. Micromethods for the assay of enzyme II. Specofic procedures. Alkaline phosphatase. *Methods Enzymol.* **1955**, *4*, 371–372.
17. Kelder, C.; Hogervorst, J.M.A.; Wismeijer, D.; Kleverlaan, C.J.; de Vries, T.J.; Bakker, A.D. Burst, short, and sustained vitamin D3 applications differentially affect osteogenic differentiation of human adipose stem cells. *Int. J. Mol. Sci.* **2020**, *21*.
18. Boughton, O.R.; Ma, S.; Zhao, S.; Arnold, M.; Lewis, A.; Hansen, U.; Cobb, J.P.; Giuliani, F.; Abel, R.L. Measuring bone stiffness using spherical indentation. *PLoS One* **2018**, *13*, e0200475.
19. Zhang, J.; Wehrle, E.; Vetsch, J.R.; Paul, G.R.; Rubert, M.; Müller, R. Alginate dependent changes of physical properties in 3D bioprinted cell-laden porous scaffolds affect cell viability and cell morphology. *Biomed. Mater.* **2019**, *14*, 065009.
20. Chiesa, I.; de Maria, C.; Lapomarda, A.; Maria Fortunato, G.; Montemurro, F.; Di Gesù, R.; S Tuan, R.; Vozzi, G.; Gottardi, R. Endothelial cells support osteogenesis in an in vitro vascularized bone model developed by 3D bioprinting. *Biofabrication* **2020**, *12*.
21. Engler, A.J.; Sen, S.; Sweeney, H.L.; Discher, D.E. Matrix Elasticity Directs Stem Cell Lineage Specification. *Cell* **2006**, *126*, 677–689.
22. Lim, Y.M.; Gwon, H.J.; Choi, J.H.; Shin, J.; Nho, Y.C.; Jeong, S.I.; Chong, M.S.; Lee, Y.M.; Kwon, I.K.; Kim, S.E. Preparation and biocompatibility study of gelatin/kappa-carrageenan scaffolds. *Macromol. Res.* **2010**, *18*, 29–34.
23. Özerkan, D.; Ozsoy, N.; Yilmaz, E. Vitamin D and melatonin protect the cell's viability and ameliorate the CCl4 induced cytotoxicity in HepG2 and Hep3B hepatoma cell lines. *Cytotechnology* **2014**, *66*.
24. Liu, P.; Oyajobi, B.O.; Russell, R.G.G.; Scutt, A. Regulation of Osteogenic Differentiation of Human Bone Marrow Stromal Cells: Interaction Between Transforming Growth Factor-β and 1,25(OH)2 Vitamin D3In Vitro. *Calcif. Tissue Int.* **1999**, *65*, 173–180.
25. Luo, X.; Chen, J.; Song, W.X.; Tang, N.; Luo, J.; Deng, Z.L.; Sharff, K.A.; He, G.; Bi, Y.; He, B.C.; et al. Osteogenic BMPs promote tumor growth of human osteosarcomas that harbor differentiation defects. *Lab. Investig.* **2008**, *88*, 1264–1277.
26. Takahashi, N.; Udagawa, N.; Suda, T. Vitamin D endocrine system and osteoclasts. *Bonekey Rep.* **2014**, *3*.
27. Blanchard, F.; Duplomb, L.; Baud'huin, M.; Brounais, B. The dual role of IL-6-type cytokines on bone remodeling and bone tumors. *Cytokine Growth Factor Rev.* 2009, *20*, 19–28.
28. Franchimont, N.; Wertz, S.; Malaise, M. Interleukin-6: An osteotropic factor influencing bone formation? *Bone* 2005, *37*, 601–606.
29. Liu, X.H.; Kirschenbaum, A.; Yao, S.; Levine, A.C. The Role of the Interleukin-6/gp130 Signaling Pathway in Bone Metabolism. *Vitam. Horm.* 2006, *74*, 341–355.

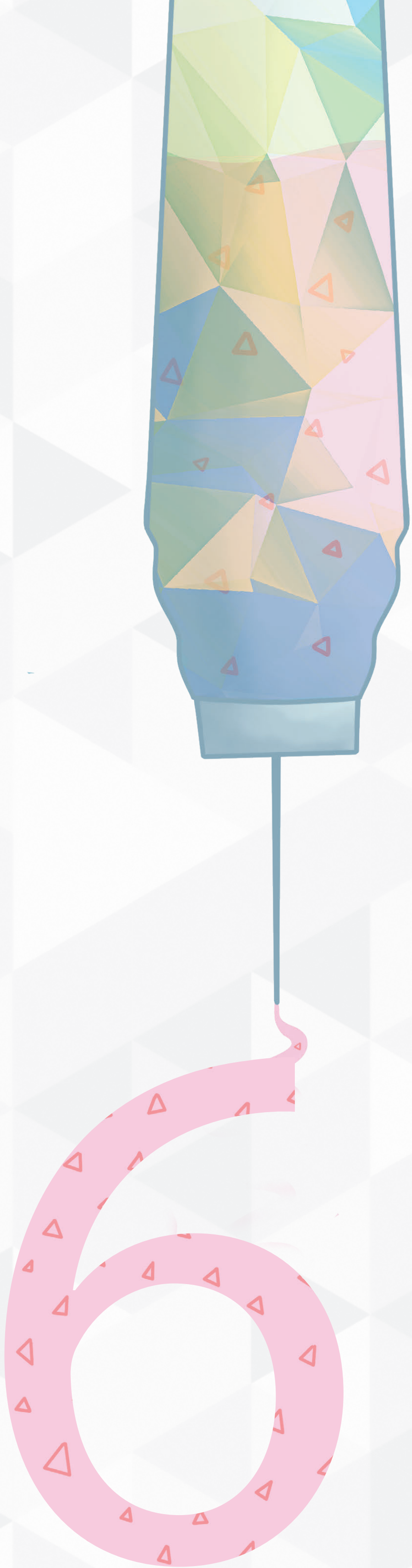
6

General Discussion

The main objective of this thesis was to develop a method to 3D-print calcium phosphate combined with biological components that are released from the construct while retaining their biological activity, in order to enable or accelerate bone healing.

The 'ideal' tissue engineering construct

In tissue engineering, biomaterials, the type of cells required for the specific approach, and chemical and/or mechanical stimuli, are usually combined to generate a construct. Regarding the construct, according to literature the 'ideal' biomaterial for bone tissue engineering should have the following properties: biocompatible or bioinert, biodegradable, both osteoconductive and osteoinductive, porous, and mechanically compatible with native bone. Currently, most developed biomaterials only have some, but never all of these required properties [1–3]. In this final chapter, I will discuss how the current thesis contributes to the making of the 'ideal' bone tissue engineering construct.

Biocompatibility

Biocompatibility is the ability of a material to be placed in contact with human tissues without causing an unacceptable reaction of the body [4]. Natural polymers that are biocompatible and often used as biomaterials are collagen, gelatin, or chitosan [5]. Synthetic polymers that are generally considered to be biocompatible are e.g. poly-L-lactic acid (PLLA) and polycaprolactone diol (PCL)[6]. In this thesis, we used a printable material or bioink consisting of a combination of calcium phosphate and κ-carrageenan. Calcium phosphates are widely accepted to be biocompatible, and κ-carrageenan, which resembles glycosaminoglycans (GAGs), is used in the food industry and therefore can be considered as a bio acceptable material. Popa et al. studied both the in vitro and in vivo biocompatibility of κ-carrageenan hydrogels and showed a slightly lower metabolic activity in a cultured mouse fibroblast cell line, and no production of reactive oxygen species. A low inflammatory response in vivo was observed by the presence of only PMNs [7]. Similarly, an acute inflammatory reaction, but not a systemic reaction, was found by Lim et al. when a scaffold made of gelatin and κ-carrageenan was implanted subcutaneously in rats [8]. This lack of a systemic inflammatory reaction when using κ-carrageenan indicates that the initial immune responses to k-carrageenan were transient. Also, as stated earlier, the desired cells, being bone cells that contribute to bone formation and cells that ultimately replace the carrier, were not taken into account. We expected no, or very low, adverse effect of our bioink on cells. In **chapter 5** we measured metabolic activity and cytotoxicity of U2OS cells co-cultured with constructs made of our bioink. The metabolic activity of cells cultured together with a construct is significantly lower than cells cultured on tissue culture plastic, but adding vitD$_3$ to the bioink cancels this effect. The cytotoxicity seems higher in the condition with only the bioink, although this is not significant compared to tissue culture plastic. Again, adding vitD$_3$ reduced the cytotoxicity. This indicates that the bioink alone elicits a low cellular response, which is canceled by the addition of vitD$_{3.}$ This low response by the bioink might be improved by adjustments to the material.

Tissue engineering constructs based on materials normally present in the damaged human tissue that needs to be repaired have a good chance of being biocompatible. Several types of collagen are present in bone i.e. type I, III, and V, with collagen type I being the most abundant, comprising 90% of all organic matrix inside bone [9]. To better mimic the extracellular matrix of bone, collagen type I could be incorporated into the bioink or used as a coating. By adding collagen type I, the biocompatibility might be enhanced as collagen contains RGD binding sites to which cells can attach. We used κ-carrageenan instead of collagen because κ-carrageenan is derived from red seaweed that is abundantly available and it is much cheaper than collagen. Another adjustment that may improve the biocompatibility and cell attachment of the bioink is adding small (micrometers) CaP particles, made of the same precipitated CaP as the CaP paste used in the bioink. We have unpublished data that printing a bioink with CaP particles is possible. By adding such particles the surface roughness is likely to increase, which might enhance cell attachment [10]. With every adjustment to the material, the printability must be tested and the 3D-printing parameters optimized.

Biodegradable

Besides being biocompatible, the material should ideally also be biodegradable or at least bioinert. Biomaterials are often not intended to be permanent [11] because in time materials are affected by wear/fatigue, and cannot remodel, regenerate and adapt, while natural bone can. For these reasons it is preferred that bone will replace the biomaterial. Preferably, the material should be resorbed/dissolve at the same speed as new bone is formed.

Our bioink consists of precipitated calcium phosphate and κ-carrageenan. Calcium and phosphate ions affect bone resorption as calcium ions regulate the formation of osteoclasts [12], while phosphate ions inhibit bone resorption by interfering with RANKL signaling, thereby inhibiting osteoclast differentiation [13]. Liu et al. showed that precipitated CaP (similar to the protocol we used) is resorbed by osteoclasts *in vitro* [14]. This indicates that the CaP in our bioink might also be resorbed. However, we used a CaP paste instead of dried particles, therefore it is necessary to experimentally assess whether osteoclasts also absorb CaP paste. K-carrageenan is a naturally derived sulfated polysaccharide just like alginate. Alginate is derived from brown seaweed and is known for its biocompatibility and biodegradation [15]. Alginate and κ-carrageenan can be enzymatically degraded; however, such enzymes are not present in humans. An ionically crosslinked alginate can be dissolved by the release of the ions that crosslink the gel in the surrounding medium [16]. Furthermore, the degradation of alginate depends on the pH. In an acidic environment of pH <5 the glycosidic bonds are degraded by acid hydrolyze [17]. Based on the similarity in molecular basis and origin, we suspect that κ-carrageenan undergoes a similar degradation process as alginate. Popa et al. show that κ-carrageenan hydrogels were degraded after 15 days when placed subcutaneously in rats [7]. Taken together, we assume that our bioink, consisting of CaP paste and κ-carrageenan, is biodegradable. Whether this is indeed the case needs to be tested, as well as the degradation kinetics. Firstly, the rate of dissolving CaP can be tested in vitro. Preliminary tests (not shown) showed that a porous construct printed with CaP paste and 2.8% κ-carrageenan retained its shape for 7 days in phosphate-buffered saline. In other words, without the cellular component, at neutral pH and room temperature, these constructs are stable for at least multiple days. Further testing with 3.8% κ-carrageenan and other solvents such as simulated body fluid and culture medium would give a better understanding on the biodegradation of the construct. To assess whether cells resorb the bioink, experiments with cultured osteoclasts derived from human peripheral blood monocytes can used to give an indication.

Osteoconductive and osteoinductive

Osteoconductive materials are materials with a surface that permits the migration and growth of bone, while osteoinductive materials stimulate (stem) cells to differentiate into bone-forming cells [18,19]. To be effective, a tissue-engineered scaffold should be both, since both are needed for rapid bone formation throughout the construct and bone integration. For effective osteoconduction the scaffolds should fit the defect perfectly, thus facilitating the migration of cells from the adjacent bony environment. Therefore, 3D-printing is an appropriate production method, as it allows the creation of a custom-made scaffold to fit an individual defect e.g. based on CT scans.

Calcium phosphate-based materials are osteoconductive, and when CaP dissolves, calcium and phosphate ions are released. Calcium ions can influence bone formation and maturation through calcification [13]. Furthermore, these ions have an effect on bone regeneration as they stimulate mature bone cells and induce the proliferation of bone precursor cells [20]. Phosphate ions can also influence bone formation by regulating the differentiation and growth of osteoblasts and it increases the expression of BMPs [21].

In **chapter 5**, we have performed preliminary tests for the ability of our bioink to enhance osteogenic differentiation in U2OS cells. The bioink did not affect ALP expression, however, the bioink upregulated *Osteopontin* (OPN) release. As U2OS cells are already considered osteoblast-derived cells, this is not osteoinduction in its purest form, but it is still indicative of a positive effect on osteogenic differentiation since the balance contributing to osteoclast differentiation. Furthermore, we have tested the influence of the bioink on cells that were not in direct contact with the material. After more in vitro tests, in vivo testing of the material is needed to really state if the material is both osteoconductive and osteoinductive.

The possibility to enhance the print material with biological components (such as vitD$_3$) makes it suitable to improve osteoinductive properties with bioactive factors. Besides the often-used factors, BMP-2 and vitD$_3$ other factors such as cytokines might be useful. In the first 72 hours of bone fracture healing, several cytokines are released such as TNF-α, IL-4, and IL-6. Especially, IL-6 might be of interest, as IL-6 stimulates the osteogenic differentiation of MSCs [22] and stimulates the formation of osteoclasts, thereby aiding the degradation of the scaffold material. However, dose and timing need to be very precisely tuned when using cytokines, since prolonged exposure to cytokines are generally catabolic, where short exposures are more likely to be anabolic.

In the study by Kuttappan et al. a combination of factors (VEGF, FGF, and BMP-2) was released from nanocomposite fibrous scaffolds. The factors were released at different time intervals and led to increased bone formation and vascularization [23]. This indicates that enhancing our material with a combination of factors might be the direction in which future research should be perused, although such a strategy can become costly, as some biological components are very expensive for applications in large defects. Furthermore, the optimal release kinetics will be component-dependent, and overstimulation can lead to substantial side effects, such as ectopic bone formation and highly active osteoclasts caused by the BMP-2 [24], and growth inhibition when supraphysiological concentrations of vitD$_3$ are used [25]. Finding the optimal release of a cocktail of components is more difficult and might lead to more side effects.

In **chapter 2**, we aimed to study which release kinetics of vitD$_3$ is more optimal for osteogenic differentiation of adipose stem cells in vitro. We showed that a sustained release of vitD$_3$ is more optimal for the osteogenic differentiation of adipose stem cells [26]. Our regime of 10 nM of vitD$_3$ for 20 days highly upregulated the expression of Cyp24a1, which converts the active form of vitD$_3$ to an inactive form [27]. We suspect that by using lower concentrations of vitD$_3$ the mentioned upregulation will be less, potentially leading to better osteogenic differentiation, which is preferable for bone tissue engineering. Unfortunately, we did not measure late osteogenic differentiation markers such as OPN, *Dental Matrix protein-1* (DMP-1), and *Actin alpha 1* (ACTA1). Assessing the expression of these components is recommended as differentiation towards the later stages of osteogenic differentiation are needed to form bone [28]. The experiments performed in chapter 2 are executed *in vitro* and were precisely controlled. To make tissue engineering constructs that release biological components in such a precise manner is difficult, and most materials first release a burst before having a sustained release. It would be interesting to test *in vitro* whether a combination of a burst with a sustained release is more optimal for osteogenic differentiation than the sustained release alone. Biologically this might make sense, as the initial burst may prime the surrounding cells to differentiate towards the osteogenic lineage. Overman et al. show that a 15-minute treatment of BMP-2 can already prime cells towards the osteogenic lineage. The sustained release can further differentiate the cells and also differentiate possible recruited stem cells towards the osteogenic lineage.

In **chapters 3** and **5**, we cultured cells in 2D. The advantage of 2D culturing is higher throughput and microscopical and biochemical analyses are easier. However, it is known that 2D culture does not fully mimic the *in vivo* environment, as it lacks cell-cell interactions from all sites and provides a different mechanical environment. Furthermore, many cell types, when cultured in 2D, become flattened and lose their differentiated phenotype [29]. Based on the study of Xiao et al. alveolar bone cells maintain their osteogenic properties more when cultured in a 3D environment [30]. This suggests the results we see in chapter 3 for alveolar bone cells might be different when performed in 3D, however, this might also be the case for long bone cells. We suspect that the results we see in our 2D studies will be more pronounced when it would be conducted in 3D. Taken together our bioink, with the vitD_3 concentration we used only seems to have a slight osteogenic effect on U2OS cells. To really assess the osteoinduction properties of the bioink more studies, such as differentiation studies with stem cells, are needed.

Porous

Scaffolds for tissue engineering should have a porous structure as this is essential for the exchange of nutrients, proliferation, and migration of cells for vascularization and tissue formation [31]. It is especially important for large constructs to have interconnected pores, to allow for cell migration throughout the construct, and to allow rapid invasion of the construct with blood vessels to ensure oxygen delivery inside the complete construct, including the (often severely hypoxic) center. The ideal pore size for bone tissue engineering is not completely clear but is estimated to range between 100-1000 µm [32]. The minimal scaffold pore size for cell migration and exchange of nutrients has been claimed to be 100 µm, but other studies show that pores above 200 µm promote deep vascularization [33].

In **chapter 4** and **5** we used 3D-printing to design and create constructs with a pre-defined internal structure. By using 3D-printing, we created constructs with pores of approximately 2.2 mm^3 with 3.8% κ-carrageenan. These pores are large enough for angiogenesis and bone ingrowth [34]. Unfortunately, these pores are only one way (vertically) and not interconnected which would be preferable. This is the result of the viscosity of the material which causes it to spread when printed on a surface and is not strong enough to stack the layers and create interconnected pores. To overcome this, embedded printing methods can be used, where the bioink is extruded in a supporting material such as a hydrophobic high-density fluid [35–37]. Indirect printing is another way to make interconnected pores. With this method, a sacrificial mold is created, followed by casting the scaffold material in the mold and then removal of the mold [38,39]. We did some tests with this method; however, we encountered some obstacles such as removing the mold without breaking the printed construct. One more way to create interconnected pores with our bioink is printing simultaneously with sacrificial material. By removing the sacrificial material pores are created. The sacrificial material would preferably dissolve when the bioink is crosslinked or washed. Extensive steps to dissolve the sacrificial material are likely to affect the activity of the incorporated bioactive factors and are therefore undesirable. The ready-to-print sacrificial and support ink of Cellink (commercially available) might be a good option to use.

Mechanically compatible with native bone

Materials have different mechanical properties such as the stiffness of the material which cells feel, or the mechanical properties of the bulk of the material made into a scaffold. When it is proposed that an ideal tissue engineering construct should be mechanically compatible with the native bone it suggests that the bulk mechanical properties should be in the same range and therefore can carry some load. The material should not be too stiff as this will lead to stress shielding [40], a phenomenon characterized by the reduction of bone density as a result of the removal of mechanical load from the bone by the material. In **chapter 5**, we show that mechanically, our print material is not in the range of native bone, namely the compression modulus of our bioink is ~10.000 times lower. For the use in non-load defects such as the sinus floor elevation, this is less important and load-bearing defects can initially be stabilized with screws. However, there are some options to try and improve the mechanical properties of our print material. First of all, adding small CaP particles or rods to the mixture of paste and κ-carrageenan. In the study of Nejati et al. both precipitated rods as commercially bought particles were added to PLLA scaffolds and both improved the mechanical properties compared to PLLA alone [41]. Another method to improve the mechanical properties can be to alternatingly print strands of our print material between strands of a biodegradable polymer such as PLGA or PCL [42]. The mechanical properties of such polymers are higher and can work as a sort of cage to protect the softer print material against mechanical loading. A downside is that less bioink is used to create a scaffold and the amount of biological component should be adjusted to the lesser amount of bioink.

Other properties

The above-discussed properties are the classical properties needed for the 'ideal' tissue engineering construct. Other properties that are useful to consider or needed such as vascularization. Vascularization is crucial in tissue engineering and therefore scaffolds should induce angiogenesis [43]. One of the most used factors to induce vascularization is VEGF as it promotes the first phases of angiogenesis such as endothelial cell sprouting. Other factors such as ANG1 can be used or a combination of VEGF and ANG1 as the angiopoietin–Tie signaling system seems to complement the VEGF pathway [44,45].

In addition, there are probably no uniform solutions for all bone defects. In **chapter 3**, we aimed to study if skeletal sites react differently to possible cues from such tissue engineering constructs. We did this by comparing cells derived from human alveolar bone with cells derived from human long bone when studying their osteogenic and osteoclastogenic potential with and without vitD$_3$. Our results showed that cells from different skeletal sites have site-specific differences. Cells derived from long bone are more differentiated within the osteogenic lineage, while alveolar bone cells proliferate faster. Furthermore, long bone cells have increased osteoclastogenic potential compared to alveolar bone cells [46]. These differences indicate that the 'ideal' tissue engineering construct should take the site of an implant into account.

To be clinically applicable, other properties such as sterilizability, costs, shelf life, and production time need to be considered.

Taken together, did we make the ideal bone tissue engineering construct suitable for each site? No, we are not there yet. However, we did lay a firm foundation for a bioink that might have the potential to be optimized and used for bone tissue engineering.

References

1. Das, R. Application of nanobioceramics in bone tissue engineering. In *Nanobiomaterials in Hard Tissue Engineering: Applications of Nanobiomaterials*; Elsevier Inc., 2016; pp. 353–379 ISBN 9780323428620.
2. Polo-Corrales, L.; Latorre-Esteves, M.; Ramirez-Vick, J.E. Scaffold design for bone regeneration. *J. Nanosci. Nanotechnol.* 2014, *14*, 15–56.
3. Sanz-Herrera, J.A.; García-Aznar, J.M.; Doblaré, M. On scaffold designing for bone regeneration: A computational multiscale approach. *Acta Biomater.* **2009**, *5*, 219–229.
4. Williams, D.F. On the mechanisms of biocompatibility. *Biomaterials* **2008**, *29*, 2941–2953.
5. Akilbekova, D.; Shaimerdenova, M.; Adilov, S.; Berillo, D. Biocompatible scaffolds based on natural polymers for regenerative medicine. *Int. J. Biol. Macromol.* **2018**, *114*, 324–333.
6. Maitz, M.F. Applications of synthetic polymers in clinical medicine. *Biosurface and Biotribology* **2015**, *1*, 161–176.
7. Popa, E.G.; Carvalho, P.P.; Dias, A.F.; Santos, T.C.; Santo, V.E.; Marques, A.P.; Viegas, C.A.; Dias, I.R.; Gomes, M.E.; Reis, R.L. Evaluation of the *in vitro* and *in vivo* biocompatibility of carrageenan-based hydrogels. *J. Biomed. Mater. Res. Part A* **2014**, *102*, 4087–4097.
8. Lim, Y.M.; Gwon, H.J.; Choi, J.H.; Shin, J.; Nho, Y.C.; Jeong, S.I.; Chong, M.S.; Lee, Y.M.; Kwon, I.K.; Kim, S.E. Preparation and biocompatibility study of gelatin/kappa-carrageenan scaffolds. *Macromol. Res.* **2010**, *18*, 29–34.
9. Lin, X.; Patil, S.; Gao, Y.G.; Qian, A. The Bone Extracellular Matrix in Bone Formation and Regeneration. *Front. Pharmacol.* 2020, *11*, 757.
10. Deligianni, D.D.; Katsala, N.D.; Koutsoukos, P.G.; Missirlis, Y.F. Effect of surface roughness of hydroxyapatite on human bone marrow cell adhesion, proliferation, differentiation and detachment strength. *Biomaterials* **2000**, *22*, 87–96.
11. O'Brien, F.J. Biomaterials & scaffolds for tissue engineering. *Mater. Today* 2011, *14*, 88–95.
12. Asagiri, M.; Takayanagi, H. The molecular understanding of osteoclast differentiation. *Bone* 2007, *40*, 251–264.
13. Jeong, J.; Kim, J.H.; Shim, J.H.; Hwang, N.S.; Heo, C.Y. Bioactive calcium phosphate materials and applications in bone regeneration. *Biomater. Res.* 2019, *23*, 1–11.
14. Liu T Zheng Y, Wismeijer D, Everts V, Liu Y., W.G. Cell-mediated BMP-2 release from a novel dual-drug delivery system promotes bone formation. *Clin. Oral Implants Res.* **2014**, *25*.
15. Sun, J.; Tan, H. Alginate-based biomaterials for regenerative medicine applications. *Materials (Basel).* 2013, *6*, 1285–1309.
16. Lee, K.Y.; Mooney, D.J. Alginate: Properties and biomedical applications. *Prog. Polym. Sci.* 2012, *37*, 106–126.
17. Guarino, V.; Caputo, T.; Altobelli, R.; Ambrosio, L. Degradation properties and metabolic activity of alginate and chitosan polyelectrolytes for drug delivery and tissue engineering applications. *AIMS Mater. Sci.* 2015, *2*, 497–502.

18. Albrektsson, T.; Johansson, C. Osteoinduction, osteoconduction and osseointegration. *Eur. Spine J.* **2001**, *10*, S96–S101.
19. Agrawal, S.; Srivastava, R. Osteoinductive and Osteoconductive Biomaterials. In *Racing for the Surface*; Springer International Publishing, 2020; pp. 355–395.
20. Riddle, R.C.; Taylor, A.F.; Genetos, D.C.; Donahue, H.J. MAP kinase and calcium signaling mediate fluid flow-induced human mesenchymal stem cell proliferation. *Am. J. Physiol. - Cell Physiol.* **2006**, *290*, 776–784.
21. Tada, H.; Nemoto, E.; Foster, B.L.; Somerman, M.J.; Shimauchi, H. Phosphate increases bone morphogenetic protein-2 expression through cAMP-dependent protein kinase and ERK1/2 pathways in human dental pulp cells. *Bone* **2011**, *48*, 1409–1416.
22. AP, B.-C.; AD, B.; B, Z.-D.; CJ, K.; N, B.; T, F.; J, K.-N. Cytokines TNF-α, IL-6, IL-17F, and IL-4 Differentially Affect Osteogenic Differentiation of Human Adipose Stem Cells. *Stem Cells Int.* **2016**, *2016*.
23. Kuttappan, S.; Mathew, D.; Jo, J. ichiro; Tanaka, R.; Menon, D.; Ishimoto, T.; Nakano, T.; Nair, S. V.; Nair, M.B.; Tabata, Y. Dual release of growth factor from nanocomposite fibrous scaffold promotes vascularisation and bone regeneration in rat critical sized calvarial defect. *Acta Biomater.* **2018**, *78*, 36–47.
24. Zara, J.N.; Siu, R.K.; Zhang, X.; Shen, J.; Ngo, R.; Lee, M.; Li, W.; Chiang, M.; Chung, J.; Kwak, J.; et al. High doses of bone morphogenetic protein 2 induce structurally abnormal bone and inflammation in vivo. *Tissue Eng. - Part A* **2011**, *17*, 1389–1399.
25. Skjødt, H.; Gallagher, J.A.; Beresford, J.N.; Couch, M.; Poser, J.W.; Russell, R.G.G. Vitamin D metabolites regulate osteocalcin synthesis and proliferation of human bone cells in vitro. **1985**, *105*, 391.
26. Kelder, C.; Hogervorst, J.M.A.; Wismeijer, D.; Kleverlaan, C.J.; de Vries, T.J.; Bakker, A.D. Burst, Short, and Sustained Vitamin D3 Applications Differentially Affect Osteogenic Differentiation of Human Adipose Stem Cells. *Int. J. Mol. Sci.* **2020**, *21*, 3202.
27. Yu, O.B.; Arnold, L.A. Calcitroic Acid–A Review. *ACS Chem. Biol.* **2016**, *11*, 2665–2672.
28. Infante, A.; Rodríguez, C.I. Osteogenesis and aging: lessons from mesenchymal stem cells. *Stem Cell Res. Ther.* 2018, *9*, 244.
29. Baker, B.M.; Chen, C.S. Deconstructing the third dimension-how 3D culture microenvironments alter cellular cues. *J. Cell Sci.* 2012, *125*, 3015–3024.
30. Xiao, Y.; Qian, H.; Young, W.G.; Bartold, P.M. Tissue Engineering for Bone Regeneration Using Differentiated Alveolar Bone Cells in Collagen Scaffolds. *Tissue Eng.* **2003**, *9*, 1167–1177.
31. Loh, Q.L.; Choong, C. Three-dimensional scaffolds for tissue engineering applications: Role of porosity and pore size. *Tissue Eng. - Part B Rev.* 2013, *19*, 485–502.
32. Zhang, B.; Pei, X.; Song, P.; Sun, H.; Li, H.; Fan, Y.; Jiang, Q.; Zhou, C.; Zhang, X. Porous bioceramics produced by inkjet 3D printing: Effect of printing ink formulation on the ceramic macro and micro porous architectures control. *Compos. Part B Eng.* **2018**, *155*, 112–121.

33. Somo, S.I.; Akar, B.; Bayrak, E.S.; Larson, J.C.; Appel, A.A.; Mehdizadeh, H.; Cinar, A.; Brey, E.M. Pore Interconnectivity Influences Growth Factor-Mediated Vascularization in Sphere-Templated Hydrogels. *Tissue Eng. - Part C Methods* **2015**, *21*, 773–785.
34. Murphy, C.M.; O'Brien, F.J. Understanding the effect of mean pore size on cell activity in collagen-glycosaminoglycan scaffolds. *Cell Adhes. Migr.* 2010, *4*, 377–381.
35. Duarte Campos, D.F.; Blaeser, A.; Weber, M.; Jäkel, J.; Neuss, S.; Jahnen-Dechent, W.; Fischer, H. Three-dimensional printing of stem cell-laden hydrogels submerged in a hydrophobic high-density fluid. *Biofabrication* **2013**, *5*, 015003.
36. Highley, C.B.; Rodell, C.B.; Burdick, J.A. Direct 3D Printing of Shear-Thinning Hydrogels into Self-Healing Hydrogels. *Adv. Mater.* **2015**, *27*, 5075–5079.
37. Senior, J.J.; Cooke, M.E.; Grover, L.M.; Smith, A.M. Fabrication of Complex Hydrogel Structures Using Suspended Layer Additive Manufacturing (SLAM). *Adv. Funct. Mater.* **2019**, *29*, 1904845.
38. Miller, J.S.; Stevens, K.R.; Yang, M.T.; Baker, B.M.; Nguyen, D.H.T.; Cohen, D.M.; Toro, E.; Chen, A.A.; Galie, P.A.; Yu, X.; et al. Rapid casting of patterned vascular networks for perfusable engineered three-dimensional tissues. *Nat. Mater.* **2012**, *11*, 768–774.
39. Zhang, Y.S.; Yue, K.; Aleman, J.; Mollazadeh-Moghaddam, K.; Bakht, S.M.; Yang, J.; Jia, W.; Dell'Erba, V.; Assawes, P.; Shin, S.R.; et al. 3D Bioprinting for Tissue and Organ Fabrication. *Ann. Biomed. Eng.* **2017**, *45*, 148–163.
40. Huiskes, R.; Weinans, H.; Van Rietbergen, B. *The Relationship Between Stress Shielding and Bone Resorption Around Total Hip Stems and the Effects of Flexible Materials*; 1992;
41. Nejati, E.; Mirzadeh, H.; Zandi, M. Synthesis and characterization of nano-hydroxyapatite rods/poly(l-lactide acid) composite scaffolds for bone tissue engineering. *Compos. Part A Appl. Sci. Manuf.* **2008**, *39*, 1589–1596.
42. Zamani, Y.; Mohammadi, J.; Amoabediny, G.; Helder, M.N.; Zandieh-Doulabi, B.; Klein-Nulend, J. Bioprinting of Alginate-Encapsulated Pre-osteoblasts in PLGA/β-TCP Scaffolds Enhances Cell Retention but Impairs Osteogenic Differentiation Compared to Cell Seeding after 3D-Printing. *Regen. Eng. Transl. Med.* **2020**, 1–9.
43. Mastrullo, V.; Cathery, W.; Velliou, E.; Madeddu, P.; Campagnolo, P. Angiogenesis in Tissue Engineering: As Nature Intended? *Front. Bioeng. Biotechnol.* 2020, *8*, 188.
44. Augustin, H.G.; Young Koh, G.; Thurston, G.; Alitalo, K. Control of vascular morphogenesis and homeostasis through the angiopoietin - Tie system. *Nat. Rev. Mol. Cell Biol.* 2009, *10*, 165–177.
45. Thurston, G.; Daly, C. The complex role of angiopoietin-2 in the angiopoietin-Tie signaling pathway. *Cold Spring Harb. Perspect. Med.* **2012**, *2*.
46. Kelder, C.; Kleverlaan, C.J.; Gilijamse, M.; Bakker, A.D.; de Vries, T.J. Cells derived from human long bone appear more differentiated and more actively stimulate osteoclastogenesis compared to alveolar bone-derived cells. *Int. J. Mol. Sci.* **2020**, *21*, 1–17.

7

Summary

Bone defects can arise as a consequence of trauma, cancer, inflammation, or overloading. Even though natural bone has good intrinsic healing capacity, the reconstruction of critical size bone defects remains a challenge. Currently, the “golden standard” for this type of defects is the use of autologous bone grafts. These grafts are taken from the patient, often from the iliac crest, or in the case of orofacial defects from the symphysis of the chin or ascending ramus. Autologous bone grafts provide both an osteoconductive and osteogenic environment, as a result of the presence of living cells and the cocktail of growth factors in the matrix. This method, however, has major drawbacks: bone grafts are only available in limited volumes and this procedure can cause long-lasting donor site morbidity and pain. These drawbacks could be overcome by alternative approaches for bone reconstruction, such as methods employing principles of bone tissue engineering, combining scaffolds, cells, and/or chemical stimuli.

Biological components such as growth factors and cytokines can be used as chemical stimuli aiding bone tissue engineering. The kinetics of delivery of biological components will influence the biological effect of the component, or the occurrence of side effects. In **chapter 2**, we shed light on the continuing debate whether short, burst or sustained release is the best mechanism for the application of biological components for bone tissue engineering. We mimicked the in vivo situation in a cell culture environment by seeding human adipose stem cells (hASCs) on clinically applicable biphasic calcium phosphate (BCP) particles, allowing precise manipulation of doses and timing of application. We aimed to investigate which application of vitD$_3$ i.e. mimicking short exposure of cells ([200 nM] for 30 minutes), burst release from scaffolds ([100 nM] for 2 days), or sustained release from scaffolds ([10 nM] for 20 days), leads to optimal osteogenic differentiation of hASCs. Our results suggest that mimicking sustained release by delivery of a daily dose of vitD$_3$ seems to have more effect on hASCs than the other applications. Delivery of vitD$_3$ for a longer period did not lead to apoptosis and triggers ALP activity at day 7 and day 20. It also affected the gene expression of key osteogenesis regulator gene RUNX2, and genes involved in the vitD$_3$ metabolism, VDR, and CYP24a1.

Bone tissue engineering constructs send signals to cells in the bone to form more bone and to recruit stem cells, which can differentiate into cells that form bone. Cells from different skeletal sites may react differently to such signals. Therefore, in **chapter 3** we analyzed the degree of differentiation of bone cells derived from human long bone and alveolar bone. Furthermore, the production of signaling molecules by these cells and their capacity to induce osteoclast formation was measured in the presence or absence of biological component vitD3. The results show that under basic culturing conditions long bone cells seemed more differentiated compared to alveolar bone cells. Furthermore, long bone-derived cells have stronger osteoclastogenic potential than alveolar bone cells. Taken together, these differences reveal that skeletal sites generate site-specific differences between the cells and indicate that for the regeneration of specific sites, such as the alveolar bone, more research on site-specific tissue engineering constructs is needed.

3D-printing can be used to make scaffolds for bone tissue engineering. By using this technique patient-specific scaffolds can be created that fits the defect perfectly. Calcium phosphates are often used in bone tissue engineering as it resembles the crystals of hydroxyapatite in bone. 3D printing of calcium phosphates with a chemical stimulus such as growth factors is a challenge since methods using high temperatures or aggressive chemicals, such as Selective laser sintering and 3D-powder printing, impede the bioactivity of the incorporated biological components. Cells and proteins that are active at body temperature lose their life or bioactivity at such high temperatures, or are denatured by the chemicals. In **chapter 4**, we developed a method to 3D print calcium phosphate with a biological binder allowing for the incorporation of biologically active components as chemical stimuli. We show that it is possible to 3D print with a mixture of precipitated calcium phosphate paste and κ-carrageenan. To show the ability to incorporate biological components BSA-FITC was used as a model. We show the incorporation of the BSA-FITC inside the print material and also show that the BSA-FITC is released, indicating that this method can be used to 3D print constructs with biological components. More research on the clinical relevance of this method is needed.

Finally, in **chapter 5**, as the next step towards a clinical application, we assessed if constructs printed with the method described in chapter 4, and enhanced with 1,25(OH)2vitD_3 as a biological component, can be clinically relevant. In order to meet clinical relevance, the material should have the following features: The material should have a certain rigidity, so the surgeon can handle the construct and it should be tolerated by cells, so no adverse body reaction takes place. We investigated these features by measuring the printability, compressive stiffness, and cytotoxicity of the material and the effect of the material on U2OS human osteosarcoma-derived cells when cultured in close proximity to the print material. The results show that the material is printable, is rigid enough to handle, and did not have an adverse effect on the proliferation of U2OS cells when co-cultured. We also showed that the vitD_3 is released from the material, and most importantly, is bioactive.

Taken together, the combined results in this thesis suggest that constructs made of CaP paste and κ-carrageenan could be clinically relevant and that 1,25(OH)2vitD$_3$ could be a biological additive that enhances the osteoinductive potential of the construct. However, precise tuning of the release characteristics may be necessary to increase the effectivity 1,25(OH)2vitD3. In addition, when the construct is made for the purpose of healing large bone defects in the orofacial area, research into other osteoinductive components to enhance the construct may be necessary as alveolar bone cells are different and react differently to 1,25(OH)2vitD$_3$ than long bone cells.

8

Nederlandse samenvatting

Botdefecten kunnen ontstaan als gevolg van onder andere trauma, kanker, ontsteking of overbelasting. Hoewel bot van nature goed geneest, blijft de reconstructie van botdefecten van kritische grootte (CSBD) een uitdaging. Momenteel is de “gouden standaard” om dit soort defecten te reconstrueren het gebruik van autologe bottransplantaties. Bot voor deze transplantaties wordt bij de patiënt zelf afgenomen, vaak van de bekkenkam en voor aangezichtsdefecten vanuit de kin of de ramus. Autologe bottransplantaties zorgen voor zowel een botgroei-geleidende omgeving als een botvorming-inducerende omgeving, omdat het levende cellen bevat, alsmede een cocktail van groeifactoren in de extracellulaire matrix. Deze methode heeft echter grote nadelen: Bot voor de bottransplantaties is slechts in beperkte hoeveelheden beschikbaar, past meestal niet naadloos in het op te vullen defect, en het oogsten kan langdurige pijn veroorzaken. Deze nadelen kunnen worden overwonnen door alternatieve behandelmethoden te gebruiken, zoals tissue engineering, waarbij een combinatie van dragermaterialen (scaffolds), cellen, en/of chemische stimuli wordt gebruikt.

Biologische componenten zoals groeifactoren en cytokinen kunnen worden gebruikt als chemische stimuli om botweefsel vorming te ondersteunen. De kinetiek van afgifte van biologische componenten, uit bijvoorbeeld een dragermateriaal, kan het effect van de betreffende component, of het optreden van bijwerkingen beïnvloeden. In **hoofdstuk 2** werpen we licht op de voortgaande discussie of een piek, kortstondige, of langdurige afgifte van biologische componenten vanuit dragermaterialen, specifiek gebouwd voor botweefsel tissue engineering, botgroei het meest stimuleert. We hebben daarvoor de in vivo situatie gedeeltelijk nagebootst in een celkweekomgeving. Dit hebben we gedaan door menselijke stamcellen verkregen uit vetweefsel (hASC’s) op klinisch toepasbare calciumfosfaat deeltjes te zaaien, waardoor een nauwkeurige manipulatie van de dosering en timing van afgifte van de onderzochte componenten mogelijk is. Ons doel was om te onderzoeken welke toediening van 1,25(OH)2vitamineD_3 (vitD_3) leidt tot een optimale osteogene differentiatie van hASCs. We hebben gekozen voor het nabootsen van de volgende situaties: een zeer korte blootstelling van cellen aan vitD_3 ([200 nM] gedurende 30 minuten), het kortstondig toevoegen van vitD_3 ([100 nM] gedurende 2 dagen), of het langdurig toevoegen van vitD_3 ([10 nM] gedurende 20 dagen). Onze resultaten suggereren dat het nabootsen van langdurige afgifte, door het toedienen van een dagelijkse dosis vitD_3, meer effect lijkt te hebben op de osteogene differentiatie van hASC’s dan de kortere toepassingen. Het toedienen van vitD_3 voor een langere periode leidde niet tot apoptose en stimuleert de ALP-activiteit op dag 7 en dag 20. Daarnaast beïnvloedde het ook de genexpressie RUNX2, een belangrijke regulator voor osteogenese, en de genen die betrokken zijn bij het vitD3-metabolisme, VDR en CYP24a1.

Constructen die geschikt zijn voor bot tissue engineering sturen signalen naar cellen in het bot om meer bot te vormen en om stamcellen aan te trekken. Deze stamcellen kunnen vervolgens 120 differentiëren in cellen die botmatrix vormen. Cellen van verschillende plekken in het skelet kunnen echter mogelijk verschillend reageren op signalen afkomstig van tissue engineering constructen. Daarom hebben we in **hoofdstuk 3** de respons van mesenchymale botcellen (osteoblasten) afkomstig van menselijke pijpbeenderen en alveolair bot op biologische componenten geanalyseerd. Daarnaast hebben we de productie van signaalmoleculen door deze cellen gemeten, alsmede hun vermogen om osteoclast vorming te induceren in de aanwezigheid of afwezigheid van vitD3. De resultaten tonen aan dat onder standaard celkweekcondities cellen van pijpbeen meer gedifferentieerd leken dan alveolaire botcellen. Bovendien hebben pijpbeencellen een sterker osteoclastogeen potentieel dan alveolaire botcellen. Samen laten deze verschillen zien dat de locatie van het bot in het skelet voor specifieke verschillen tussen de cellen zorgt. Dit geeft aan dat voor de regeneratie van specifieke locaties, zoals het alveolaire bot, meer onderzoek nodig is naar locatie-specifieke tissue-engineering constructen.

3D-printing kan worden gebruikt om scaffolds te maken voor botweefsel engineering. Door gebruik te maken van deze techniek kunnen patiënt-specifieke scaffolds worden gemaakt die perfect passen in het defect. Calciumfosfaten worden vaak gebruikt voor bot tissue engineering omdat deze in samenstelling lijken op het hydroxyapatiet in bot. Het 3D printen van calciumfosfaten met daarin biologisch actieve factoren zoals groeifactoren is een uitdaging, omdat de meeste gangbare 3D print-methoden gebruik maken van hoge temperaturen of agressieve chemicaliën die de bioactiviteit van de geïncorporeerde biologische componenten negatief beïnvloeden. Cellen en eiwitten, die actief zijn bij lichaamstemperatuur, gaan dood of verliezen hun bioactiviteit bij zulke hoge temperaturen, of worden gedenatureerd door de chemicaliën. In **hoofdstuk 4** hebben we een methode ontwikkeld om calciumfosfaat te 3D printen met een biologisch bindmiddel dat de opname van biologisch actieve componenten als chemische stimulans mogelijk maakt. De combinatie van calciumfosfaat en bindmiddel noemen wij een “bioinkt”. We laten zien dat het mogelijk is om een 3D construct te printen van een bioinkt bestaande uit neergeslagen calciumfosfaat, in de vorm van een pasta, en κ-carrageenan, een uit zeewier verkregen materiaal dat lijkt op de glycosaminoglycanen in extracellulaire matrix. Om de mogelijkheid om biologische componenten in te bouwen aan te tonen werd BSA-FITC aan de bioinkt toegevoegd. We tonen de integratie van de BSA-FITC in het printmateriaal aan, en laten ook zien dat de BSA-FITC vrijkomt na het printen. We laten zo zien dat deze methode kan worden gebruikt om 3D geprinte constructen met biologische componenten te maken. Echter, of de biologische component nog bioactief is, is hiermee niet aangetoond, en meer onderzoek naar de klinische relevantie van deze methode is nodig.

Als eerste stap naar een klinische toepassing hebben we tot slot in **hoofdstuk 5**, onderzocht of de constructen geprint met de methode beschreven in hoofdstuk 4, met vitD_3 als biologische component, klinisch relevant kunnen zijn. Om aan de klinische relevantie te voldoen, moet het materiaal ten minste de volgende kenmerken hebben: Het materiaal moet een bepaalde mechanische stijfheid hebben, zodat het hanteerbar is, en het moet door de cellen worden getolereerd, zodat er geen bijwerkingen in het lichaam plaatsvinden. We hebben deze kenmerken onderzocht door de printbaarheid, de compressiestijfheid en de cytotoxiciteit van het materiaal te meten. Daarnaast hebben we het effect van het materiaal op menselijke osteoblast-achtige cellen (U2OS) getest wanneer deze worden gekweekt in de nabijheid van de bioinkt. De resultaten tonen aan dat het materiaal printbaar is, stijf genoeg is om voorzichtig vast te kunnen houden en geen nadelig effect heeft op de proliferatie van U2OS-cellen wanneer deze worden gekweekt in de nabijheid van de bioinkt. We hebben ook aangetoond dat de vitD_3 uit het materiaal vrijkomt, en het belangrijkste is dat het vitD_3 nog bioactief is als het vrijkomt.

De gecombineerde resultaten in dit proefschrift suggereren dat constructen gemaakt van CaPpasta en κ-carrageenan klinisch relevant zouden kunnen zijn, en dat 1,25(OH)2vitD_3 een biologisch additief zou kunnen zijn dat het osteo- inductief potentieel van het construct versterkt. Een nauwkeurige afstemming van de afgifte kan echter nodig zijn om de effectiviteit van vitD_3 te verhogen. Bovendien kan, wanneer het construct is gemaakt voor het genezen van grote botdefecten in het orofaciale gebied, onderzoek naar andere osteo-inductieve componenten nodig zijn om het construct te verbeteren, omdat alveolaire botcellen anders zijn en anders reageren op vitD_3 dan pijpbeen cellen.

9

Appendices

List of publications

Peer reviewed full-text publications

1. **Kelder, C**.; Kleverlaan, C.J.; Gilijamse, M.; Bakker, A.D.; de Vries, T.J. Cells Derived from Human Long Bone Appear More Differentiated and More Actively Stimulate Osteoclastogenesis Compared to Alveolar Bone-Derived Cells. *Int. J. Mol. Sci.* 2020, *21*, 5072.
2. **Kelder, C**.; Hogervorst, J.M.A.; Wismeijer, D.; Kleverlaan, C.J.; de Vries, T.J.; Bakker, A.D. Burst, short, and sustained vitamin D_3 applications differentially affect osteogenic differentiation of human adipose stem cells. *Int. J. Mol. Sci.* 2020, *21*.
3. Kamperman, T.; Koerselman, M.; **Kelder, C**.; Hendriks, J.; Crispim, J.F.; de Peuter, X.; Dijkstra, P.J.; Karperien, M.; Leijten, J. Spatiotemporal material functionalization via competitive supramolecular complexation of avidin and biotin analogs. *Nat. Commun.* 2019, *10*, 1–11.
4. **Kelder, C.**; Bakker, A.D.; Klein-Nulend, J.; Wismeijer, D. The 3D printing of calcium phosphate with k-carrageenan under conditions permitting the incorporation of biological components—A method. *J. Funct. Biomater.* 2018, *9*.
5. Ghebes, C.A.; **Kelder, C.**; Schot, T.; Renard, A.J.; Pakvis, D.F.M.; Fernandes, H.; Saris, D.B. Anterior cruciate ligament- and hamstring tendon-derived cells: in vitro differential properties of cells involved in ACL reconstruction. *J. Tissue Eng. Regen. Med.* 2017, *11*.
6. Thakkar, S.; Ghebes, C.A.; Ahmed, M.; **Kelder, C.**; Van Blitterswijk, C.A.; Saris, D.; Fernandes, H.A.M.; Moroni, L. Mesenchymal stromal cell-derived extracellular matrix influences gene expression of chondrocytes. *Biofabrication* 2013, *5*.

Other relevant publications and scientific contributions

1. Onder de loep! *Cindy Kelder*. Nederlands tijdschrift voor Tandheelkunde. Oktober 2018
2. The European Calcified Tissue Society PhD training course/conference, Paris, France, *Calcium phosphate as carrier for active proteins to create 3D-printed bone substitutes*. (oral presentation)
3. NBTE annual meeting 2018, Lunteren, the Netherlands, *The 3D-printing of calcium phosphate with κ-carrageenan under conditions permitting the incorporation of biological components-a method.* (poster presentation)
4. NVCB annual meeting 2018, Zeist, the Netherlands, *The 3D-printing of calcium phosphate with κ-carrageenan under conditions permitting the incorporation of biological components-a method.* (oral presentation)
5. EORS annual meeting 2019, Maastricht, the Netherlands, *The effect of Duration of Vitamin D_3 application on the osteogenic differentiation of human adipose stem cells*. (oral presentation)

6. NVCB annual meeting together with HSSBM 2019, Athens, Greece, *The effect of Duration of Vitamin* D_3 *application on the osteogenic differentiation of human adipose stem cells.* (oral presentation)

List of contributing authors of the manuscripts in this thesis

D. Wismeijer
Department of Oral Implantology and Prosthodontics, Academic Centre for Dentistry Amsterdam (ACTA), University of Amsterdam and Vrije Universiteit Amsterdam, Amsterdam, the Netherlands

A.D Bakker
Department of Oral Cell Biology, Academic Centre for Dentistry Amsterdam
University of Amsterdam and Vrije Universiteit Amsterdam, Amsterdam, the Netherlands

T.J de Vries
Department of Periodontology, Academic Centre for Dentistry Amsterdam,
University of Amsterdam and Vrije Universiteit Amsterdam, Amsterdam, the Netherlands

C.J Kleverlaan
Department of Dental Material Sciences, Academic Center for Dentistry Amsterdam,
University of Amsterdam and Vrije Universiteit, Amsterdam, the Netherlands

J. Klein-Nulend
Department of Oral Cell Biology, Academic Centre for Dentistry Amsterdam,
University of Amsterdam and Vrije Universiteit Amsterdam, Amsterdam, the Netherlands

J.M.A Hogervorst
Department of Oral Cell Biology, Academic Centre for Dentistry Amsterdam,
University of Amsterdam and Vrije Universiteit Amsterdam, Amsterdam, the Netherlands

B. Zandieh Doulabi
Department of Oral Cell Biology, Academic Centre for Dentistry Amsterdam,
University of Amsterdam and Vrije Universiteit Amsterdam, Amsterdam, the Netherlands

M. Gilijamse
Department of Oral and Maxillofacial Surgery and Oral Pathology, Amsterdam University Medical Centre (Amsterdam UMC), location VUmc, Amsterdam, The Netherlands
Department of Oral and Maxillofacial Surgery, OLVG, Amsterdam, The Netherlands

S. Matsukawa
Graduate School of Food Science and Technology, Tokyo University of Marine Science and Technology, Tokyo, Japan

L.C Geonzon
Graduate School of Food Science and Technology, Tokyo University of Marine Science and Technology, Tokyo, Japan

R.G Bacabac
Department of Physics, Medical Biophysics Group, University of San Carlos, Philippines

C. Kelder
Department of Oral Implantology and Prosthodontics, Academic Centre for Dentistry Amsterdam, University of Amsterdam and Vrije Universiteit Amsterdam, Amsterdam, the Netherlands
Department of Oral Cell Biology, Academic Centre for Dentistry Amsterdam, University of Amsterdam and Vrije Universiteit Amsterdam, Amsterdam, the Netherlands

List of contributing authors of the manuscripts in this thesis

Authors	**Initials**
D. Wismeijer	*DW*
A.D Bakker	*ADB*
T.J de Vries	*TDV*
C.J Kleverlaan	*CJK*
J. Klein-Nulend	*JKN*
J.M.A Hogervorst	*JMH*
B. Zandieh Doulabi	*BZD*
M. Gilijamse	*MG*
S. Matsukawa	*SK*
L.C Geonzon	*LCG*
R.G Bacabac	*RGB*
C. Kelder	*CK*

Chapter 2

Published as:

Burst, Short, and Sustained Vitamin D_3 Applications Differentially Affect Osteogenic Differentiation of Human Adipose Stem Cells

Authors:
C.Kelder, J.M.A Hogervorst, D. Wismeijer, C.J KLeverlaan, T.J de Vries and A.D Bakker

Published in: International journal of Molecular Sciences, 2020

Author contributions:
Conceived and designed the study: CK, JMH, ADB
Performed the study: CK, JMH
Analyzed the data: CK, ADB
Critically revised the manuscript: CK, JMH, DW, CJK, TDV, ADB
Funding sources:

No external funding, apart from the support of the authors' institution (Academic Centre for Dentistry Amsterdam), was available for this study.

Conflict of interest statement:
The authors declare that the research was conducted in the absence of any commercial or financial relationships that could be construed as a potential conflict of interest.

Chapter 3

Published as:

Cells Derived from Human Long Bone Appear More Differentiated and More Actively Stimulate Osteoclastogenesis Compared to Alveolar Bone-Derived Cells

Authors:
C.Kelder, C.J KLeverlaan, M. Gilijamse, A.D Bakker and T.J de Vries

Published in: International journal of Molecular Sciences, 2020

Author contributions:

Conceived and designed the study:	CK, TDV
Sample collection for this study:	MG
Performed the study:	CK, TDV
Analyzed the data:	CM, TDV, ADB
Critically revised the manuscript:	CJK, MG, ADB, TDV

Funding sources:
No external funding, apart from the support of the authors' institution (Academic Centre for Dentistry Amsterdam), was available for this study.

Conflict of interest statement:
The authors declare that the research was conducted in the absence of any commercial or financial relationships that could be construed as a potential conflict of interest.

Chapter 4

Published as:

The 3D Printing of Calcium Phosphate with K-Carrageenan under Conditions Permitting the Incorporation of Biological Components-A Method

Authors:
C. Kelder, A.D Bakker, J. Klein-Nulend and D. Wismeijer

Published in:

Journal of functional biomaterials (2018)

Author contributions:

Conceived and designed the study:	CK, JKN, DW
Performed the study:	CK
Analyzed the data:	CK
Critically revised the manuscript:	CK, ADB, JKN, DW

Funding sources:
No external funding, apart from the support of the authors' institution (Academic Centre for Dentistry Amsterdam), was available for this study.

Conflict of interest statement:
The authors declare that the research was conducted in the absence of any commercial or financial relationships that could be construed as a potential conflict of interest.

Chapter 5

Physical and biological aspects of 3D calcium phosphate scaffolds containing vitamin D_3

Cindy Kelder[1,2], Jolanda M.A. Hogervorst[2], Behrouz Zandieh Doulabi[2], Cornelis, J. Kleverlaan[3], Teun J. de Vries[4], Jenneke Klein-Nulend[2], Lester C. Geonzon[5], Shingo Matsukawa[5], Rommel G. Bacabac[6], Daniel Wismeijer[1], Astrid D. Bakker[2]

Authors:
C. Kelder, J.M.A Hogervorst, B. Zandieh Doulabi, C.J Kleverlaan, T.J de Vries, J. Klein-Nulend, L.C Geonzon, S. Matsukawa, R.G Bacabac, D. Wismeijer and A.D Bakker

Author contributions:

Conceived and designed the study:	CK, CJK, ADB
Providing material:	LCG, SM, RGB, JKN
Performed the study:	CK, JMH, BZD
Analyzed the data:	CK, BZD, ADB, TDV
Critically revised the manuscript:	CK, JMH, CJK, TDV, JKN, LCG, DW, ADB

Funding sources:
No external funding, apart from the support of the authors' institution (Academic Centre for Dentistry Amsterdam), was available for this study.

Conflict of interest statement:
The authors declare that the research was conducted in the absence of any commercial or financial relationships that could be construed as a potential conflict of interest.

PhD Portfolio

PhD student:	Cindy L. Kelder
PhD Period:	October 2016 – October 2020
PhD supervisors:	prof. dr. Daniel Wismeijer dr. Astrid D. Bakker prof. dr. Cornelis J. Kleverlaan dr. ir. Teun J. de Vries

General courses	**Year**	**ECTS**
Dentistry for non-dentists	*2018*	*1.0*
Oral biology	*2017*	*4.0*
Scientific writing and presenting in English	*2019*	*4.0*
Statistics and Methodology	*2019*	*3.0*

Specific courses	**Year**	**ECTS**
The European Calcified Tissue Society PhD training course/conference, Paris	*2017*	*2.0*
Scientific integrity, ACTA Graduate School of Dentistry, Amsterdam, the Netherlands *- Research Integrity – biomedical Sciences, Epigeum, Oxford University Press* *- Research integrity – arts and humanities, Epigeum, Oxford University Press*	*2018*	*2.0*

(Inter)national conferences	**Presentation**	**Year**	**ECTS**
3D printing in healthcare	-	*2016*	*1.0*
Netherlands society for Biomaterials and Tissue Engineering (NBTE) annual meeting, Lunteren, the Netherlands	-	*2016*	*1.0*
NBTE annual meeting, Lunteren, the Netherlands	-	*2017*	*1.0*
Nederlandse Vereniging voor Calcium- en Botstofwisseling (NVCB), Annual meeting, Zeist, the Netherlands	*Oral*	*2018*	*1.0*
NBTE annual meeting, Lunteren, the Netherlands	*Poster*	*2018*	*1.0*
European Orthopaedic Research Society (EORS) annual meeting, Maastricht, the Netherlands	*Oral*	*2019*	*2.0*
NVCB annual meeting together with Hellenic Society for the Study of Bone Metabolism, Athens, Greece	*Oral*	*2019*	*2.0*

Supervising	**Year**	**ECTS**
Training and guidance in the workplace by supervisors	*2016 2020*	*6.0*
Boardmember ACTApro	*2017* *2018*	*1.0*

Total ECTS	**32.0**

Acknowledgements

Het moment is daar! Ik ben aan het einde van een spannend en uitdagend hoofdstuk uit mijn leven, en uitdagend is het geweest. Daarom ben ik alleen maar trotser dat ik het einde heb gehaald en mijn PhD kan afronden. Ik had dit niet alleen gekund en wil mijn dankbaarheid tonen aan iedereen die mij heeft geïnspireerd, geholpen en gesteund.

Allereerst wil ik **prof.dr. Daniel Wismeijer** en **prof.dr. Jenneke Klein Nulend** bedanken voor de geweldige kans die ze mij hebben gegeven om dit PhD project te mogen doen. Daarnaast wil ik jullie beide bedanken voor alle feedback om mijn artikelen zo goed mogelijk te maken.

Dr. Astrid Bakker, beste Astrid, ik wil je bedanken dat je mijn begeleiding hebt overgenomen. Jouw kennis en kunde is heel motiverend. Ook wil ik je bedanken voor het pushen, het beste uit mijzelf te halen, maar ook voor de bemoedigende woorden wanneer ik het zwaar had. Je bent een voorbeeld voor mij en ik hoop dat we contact houden.

Dr.ir. Teun de Vries, beste Teun, jij hebt mij onder je vleugels genomen toen ik dat het hardst nodig had. Onze experimenten samen in het lab waren leerzaam en gezellig. Dat ik nog vaak dansjes mag doen die jij dan nadoet!

prof.dr. Cees Kleverlaan, beste Cees, bedankt dat jij geholpen hebt om mijn project weer op de rit te krijgen en voor alle steun op de juiste momenten.

I want to thank the committee members for the time they spent on reading my thesis. It is an honor to have you at my defense ceremony.

In het bijzonder wil ik mijn paranimfen **Jolanda** en **Wessel** bedanken. Lieve Jolanda, na het eerste jaar werd jij aan mij gekoppeld en sindsdien waren we labmaatjes. Jij hebt mij door dik en dun gesteund (met en zonder prosecco) en jouw hulp was van onschatbare waarde. Bedankt voor alles wat je hebt gedaan en voor de leuke borrels. Dat we nog heel lang samen bubbels mogen drinken. Lieve Wessel, bedankt! Volgens jou was dit genoeg maar dat vind ik niet. Ik ben heel blij dat jij naast mij staat bij deze belangrijke gebeurtenis want jij bent mijn belangrijkste steunpilaar buiten ACTA geweest. Ik kon altijd bij je terecht en jij hebt altijd in mij geloofd ook wanneer ik dat zelf soms niet deed. Bedankt voor alle filmavonden met hele slechte films en veel sniper.

Ik wil ook het geweldige ondersteuningsteam van de 11^{e} verdieping bedanken. **Cor**, bedankt voor al je hulp! Ook al wist je helemaal niets ;). **Marion** jij bent de stille kracht op de afdeling. **Jolanda**, zonder jouw geweldige lach zou niemand weten dat er een 11de verdieping bestond. **Ton**, bedankt voor al je advies tijdens de lekkere biertjes en je bent zooo grappig ;). **Behrouz**, jij bent een wandelende encyclopedie.

Daarnaast wil ik mijn PhD maatjes Carolyn, Tijmen, Ursula en Yvon bedanken. Lieve **Carolyn**, jij bent een geweldig voorbeeld voor mij geweest en ik wil je bedanken voor alle lieve steun die jij mij hebt gegeven. Jij wist precies waar ik soms doorheen ging en was niet bang om dit te delen, daar ben ik je heel dankbaar voor. Ook onze shoppinguitjes en lunchdates nadat we weer in het weekend moesten werken zal ik missen. Ik ben super dankbaar voor de mooie vriendschap die is ontstaan. Beste **Tijmen**, mijn mede biomedical engineer, bedankt voor alle sparringrondes en theetjes, die heb ik altijd erg gewaardeerd. Ook bedankt voor de toffe tijd in Athene, mijn voeten doen nog steeds pijn van al het lopen. Ik zal alle leuke borrels en onze 'inside' nerd grapjes, die alleen wij snapten, missen. Dear **Ursula**, my sweet Brazilian girl, thank you for all your support and pep talks while eating Kinder chocolate. Lieve **Yvon**, ook al was je niet de hele week op ACTA ik kon altijd bij je terecht. Bedankt voor de gezellige theetjes, etentjes en het verven van mijn haar.

I want to thank my sweet roomies for all the great times, but also support in the more difficult times. You all believed in me! **Ivana**, you are such a great woman and scientist. Thanks for all your advice, nice talks and our squat moments. I wish you a lovely future with Ivan and your daughter Jana. Dear **Silvia**, your enthusiasm for research has been an inspiration. I have happy memories of our trip to Paris and Disneyland! Thanks for all the support. Dear **Yasaman**, Thanks you for your positive vibes and help with the 3D printer. Dear **Jiayi**, no wonder we can call you Joy. You are always so joyful and positive. Thank you for all the nice talks and hugs. And last but not least: dear **Behrouz**, mijn 'zeer gewaardeerde collega' you are one of the nicest persons I have ever met and you are always willing to help. Thanks for everything!

Ik heb zelf geen studenten begeleid, maar er waren studenten op de afdeling waarmee ik wel een goede band heb opgebouwd. **Fenne**, bedankt voor alle leuke 'theetijd' en Disney-films. Nog heel veel succes met het afronden van je eigen PhD. **Yanaika**, bedankt voor alle gezellige treinritjes, ik ga ze echt missen! **Hanneke**, bedankt voor alle fijne gesprekken en steun in de moeilijke tijden.

Ik wil alle (oud) collega's van de 11de en 12de verdieping bedanken: **Ineke, Jinfeng, Dagmar, Vivian, Wei, Mingjie, Angela, Fereshteh, Clara, Tineke, Jan-Harm, Hans,**

Kamran, Toon, Wendy, Sara, Beatriz, Sophie, Marieke en **Victor**. Heel erg bedankt voor alle gezelligheid, borrels en lunches, maar ook voor de feedback en steun! En Victor, hierbij geef ik mijn vloek over aan jou!

Ook wil ik de mensen van de afdeling implantologie bedanken en dan in het bijzonder **Nawal**, voor het wegwijs maken met de 3D printer en **Gang**, voor het protocol van de calciumfosfaat productie.

Ik wil graag mijn lieve vrienden bedanken voor alle gezellige avonden, uitjes, drankjes en festivals. Deze afleidingen waren van cruciaal belang! Lieve **Suus**, bedankt dat ik onderdeel van jullie meubilair mag zijn en ik altijd bij je terecht kan. Je wist vaak de juiste vragen te stellen waardoor ik tot inzicht en tot rust kwam. Beste **Kevin**, jij wist maar al te goed dat je niet altijd naar mijn PhD moest vragen en ik kon altijd bij je terecht als ik er even uit moest! Jammer dat we uiteindelijk niet hebben kunnen samenwerken. Lieve **Yvette**, bedankt voor de gezellige avonden en de leuke telefoongesprekken. Lieve **Femke**, met jou kon ik altijd mijn gedachten even verzetten, met Mario karten en drankjes. We moeten zeker nog een keer touren door ’t gooi. Beste **Pascal**, ik wil je bedanken voor jouw hulp en steun tijdens mijn bachelor, (pre)-master en het eerste deel van mijn PhD.

Girls: **Rosalie, Lisa** en **Anne-Sophie**, mijn heksjes, onze meidenavonden met spelletjes, maskers en veel chocola waren altijd een goede afleiding. Bedankt voor jullie steun! Jullie zijn geweldig!

Lieve **Margo**, ook al zien we elkaar niet heel vaak zodra we weer samen zijn is het alsof we elkaar nog steeds elke dag zien! Ons jaarlijkse uitje naar de Zwarte Cross is geweldig en ik kijk er altijd naar uit. Ik hoef je maar te bellen en je staat voor mij klaar, bedankt voor al je steun.

Lieve **Rosa**, Ik ben zo blij dat ik zo’n leuke vriendin in Hilversum heb. Bedankt voor alle wijntjes en onze heerlijke wandelingen. Hopelijk kunnen we snel weer naar leuke festivals. Lieve **Ashley**, vanaf het eerste moment op het vliegveld naar Bali hadden wij een klik. Thanks voor alle leuke dagjes uit en alle steun. Ik kan altijd mijn verhaal bij je kwijt. De rest van de balichicks: **Stephanie, Gea** en **Liza**, onze uitjes waren altijd erg gezellig en een fijne afleiding. Jullie waren altijd geïnteresseerd en probeerden mij te helpen. Op naar het volgende uitje!

Als laatste wil ik mijn lieve familie bedanken. Jullie hebben altijd in mij geloofd en mij enorm gesteund. Lieve **Angelique** en **Milo**, Ik kan jullie altijd bellen en jullie hebben mij veel gesteund op de momenten dat ik het moeilijk had. Bedankt! Lieve **Martinke**, mijn grote zus, bedankt voor al je liefde en vertrouwen in mij. Lieve **pap** en **mam**, bedankt voor jullie onvoorwaardelijke steun en liefde. Jullie hebben mij altijd gestimuleerd om te doen wat ik graag wilde en er het beste uit te halen. Dit is het mooie resultaat!

Met een dansje sluit ik deze mooie periode af!

Cindy

About the author

Cindy L. Kelder was born on February 12th, 1990 in Wageningen, the Netherlands. She is the daughter of Elwin and Jannie Kelder and sister of Martinke.

After obtaining her VWO diploma from Johannes Fontanes College in Barneveld, she started her Bachelor of Science in Crime science at Saxion Hogeschool of Enschede in 2008. During this study, she focused on biomedical research by completing internships at the Tissue Regeneration department of the University of Twente. In 2012, she obtained her Bachelor of Science degree and started the pre-master's program in Biomedical Engineering at the University of Twente. After completing the pre-master, she started with the master Biomedical Engineering with specialization in tissue engineering in 2013. She went to the Diabetic Research Institute in Miami for her internship and completed her graduation project at the Department of Developmental BioEngineering at the University of Twente, where she investigated the biofunctionalization of dextran-tyramine microgels using avidin-biotin chemistry. She obtained her Master of Science degree in 2016.

Shortly after her graduation, she started her Ph.D. at the Department of Implantology and Prosthodontics, and Department of Oral Cell biology of the Academic Centre for Dentistry Amsterdam (ACTA). She worked under the supervision of prof. dr. Daniel Wismeijer, Dr. Astrid D. Bakker, prof. dr. Cornelis J. Kleverlaan and Dr. ir. T.J. de Vries. She started a new adventure at the Hogeschool van Utrecht, where she will supervise and coordinate research projects of students.